



Dark matter

Rui Santos

ISEL & CFTC-UL

Dark Matter, Phase transitions and Gravitational
Waves

Dark Matter

Brief history of the universe

The early years

In the “beginning” there was a hot and dense universe. The interactions between particles were frequent and energetic. Then, the primordial plasma cooled and the light elements were formed (hydrogen, helium and lithium).

With the drop in energy the first stable atoms appeared. This is also the moment when photons started to roam freely.

What we see today is the microwave radiation from this afterglow. The radiation is nearly uniform (about 2.7 K) in all directions.

There are however small variations in the cosmic microwave background in temperature at a level of 1 part in 10 000. These fluctuations reflect tiny variations in the primordial density of matter.

Over time, and under the influence of gravity, these matter fluctuations grew. Dense regions were getting denser. Eventually, galaxies, stars and planets formed.

The early years

However what we “see” today as matter and energy is barely what we have access to in experiments on earth. Most of the universe today consists of forms of strange matter and energy.

Dark matter is required to explain the stability of galaxies and the rate of formation of the large-scale structure of the universe. Dark energy is required to rationalise the striking fact that the expansion of the universe started to accelerate recently (meaning a few billion years ago). What dark matter and dark energy are is still a mystery.

Finally, there is growing evidence that the primordial density perturbations originated from microscopic quantum fluctuations, stretched to cosmic sizes during a period of inflationary expansion. The physical origin of inflation is still a topic of active research.

So what now?

Missing ingredients:

Dark matter - no good dark matter candidates in the SM

Matter-antimatter asymmetry - more CP violation is needed

Neutrino masses...

Unexplained experimental results:

Muon magnetic moment

B meson decays

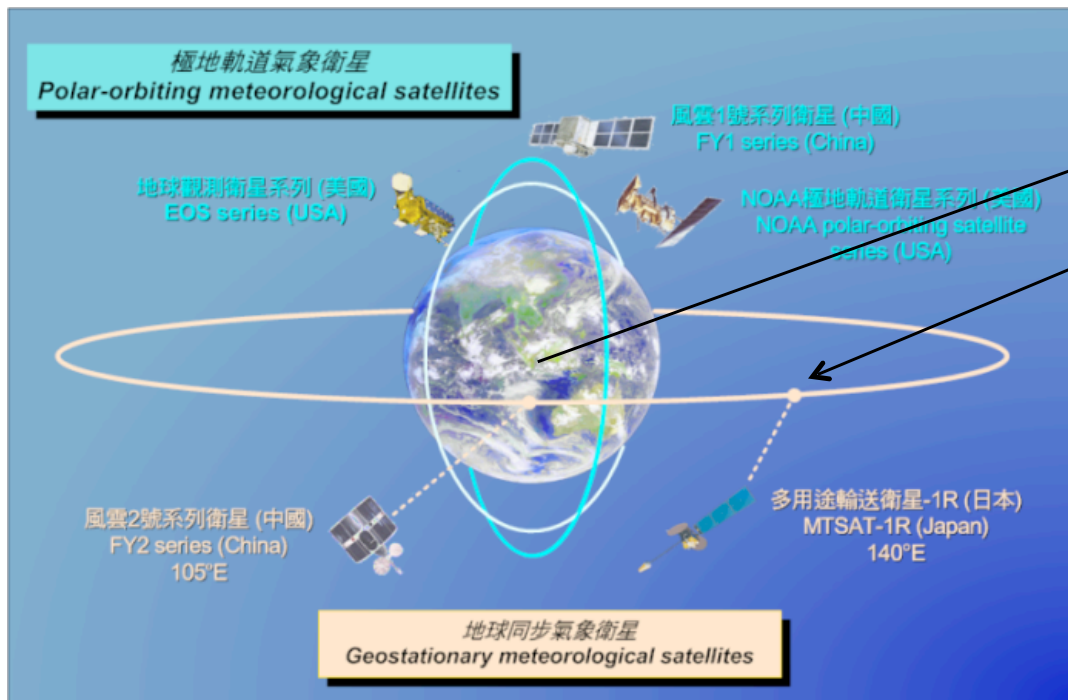


There is also gravity and dark energy

The early years

Fritz Zwicky (1930) When discussing the discrepancy between the observed and the expected rotation velocity of galaxies.

"Should this turn out to be true, the surprising result would follow that dark matter is present in a much higher density than radiating matter."



Earth

Satellite

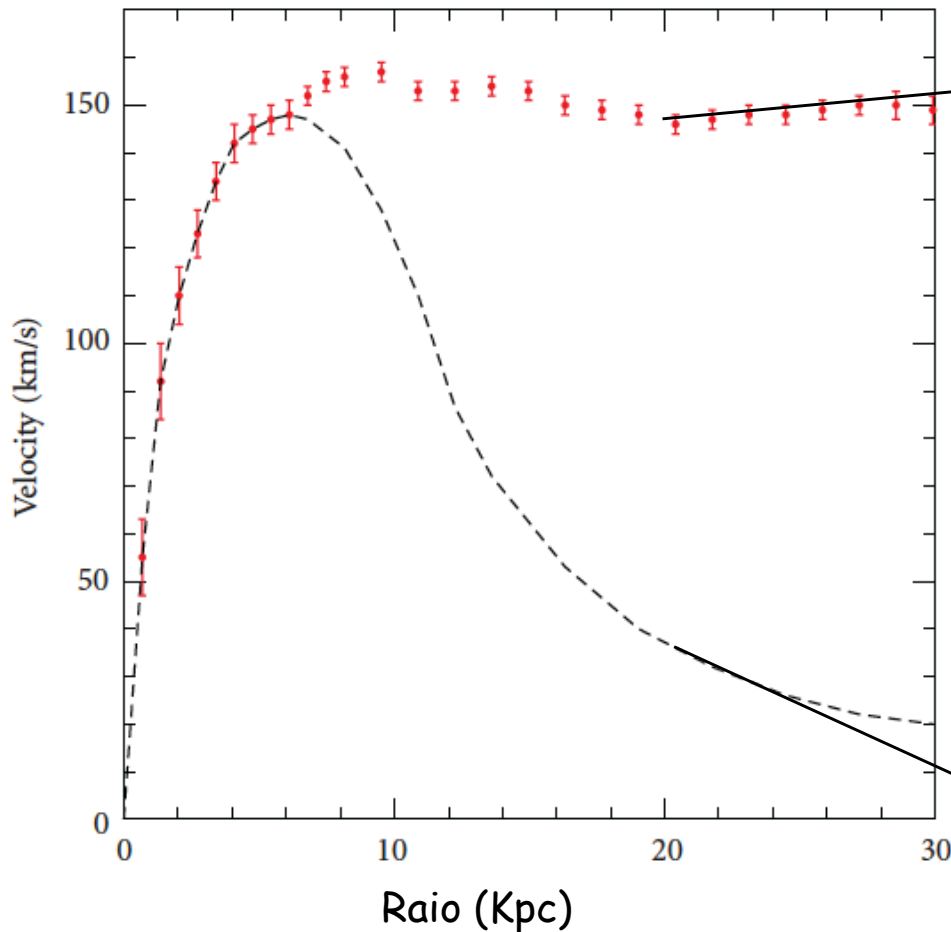
$$\frac{m v^2}{r} = G \frac{m M}{r^2}$$

$$v(r) = \sqrt{G \frac{m(r)}{r}}$$

At a distance of 640 Km, the satellite has a velocity of 27000 Km/h.

Rotation curves of galaxies

K. G. Begeman, "H I rotation curves of spiral galaxies,"
Astronomy and Astrophysics, vol. 223, pp. 47–60, 1989.



Experimental Results

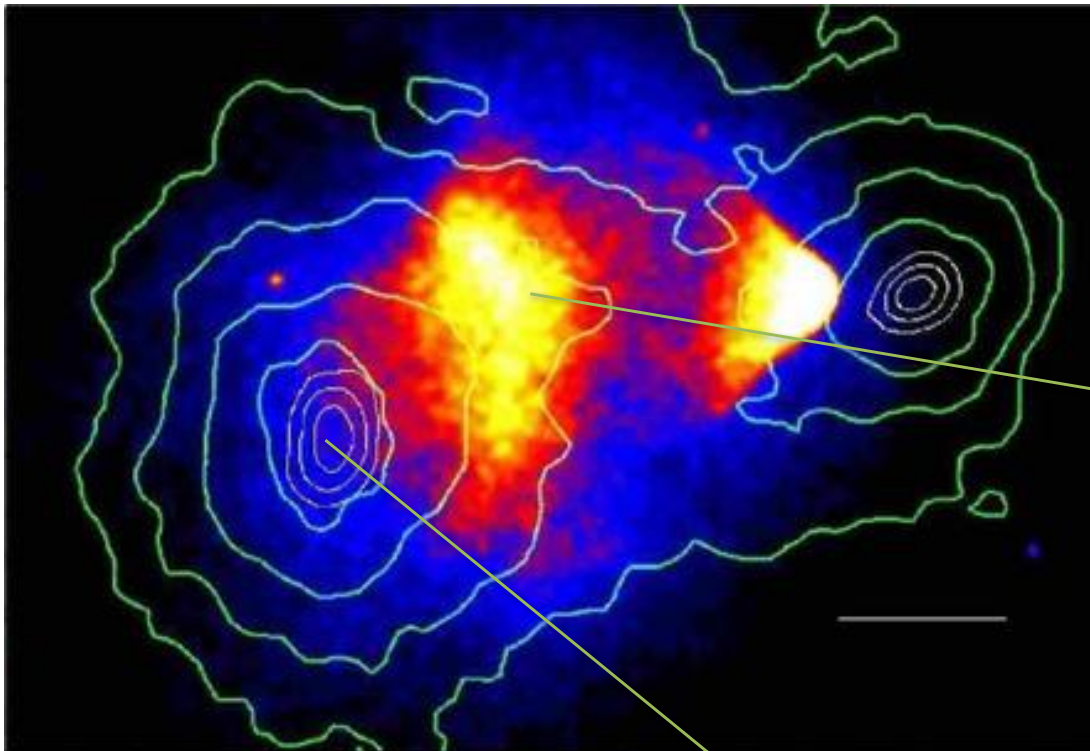
If the galaxy had only visible matter the expected behaviour for radius above 10 Kpc (for a typical spiral galaxy) would be that the velocity should decrease as:

$$v(r) = \sqrt{G \frac{m(r)}{r}}$$

Keplerian prediction

Contrary to luminosity, mass is not concentrated close to centre of spiral galaxies.
The distribution of light does not match the distribution of mass.

The Bullet Cluster



Two galaxies colliding – several sets of observational data superimposed: optical, X-ray, gravitational lensing.

Hot and dense gas. Typical shape of a high speed collision (4000 km/s).

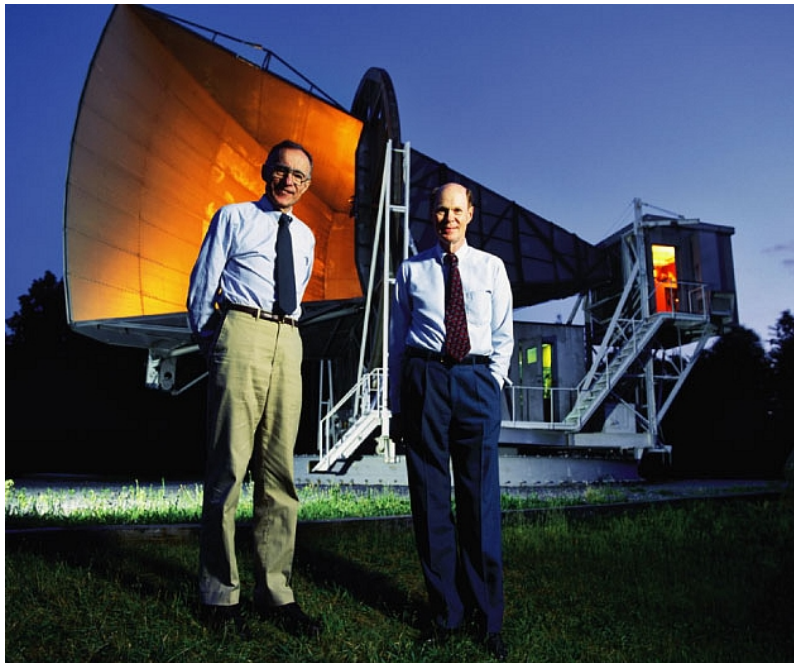
Lines of gravitation potential – from gravitational lensing show that the dark matter is concentrated around the galaxies and that it is not affected by the collisions.

Dark matter interacts very weakly!

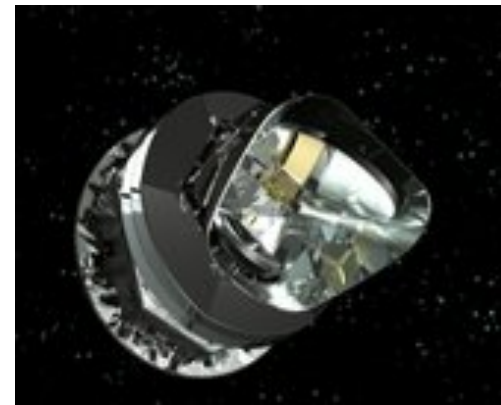
The Cosmic Microwave Background

In the Standard Model of Cosmology, it is assumed that just after the Big Bang the Universe was extremely hot, it then inflated (very rapidly) and cooled down. One effect of the rapid cooling was predicted to be a very low temperature radiation that would populate all space until today.

In 1965, astronomers Arno Penzias e Robert Wilson found (by accident – or so they say) an isotropic radiation of 2.725 Kelvin ($- 270^{\circ}$ C) (Nobel Prize 1978).

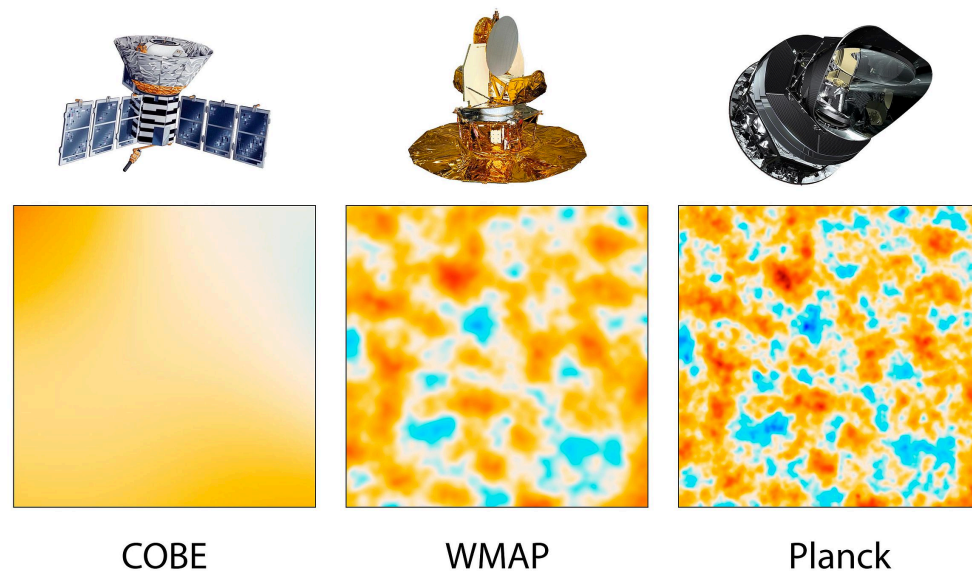


What can we learn from the
CMB?



Planck

The Cosmic Microwave Background



Planck +
cosmological model

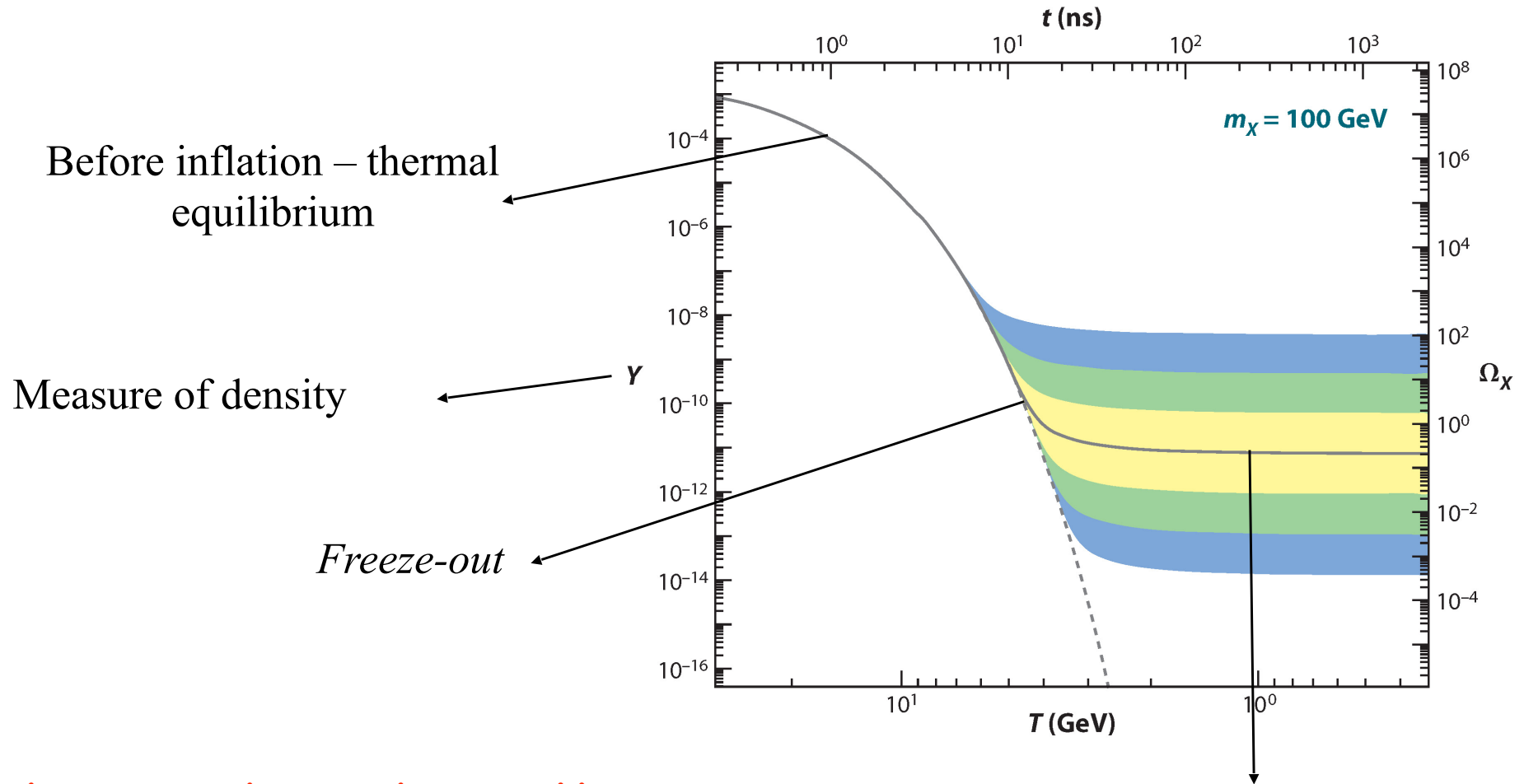
Fluctuation in the Cosmic Background Radiation are due to the matter density fluctuations in the early Universe.

Once upon a time all particles were in thermal equilibrium.

As the Universe expanded and cooled, the rate of interactions was not enough to maintain thermal equilibrium (freeze out).

The unstable particles disappeared (decayed); number of stable particles reached a constant (thermal relic density) which has still approximately the same value today.

What happened to dark matter?



There are other mechanisms like freeze-in!

$$\Omega_{CDM} \approx \frac{6 \times 10^{-27} \text{ cm}^3/\text{s}}{\langle \sigma v \rangle} \approx 0.23\%$$

Measure of the interaction rate

Why is dark matter so interesting?

- It completely changes our perception of the universe. Just a while ago we thought all matter was made of essentially the same stuff.
- It is the most interdisciplinary (inside physics) subject as it needs general relativity, nuclear physics, particle physics, cosmology, classical physics (thermodynamics and mechanics...)
- Mystery - "we know" it exists, "we know where it is", we have some hints on how it behaves but we do not know what it is ...

Why is dark matter so interesting?

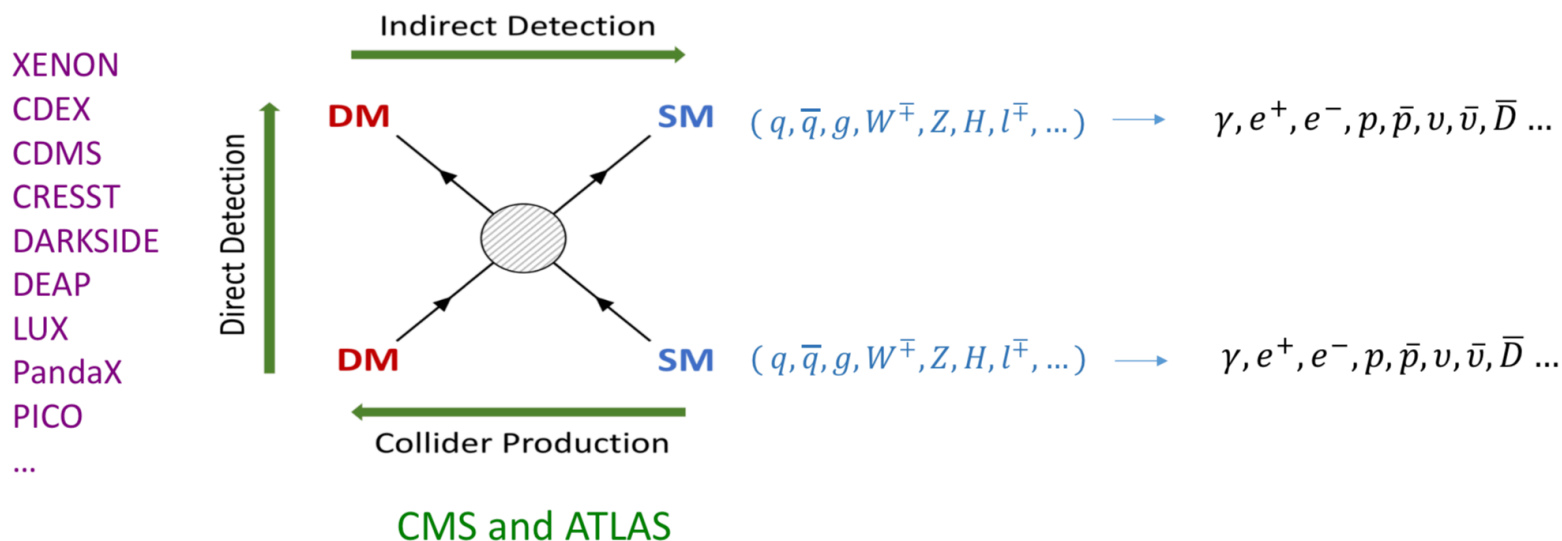
- **Massive, stable, neutral, weak (or none) interaction with SM**




















WIMP - **weakly interacting massive particles**/ Many other possibilities - **essentially no mass limits/ all spins possible**




HESS, HAWC, VERITAS, MAGIC, IceCube, ...
PAMELA, FERMI, CALET, DAMPE, AMS, ...

Searches for DM

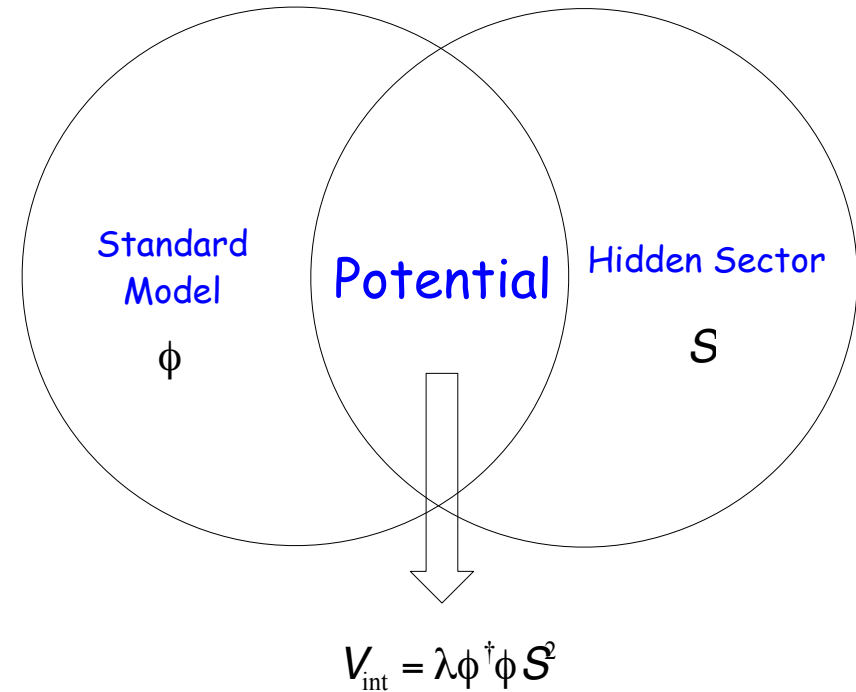


Extensions of the SM - a new model is needed

	1st gen.	2nd gen.	3rd gen.		
Q U A R K	 <i>u</i> up	 <i>c</i> charm	 <i>t</i> top	Strong Force  <i>g</i> Gluon	
	 <i>d</i> down	 <i>s</i> strange	 <i>b</i> bottom		Electro-Magnetic Force  <i>γ</i> photon
	 <i>e</i> electron	 <i>μ</i> muon	 <i>τ</i> tau		Weak Force  <i>W</i> ⁺  <i>W</i> ⁻  <i>Z</i> W bosons Z boson
L E P T O N	 <i>ν_e</i> <i>e</i> neutrino	 <i>ν_μ</i> <i>μ</i> neutrino	 <i>ν_τ</i> <i>τ</i> neutrino		

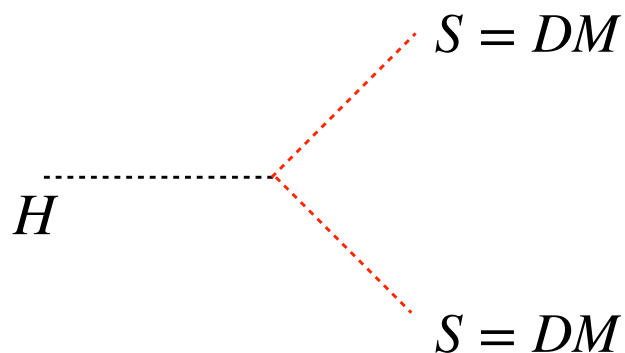
scalar particle(s)  *H*
Higgs  ?  ? . . .

Elements of the Standard Model

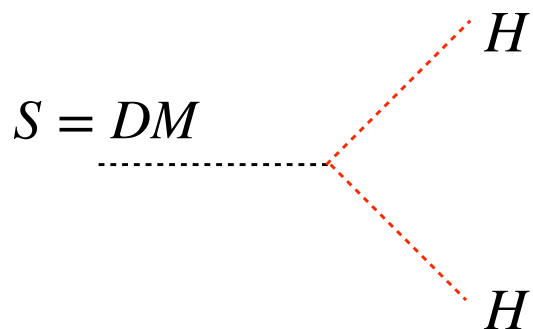


Lagrangian term that links the SM with the hidden sector. Dark Matter particle has to be stable. Can be done with a new quantum number.

Conserved quantities - darkness



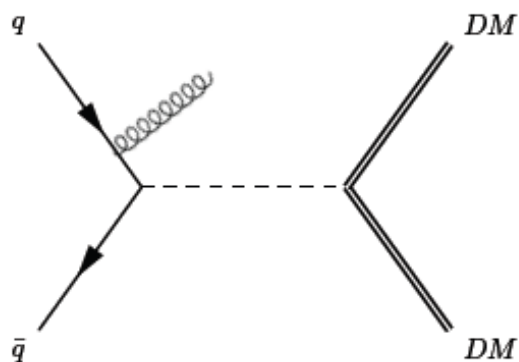
Model should conserve darkness - we need a stable particle. It is like electric charge - darkness number is constant.



Not possible - darkness not conserved.

$$Z(H) = 1; Z(DM) = -1$$

Darkness (Z) conserved



$$q\bar{q} \rightarrow g DM DM$$

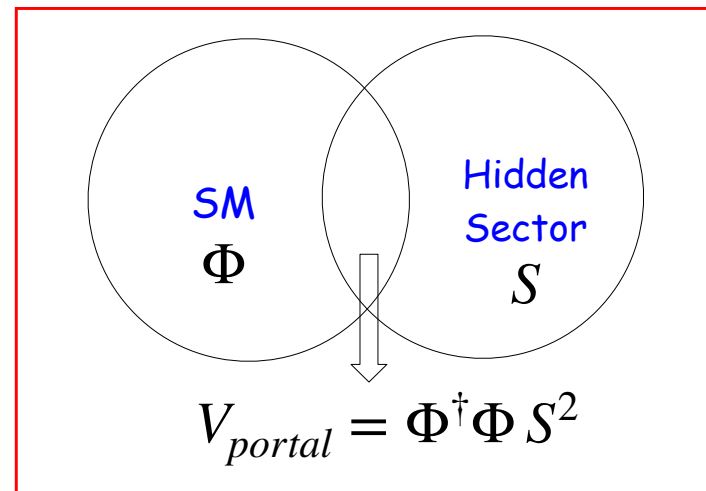
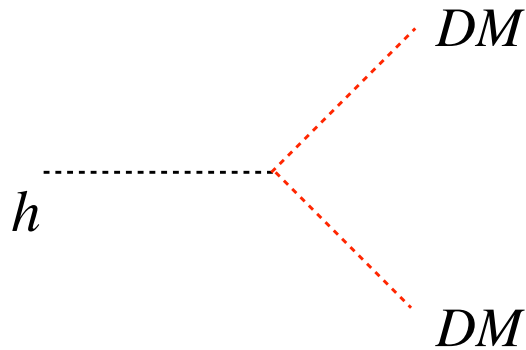
$$Z(q\bar{q}) = Z(q)Z(\bar{q}) = 1 \times 1 = 1$$

$$Z(q\bar{q}) = Z(g)Z(DM)Z(DM) = 1 \times (-1) \times (-1) = 1$$

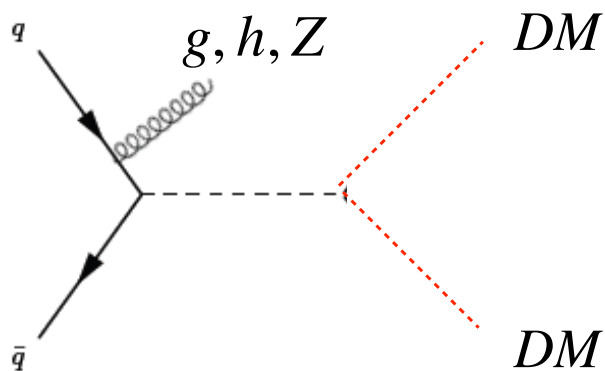
All spins allowed

Dark Matter (IDM)

Model should conserve "darkness" - we need a stable particle. The invisible width of the Higgs and the dark matter direct detection experiments set a bound on the so-called portal coupling(s).



Searches need some kind of handle

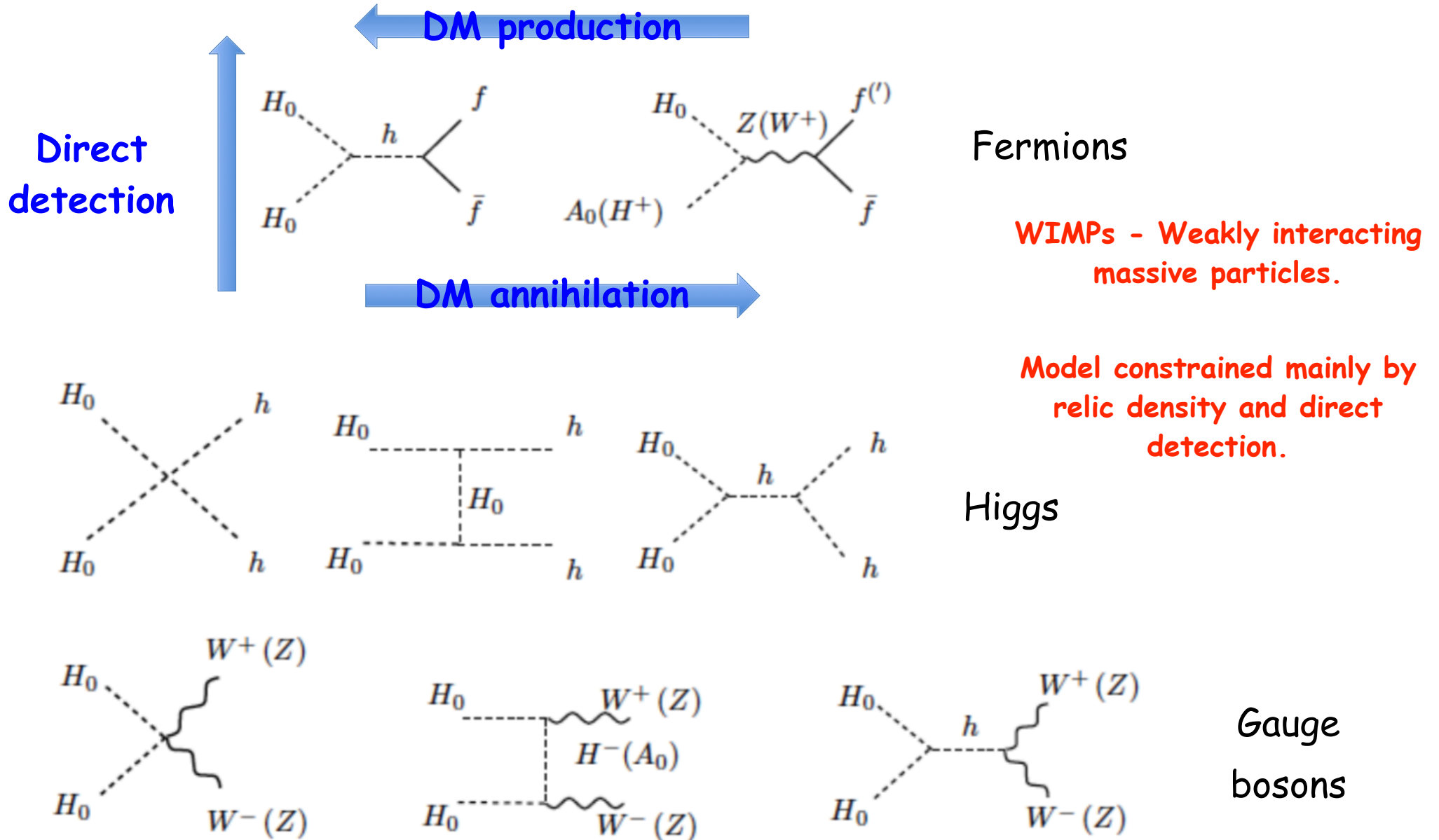


$$q\bar{q} \rightarrow (g, h, Z, \dots) DM DM$$

$$Z(q\bar{q}) = Z(q)Z(\bar{q}) = 1 \times 1 = 1$$

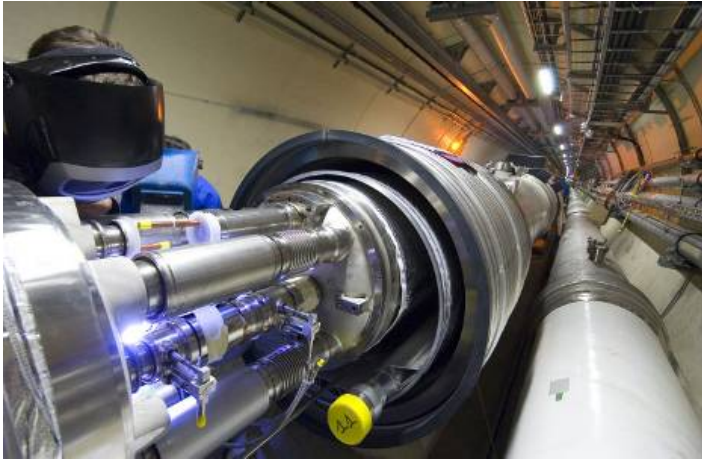
$$Z(q\bar{q}) = Z(H)Z(DM)Z(DM) = 1 \times (-1) \times (-1) = 1$$

Dark Matter (IDM)

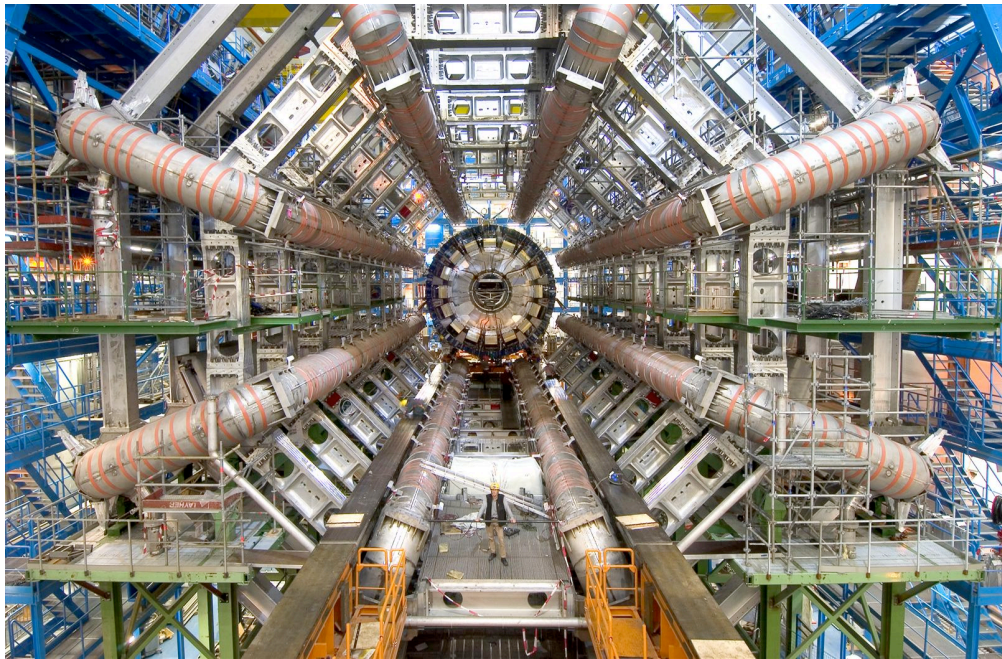


A collider is useful

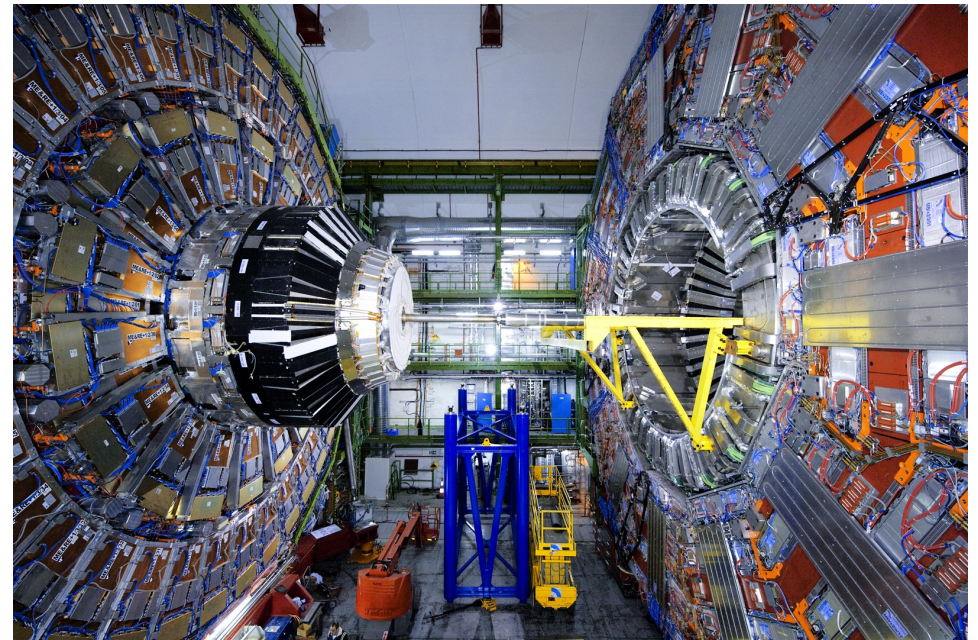
Where the protons travel



People

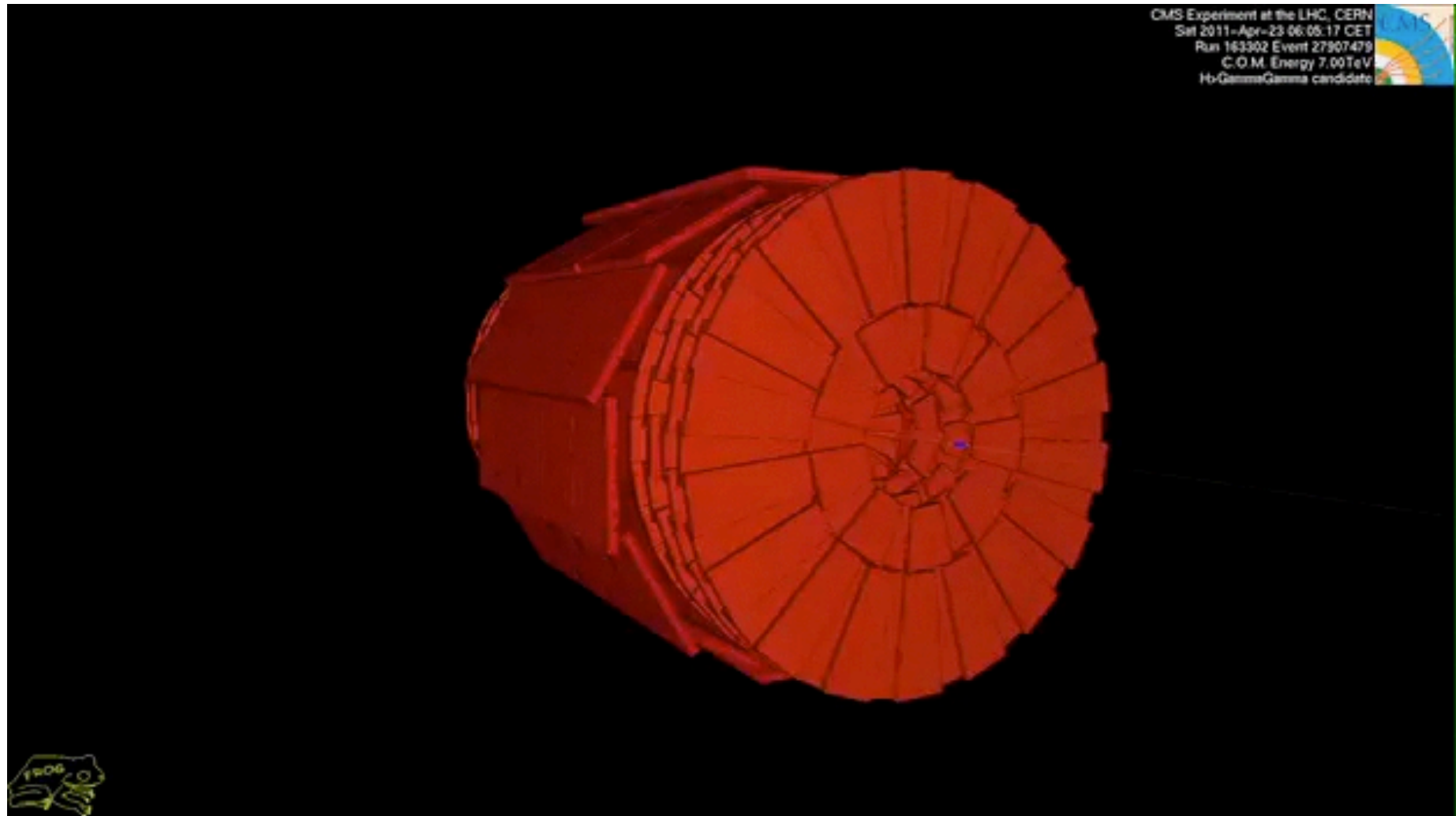


ATLAS

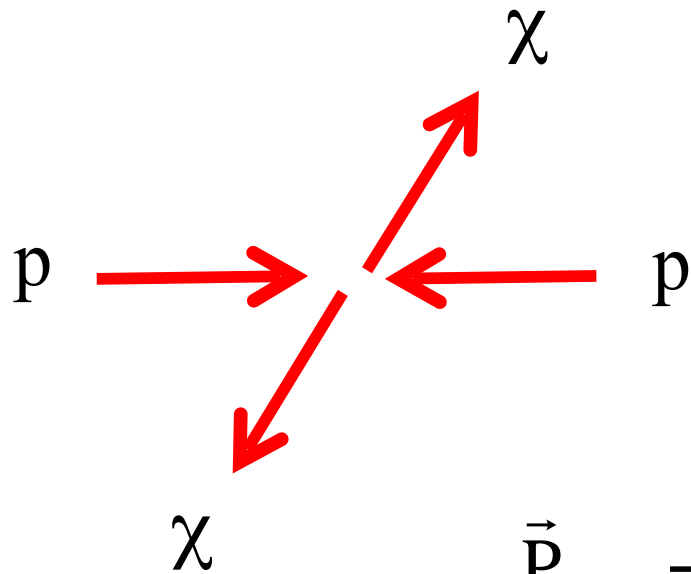


CMS

Particles collide...



Back to the LHC - Dark matter production



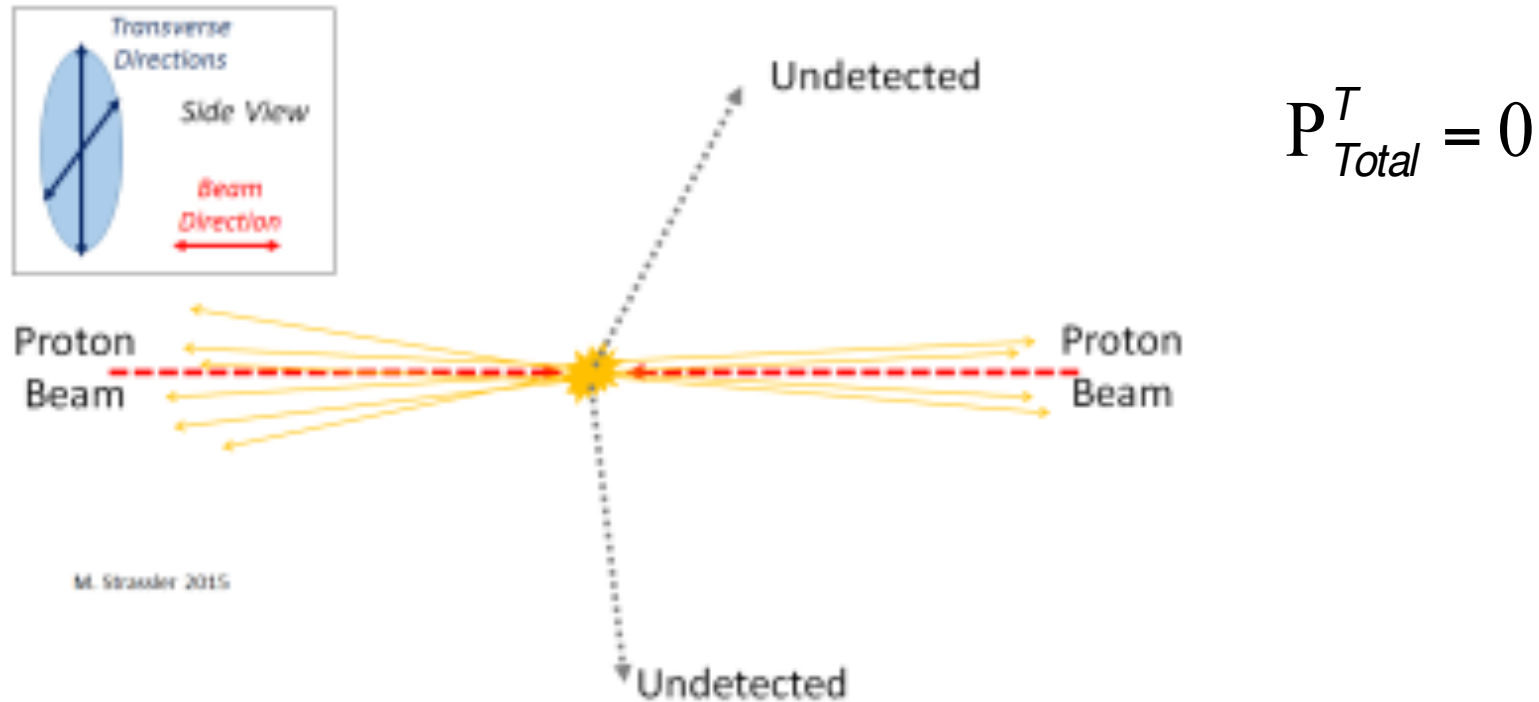
Darkness quantum number is conserved
and therefore dark particles are
produced in pairs

$$\vec{P}_{Total} = 0 \quad \xrightarrow{\text{LHC}} \quad P_{Total}^T = 0$$

But dark matter does not interact (or it does but very weakly) with the SM particles. We see nothing!

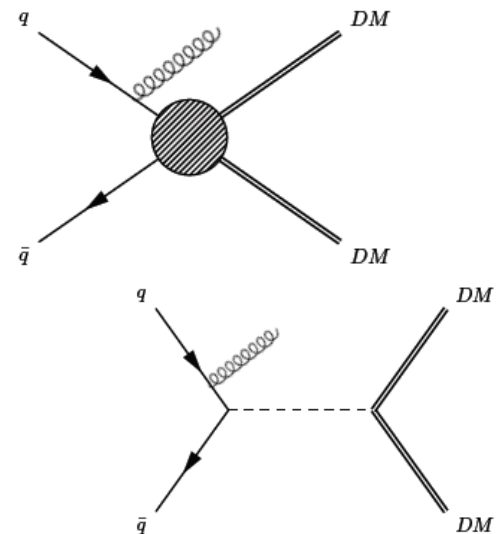
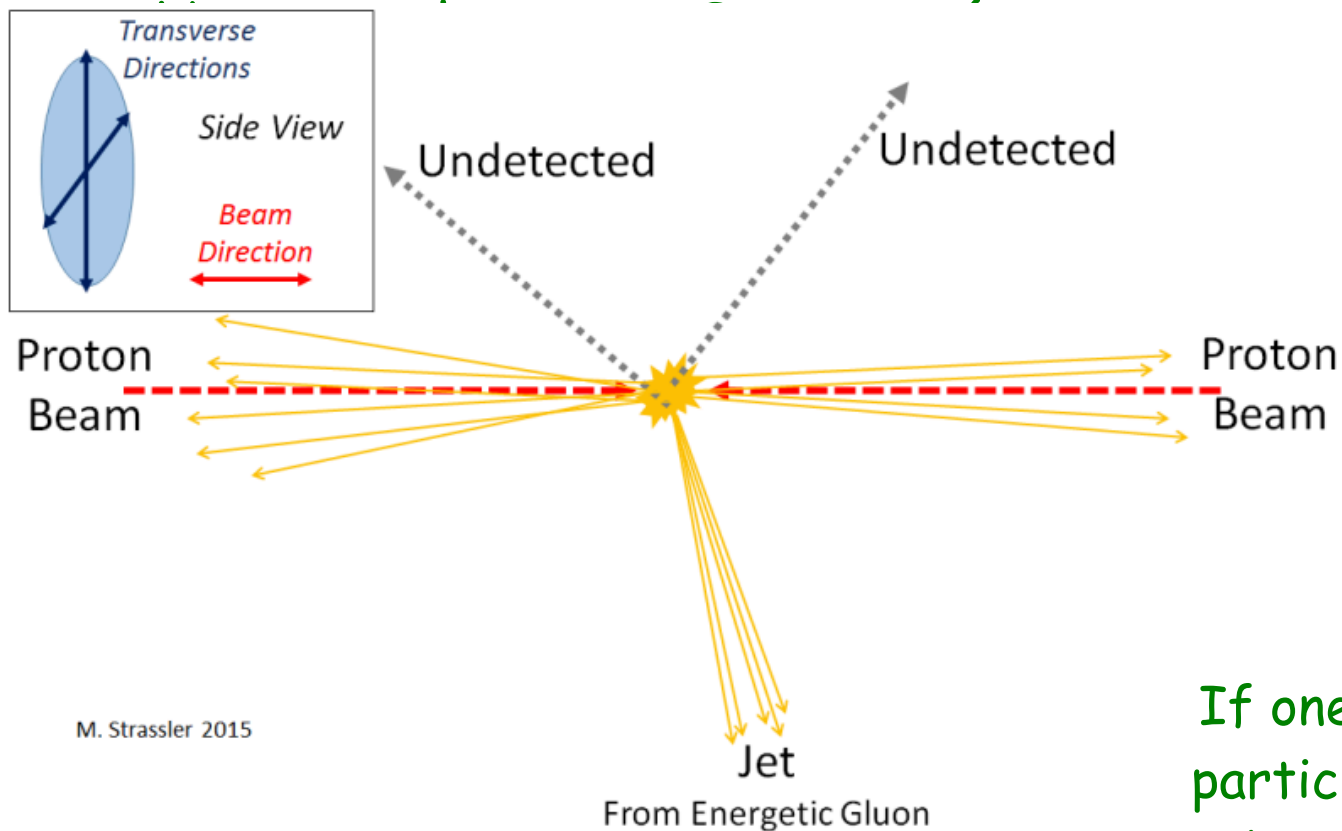
There will be MET - but still we see nothing!

Back to the LHC - Dark matter production



So the scenario where only dark matter is produced cannot simply be probed at any level.

Mono-X (X = Z, jet, Higgs...)

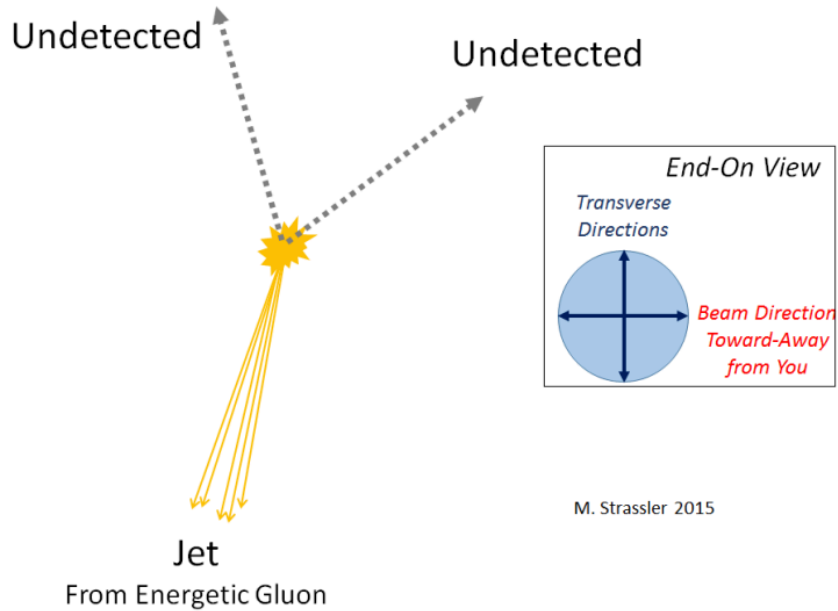


M. Strassler 2015

However, this can also be MET from neutrinos.

If one or more (high-energy) particles are also produced in the process then we have a mono-X (multi-X - still called mono-X) event! The X (for instance a jet) has a very large p_T .

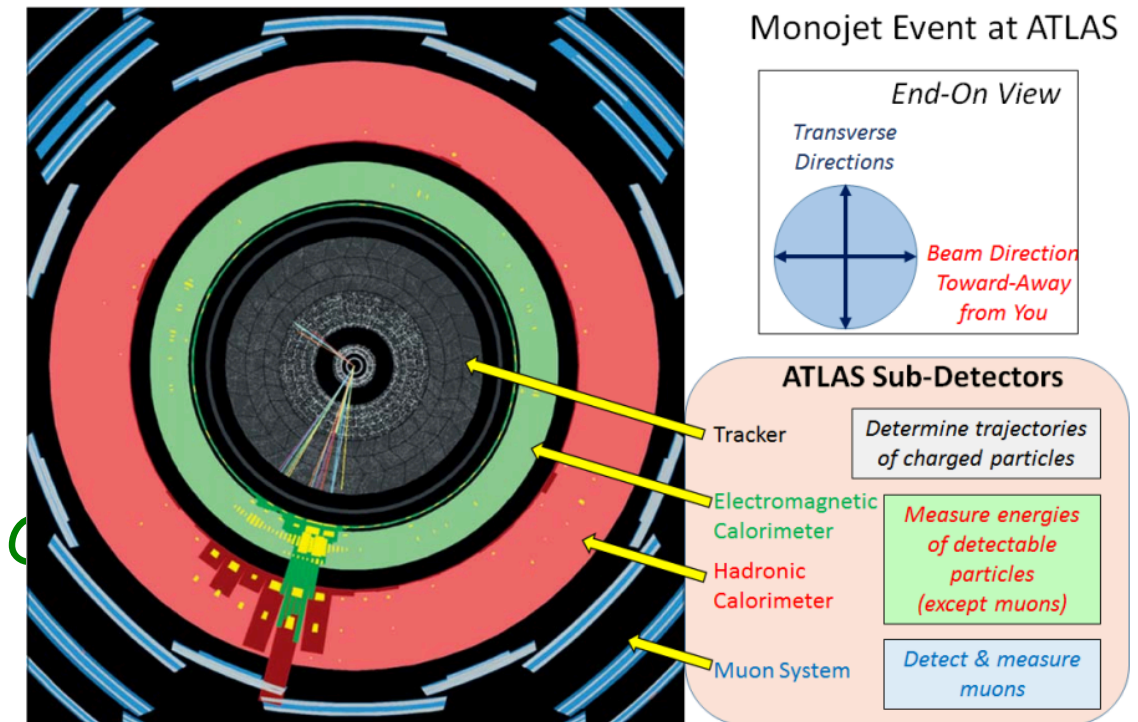
A monojet in ATLAS



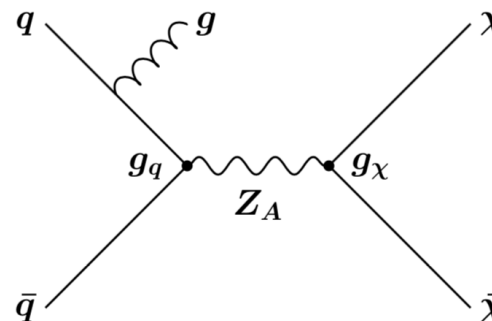
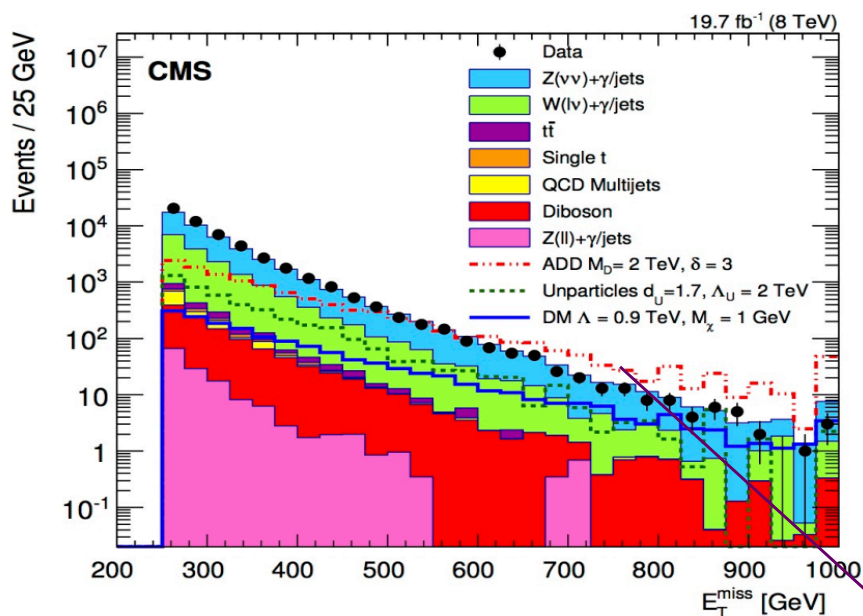
M. Strassler 2015

In the transverse plane.

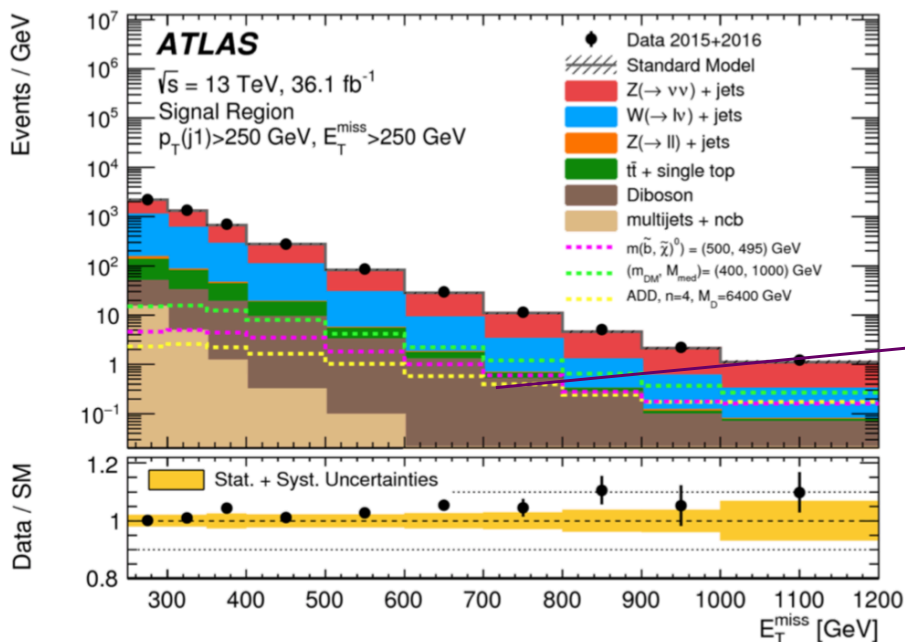
Monojet event in the ATLAS detector.



Mono-jet model interpretation in CMS

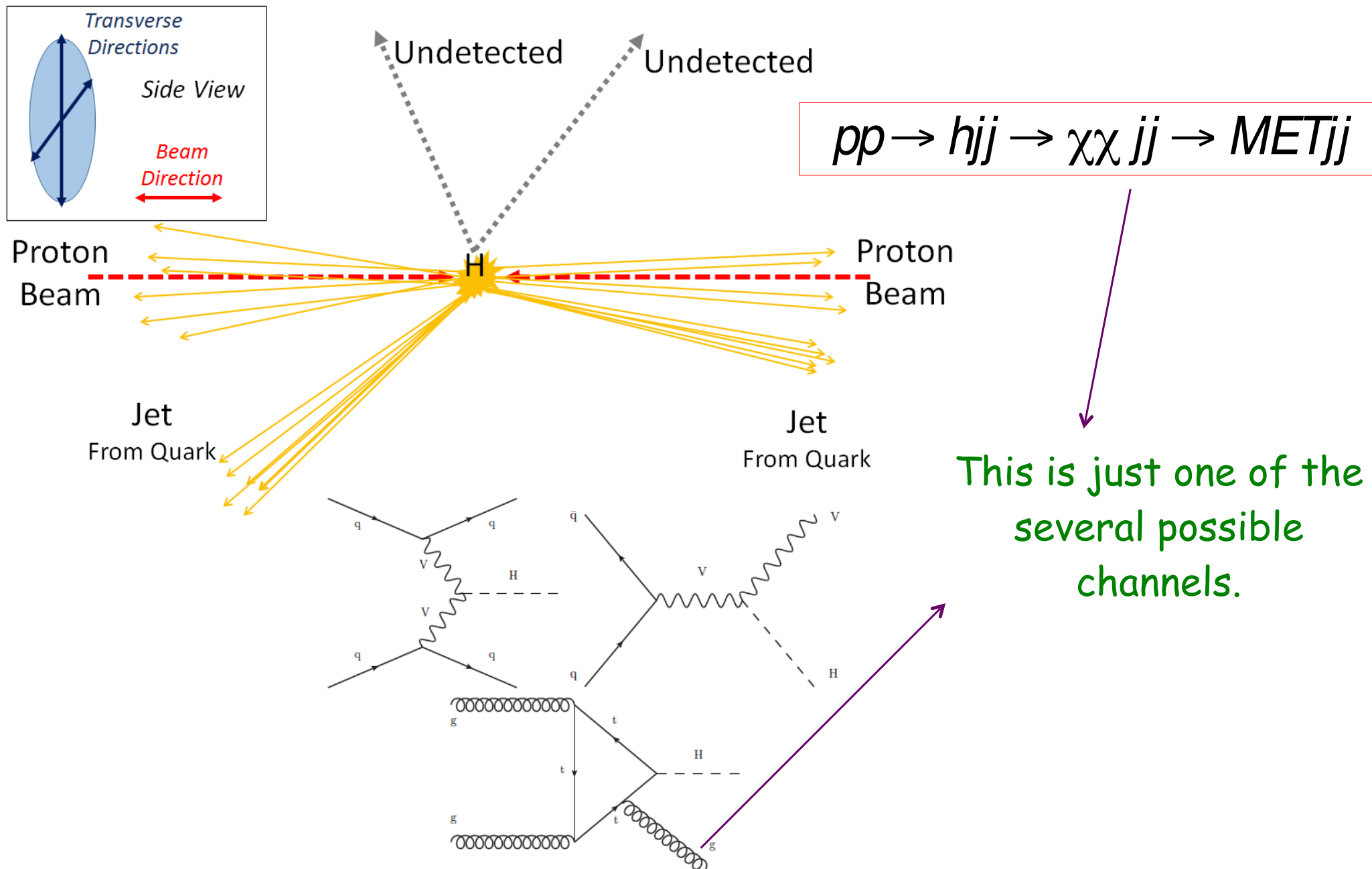


We know the SM background. This particular case is for an effective vertex with gluons.

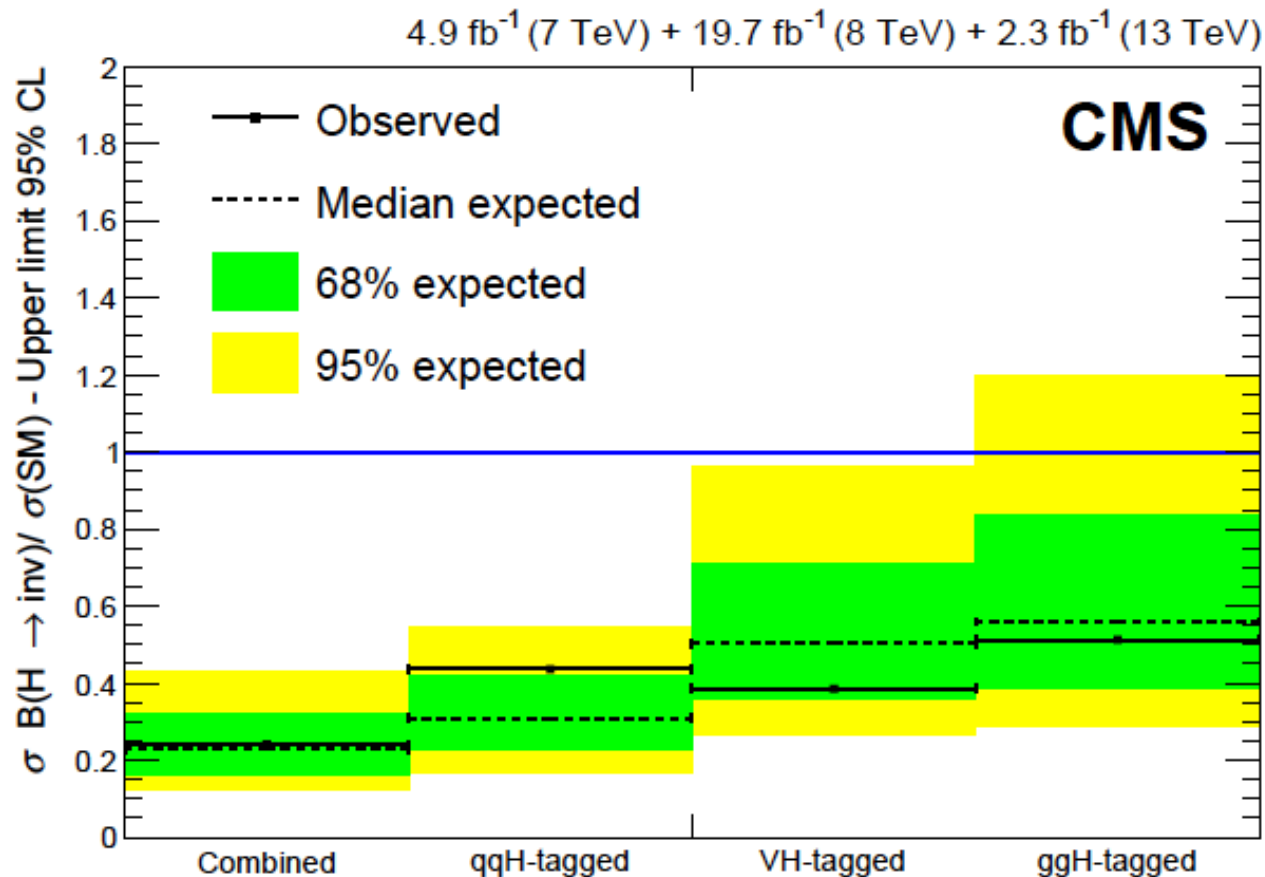


Dark matter line for a given cross section and mass of dark matter.

Another possibility



Invisible decays

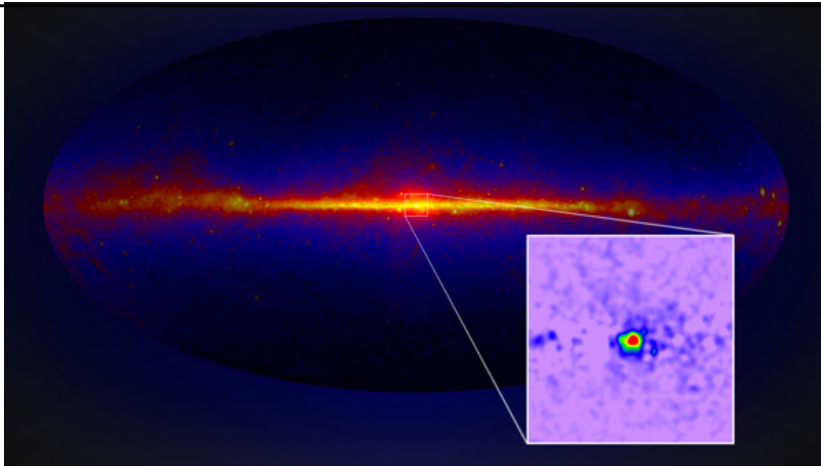


CMS results for the exclusion in the different channels

Assuming a SM production cross section for the Higgs boson, CMS obtains a limit

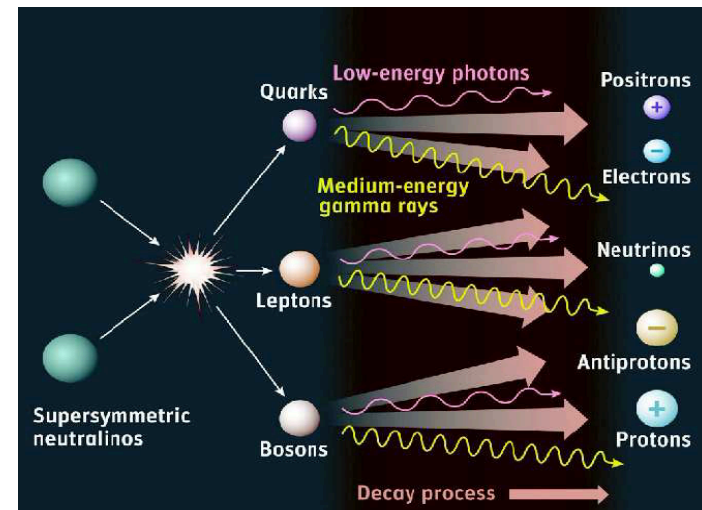
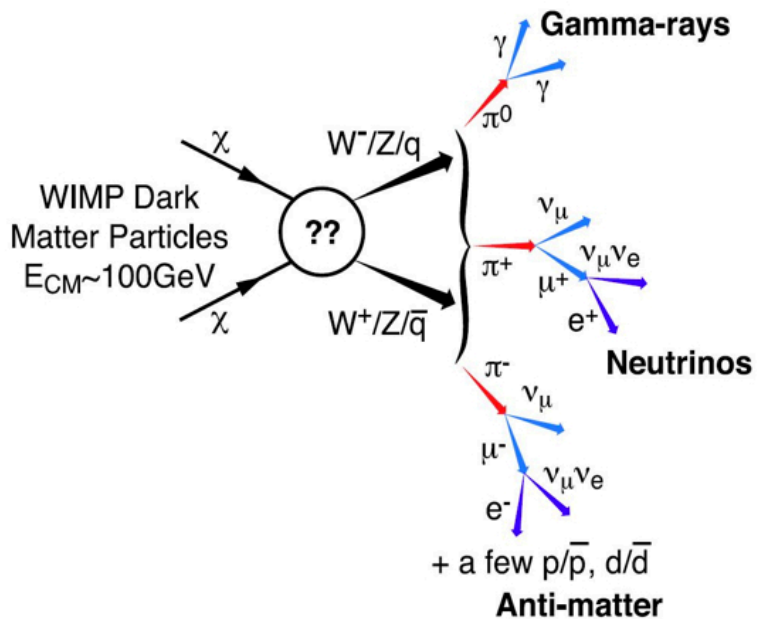
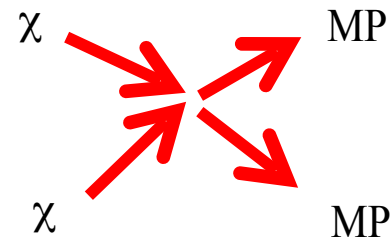
$$B(H \rightarrow \text{inv}) < 0.24 \text{ (0.23) at the 95\% CL}$$

Indirect detection

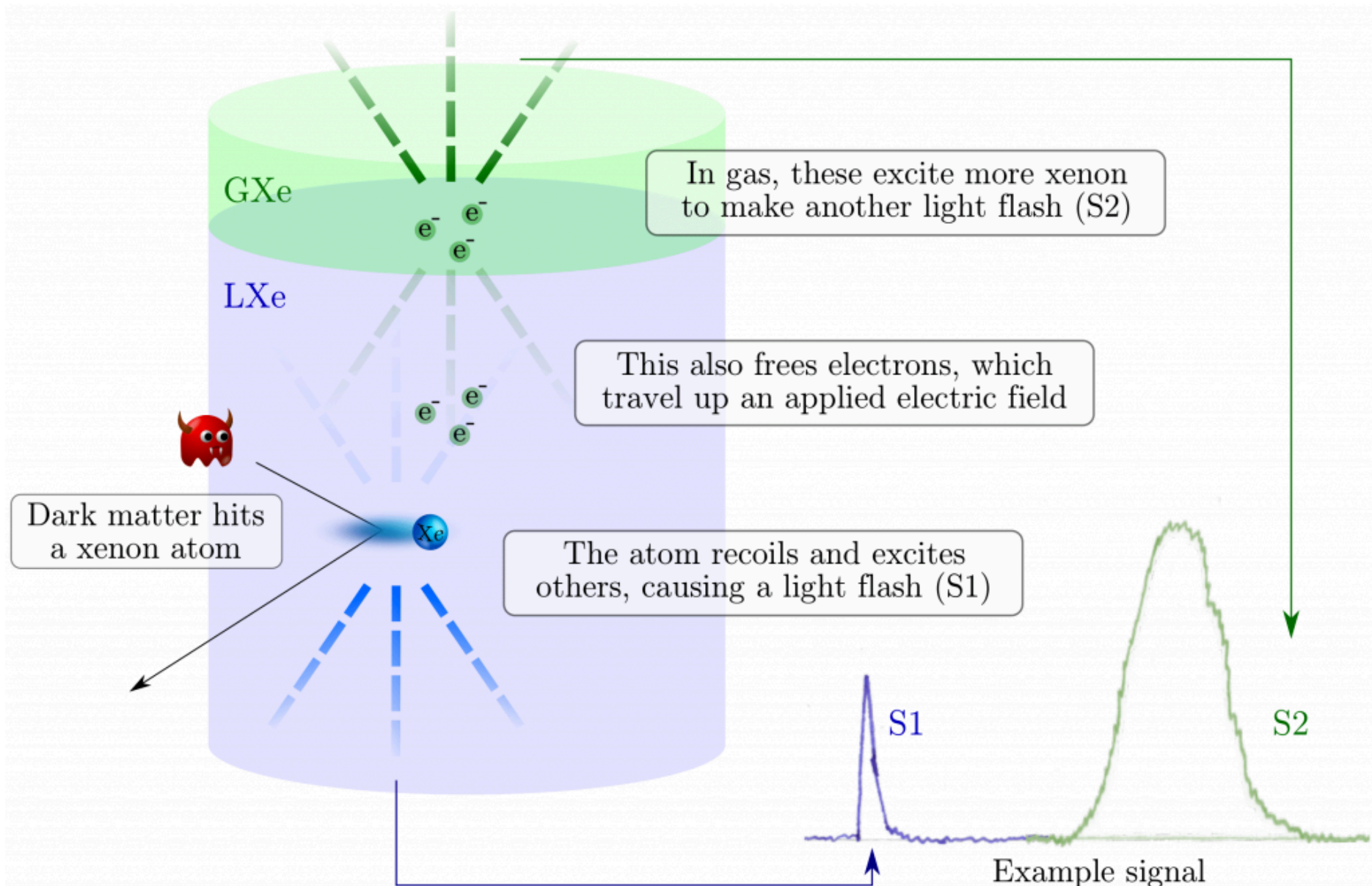


The Fermi Large Area Telescope (LAT) detects gamma radiation with energies between 0.3 and 300 GeV. It also detects electrons and positrons.

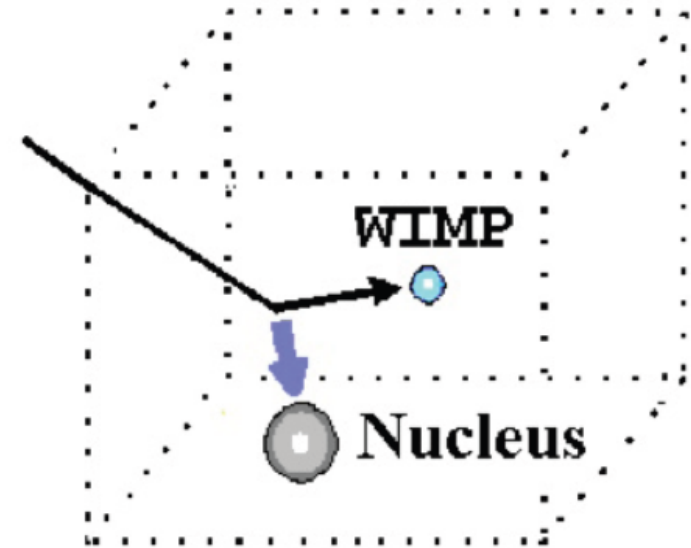
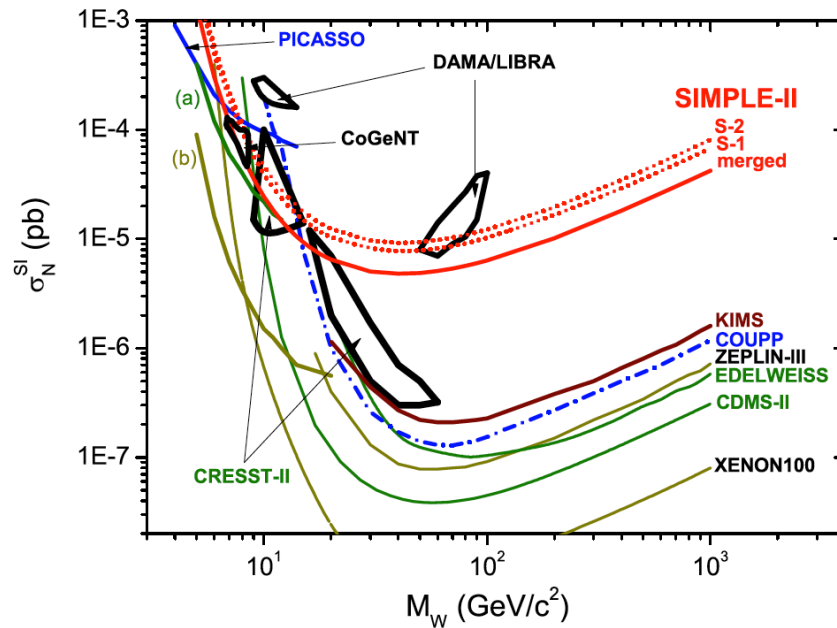
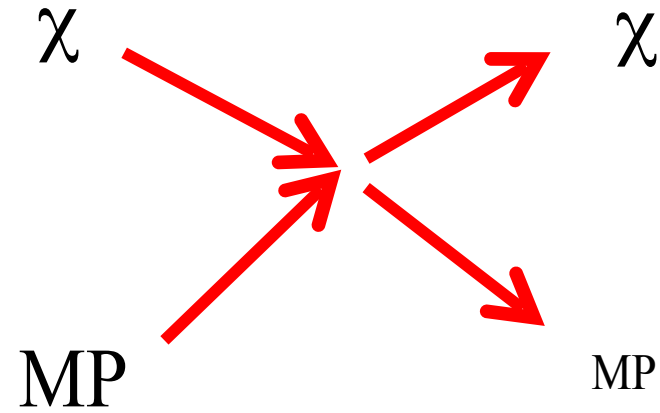
WIMPs collide producing either photons or particle anti-particle pairs.



Direct detection

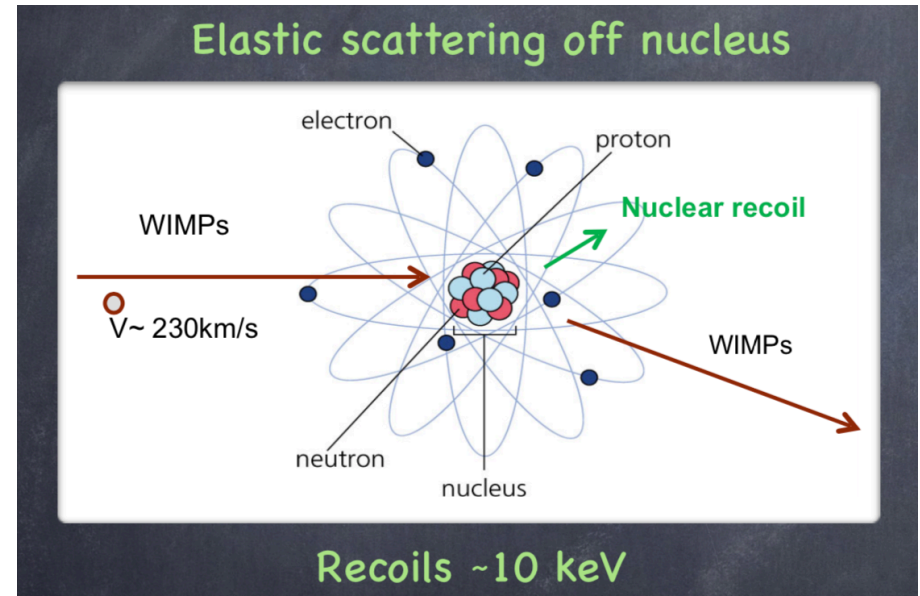
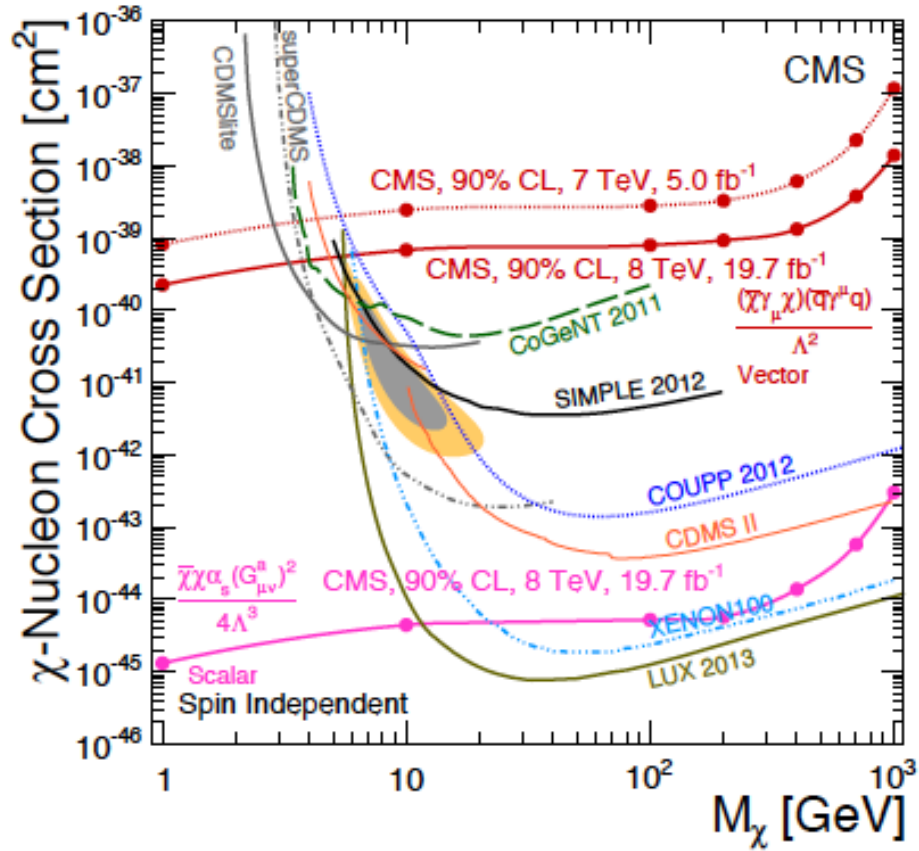


Direct detection



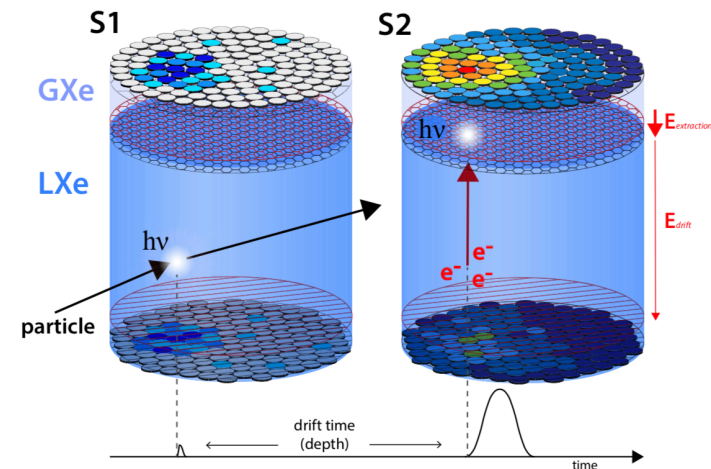
WIMP collides with nucleus - recoil energy can be measured.

Direct detection vs. LHC



Recoils ~10 keV

$$\chi N \rightarrow \chi N$$



The simplest DM models

Scalar DM Model

The spin 0 extension - real

The SM is extended by an extra real scalar singlet S . The most general Lagrangian we can write is

$$\mathcal{L} = \mathcal{L}_{SM} + \frac{1}{2}(\partial_\mu S)(\partial^\mu S) - aS - bS^2 - cS^3 - dS^4 - \kappa_1 SH^\dagger H - \kappa_2 SH^\dagger H - \mu^2 H^\dagger H - \lambda(H^\dagger H)^2$$

with (in the unitary gauge)

$$H = \begin{pmatrix} 0 \\ h \end{pmatrix}$$

If we include the Z_2 symmetry $S \rightarrow -S$, the potential reduces to

$$V_N = bS^2 + dS^4 + \kappa_1 S^2 H^\dagger H + \mu^2 H^\dagger H + \lambda(H^\dagger H)^2$$

The minimum conditions for the potential are

$$\begin{cases} \frac{\partial V}{\partial S} = 2bS + 4dS^3 + 2\kappa_1 S h^2 = 0 \\ \frac{\partial V}{\partial h} = 2h\mu^2 + 4\lambda h^3 + 2\kappa_1 S^2 h = 0 \end{cases}$$

The spin 0 extension - real

This set equation has four solutions

$$1) S = 0; h = 0; \quad 2) S = -b/(2d); h = 0; \quad 3) S = 0; h^2 = -\mu^2/(2\lambda); \quad 4) S \neq 0; h \neq 0$$

The first is the symmetric solution. So SSB does not occur. This is also true for solution 2. Solution 3 is the DM + SM one. In solution 4 the dark symmetry is broken by the vacuum.

P: Show that solution 3) has a DM candidate

P: Why doesn't SSB occur in scenario 2)?

P: Find solution 4) explicitly; find the mass eigenstates in this scenario; is there a DM candidate?

The spin 0 extension - complex

Let us now consider the extension by a complex singlet \mathbb{S} . The most general Lagrangian we can write is

$$\mathcal{L} = \mathcal{L}_{SM} + (D_\mu \mathbb{S})^\dagger (D^\mu \mathbb{S}) + \mu_S^2 |\mathbb{S}|^2 - \lambda_S |\mathbb{S}|^4 - \kappa |\mathbb{S}|^2 H^\dagger H + \mu^2 (\mathbb{S}^2 + \mathbb{S}^{*2}) \quad \mathbb{S} = \frac{1}{\sqrt{2}}(v_S + S + iA)$$

Model	Phase	VEVs at global minimum
U(1)	Higgs+2 degenerate dark	$\langle \mathbb{S} \rangle = 0$
	2 mixed + 1 Goldstone	$\langle A \rangle = 0$ (U(1) \rightarrow \mathbb{Z}'_2)
$\mathbb{Z}_2 \times \mathbb{Z}'_2$	Higgs + 2 dark	$\langle \mathbb{S} \rangle = 0$
	2 mixed + 1 dark	$\langle A \rangle = 0$ ($\mathbb{Z}_2 \times \mathbb{Z}'_2 \rightarrow \mathbb{Z}'_2$)
\mathbb{Z}'_2	2 mixed + 1 dark	$\langle A \rangle = 0$
	3 mixed	$\langle \mathbb{S} \rangle \neq 0$ (\mathbb{Z}'_2)

The spin 0 extension - complex

One particular case: black Lagrangian is U(1) symmetric. Black plus red

$$\mathcal{L} = \mathcal{L}_{SM} + (D_\mu S)^\dagger (D^\mu S) + \mu_S^2 |S|^2 - \lambda_S |S|^4 - \kappa |S|^2 H^\dagger H + \mu^2 (S^2 + S^{*2}) \quad S \rightarrow S^*$$

SM + dark matter candidate A + a new scalar that mixes with the CP-even field in the doublet such that

$$m_\pm = \lambda_H v_H^2 + \lambda_S v_S^2 \pm \sqrt{\lambda_H^2 v_H^4 + \lambda_S^2 v_S^4 + \kappa v_H^2 v_S^2 - 2\lambda_H \lambda_S v_H^2 v_S^2}$$

The mass eigenstates fields h_1 and h_2 are obtained from h and S via

$$\begin{pmatrix} h_1 \\ h_2 \end{pmatrix} = \begin{pmatrix} \cos \alpha & \sin \alpha \\ -\sin \alpha & \cos \alpha \end{pmatrix} \begin{pmatrix} h \\ S \end{pmatrix}$$

The conditions for the potential to be bounded from below are the same for the two models

$$\lambda_H > 0, \quad \lambda_S > 0, \quad \kappa > -2\sqrt{\lambda_H \lambda_S}.$$

The scalar mass matrix is

$$\mathcal{M}^2 = \begin{pmatrix} 2\lambda_H v^2 & \kappa v v_S & 0 \\ \kappa v v_S & 2\lambda_S v_S^2 & 0 \\ 0 & 0 & -4\mu^2 \end{pmatrix} \quad m_{DM} = -4\mu^2$$

Vector DM Model

A vector DM model

Dark $U(1)_X$ gauge symmetry: all SM particles are $U(1)_X$ neutral.

New complex scalar field - scalar under the SM gauge group but has unit charge under $U(1)_X$.

Lagrangian invariant under

$$X_\mu \rightarrow -X_\mu, \quad S \rightarrow S^*$$

Forbids kinetic mixing between the SM gauge boson from $U(1)_Y$ and the dark one from $U(1)_X$. The Lagrangian is

$$\mathcal{L} = \mathcal{L}_{SM} - \frac{1}{4} X_{\mu\nu} X^{\mu\nu} + (D_\mu S)^\dagger (D^\mu S) + \mu_S^2 |S|^2 - \lambda_S |S|^4 - \kappa |S|^2 H^\dagger H \quad D_\mu = \partial_\mu + ig_X X_\mu$$

with

$$H = \begin{pmatrix} G^\pm \\ \frac{1}{\sqrt{2}}(v_H + h + iG_0) \end{pmatrix} \quad S = \frac{1}{\sqrt{2}}(v_S + S + iA)$$

h is the real doublet component, S is the new real scalar component and A is the Goldstone boson related with $U(1)_X$.

P: Find the mass of the new gauge boson.

A vector DM model

With the previous definitions, the masses of the gauge bosons are

$$m_W = \frac{1}{2} g v_H; \quad m_Z = \frac{1}{2} \sqrt{g^2 + g'^2} v_H; \quad m_{DM} = g_X v_S$$

and the masses of the two scalars are

$$m_{\pm} = \lambda_H v_H^2 + \lambda_S v_S^2 \pm \sqrt{\lambda_H^2 v_H^4 + \lambda_S^2 v_S^4 + \kappa v_H^2 v_S^2 - 2\lambda_H \lambda_S v_H^2 v_S^2}$$

The mass eigenstates fields h_1 and h_2 are obtained from h and S via (and the Goldstone is eaten by the vector DM)

$$\begin{pmatrix} h_1 \\ h_2 \end{pmatrix} = \begin{pmatrix} \cos \alpha & \sin \alpha \\ -\sin \alpha & \cos \alpha \end{pmatrix} \begin{pmatrix} h \\ S \end{pmatrix}$$

I will come back to this model later.

Fermion DM model

A fermion DM model

Let us now build a model with a DM fermion. The Lagrangian is

$$\mathcal{L} = \mathcal{L}_{SM} + V_{SM} - V_{New} + \bar{\chi}(\gamma_\mu \partial^\mu - m_\chi)\chi - iy_\chi P \bar{\chi} \gamma_5 \chi + \text{scalar kinetic terms}$$

where χ is the new DM fermion for which we impose a Z_2 symmetry $\chi \rightarrow -\chi$ that is combined with $P \rightarrow P$ and $\phi_2 \rightarrow -\phi_2$ leading to the following new potential with two complex scalar doublets and one real singlet.

$$\begin{aligned} V_{New} = & m_{11}^2 |\Phi_1|^2 + m_{22}^2 |\Phi_2|^2 - m_{12}^2 (\Phi_1^\dagger \Phi_2 + h.c.) + \frac{m_S^2}{2} P^2 + \kappa (P \Phi_1^\dagger \Phi_2 + h.c.) \\ & + \frac{\lambda_1}{2} (\Phi_1^\dagger \Phi_1)^2 + \frac{\lambda_2}{2} (\Phi_2^\dagger \Phi_2)^2 + \lambda_3 (\Phi_1^\dagger \Phi_1) (\Phi_2^\dagger \Phi_2) + \lambda_4 (\Phi_1^\dagger \Phi_2) (\Phi_2^\dagger \Phi_1) \\ & + \frac{\lambda_5}{2} \left[(\Phi_1^\dagger \Phi_2)^2 + h.c. \right] + \frac{\lambda_6}{4} P^4 + \frac{\lambda_7}{2} (\Phi_1^\dagger \Phi_1) P^2 + \frac{\lambda_8}{2} (\Phi_2^\dagger \Phi_2) P^2 \end{aligned}$$

We will need an extra Z_2 symmetry $\chi \rightarrow -\chi$, to make sure that no other Yukawa terms can be built with the SM fermions.

P: Try to build one of these terms

A fermion DM model

The new dark fermion χ couples to two new fields, that come from the rotation of P and the CP -odd field from the doublet.

$$(a \cos \theta + A \sin \theta) \bar{\chi} \gamma_5 \chi$$

In turn, a and A provide the link to the remaining SM particles. So the pseudo scalar acts here as the portal.

P: Could we do this with a scalar instead of a pseudoscalar?

P: If a pseudo scalar is indeed needed, could we do this with one doublet only?

P: What are the diagrams for $pp \rightarrow \chi\chi j$? What is the background?

The spin 0 extension - complex

Let us now go back to 5th model on the list

$$\mathcal{L} = \mathcal{L}_{SM} + (D_\mu S)^\dagger (D^\mu S) + \mu_S^2 |S|^2 - \lambda_S |S|^4 - \kappa |S|^2 H^\dagger H + \mu^2 (S^2 + S^{*2}) \quad S = \frac{1}{\sqrt{2}}(v_S + S + iA)$$

Model	Phase	VEVs at global minimum
U(1)	Higgs+2 degenerate dark	$\langle S \rangle = 0$
	2 mixed + 1 Goldstone	$\langle A \rangle = 0$ ($U(1) \rightarrow \mathbb{Z}'_2$)
$\mathbb{Z}_2 \times \mathbb{Z}'_2$	Higgs + 2 dark	$\langle S \rangle = 0$
	2 mixed + 1 dark	$\langle A \rangle = 0$ ($\mathbb{Z}_2 \times \mathbb{Z}'_2 \rightarrow \mathbb{Z}'_2$)
\mathbb{Z}'_2	2 mixed + 1 dark	$\langle A \rangle = 0$
	3 mixed	$\langle S \rangle \neq 0$ (\mathbb{Z}'_2)

P: What are the diagrams for $pp \rightarrow \chi\chi j$? What is the background?

P: What are the diagrams for $\chi u \rightarrow \chi u$? And for $\chi g \rightarrow \chi g$?

P: What are the diagrams for $\chi\chi \rightarrow hh$? And for $\chi\chi \rightarrow \gamma\gamma$?

Rules for extended sectors

Extended scalar sectors

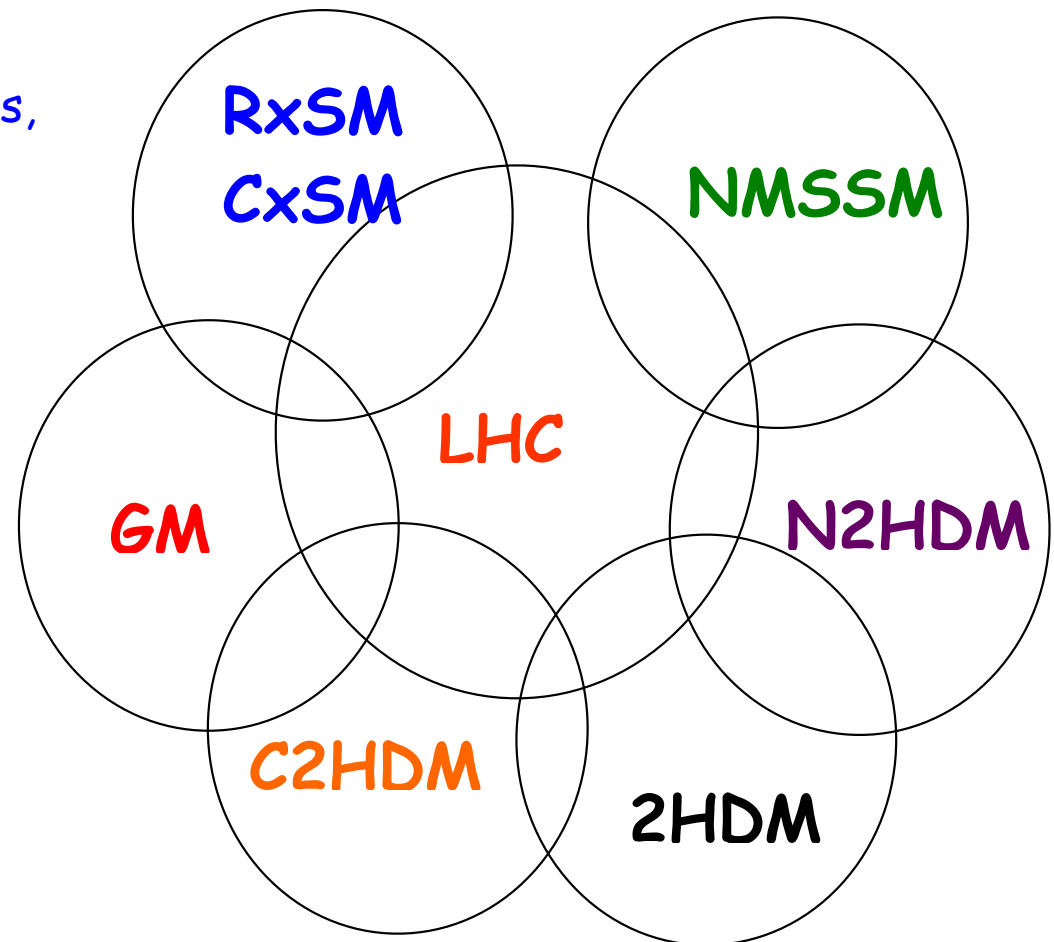
1. Direct detection of new physics - Motivate searches at the LHC in simple extensions of the scalar sector - benchmark models for searches.

2. Indirect detection of new physics (via measurements of the 125 GeV Higgs couplings)

a) Mixing effects with other Higgs bosons, e.g. singlet, doublet, CP admixtures.

b) How efficiently can the parameter space of these simple extensions be constrained through measurements of Higgs properties? Focus on CP.

c) What are higher order EW corrections (of extended models) good for?



Many simple model with new and interesting physics

	CxSM (RxSM)	2HDM	C2HDM	N2HDM
Model	SM+Singlet	SM+Doublet	SM+Doublet	2HDM+Singlet
Scalars	$h_{1,2,(3)}$ (CP even)	H, h, A, H^\pm	$H_{1,2,3}$ (no CP), H^\pm	$h_{1,2,3}$ (CP-even), A, H^\pm
Motivation	DM, Baryogenesis	+ H^\pm	+ CP violation	+ ...

Similar neutral Higgs sector but different underlying symmetries

- There is a 125 GeV Higgs (other scalars can be lighter and/or heavier).
- From the 2HDM on, $\tan \beta = v_2/v_1$. Also charged Higgs are present.
- Models (except singlet extensions) can be CP-violating.
- They all have $\rho=1$ at tree-level.
- You get a few more scalars (CP-odd or CP-even or with no definite CP)
- In case all neutral scalars mix there will be three mixing angles
- They can have dark matter candidates (or not)

Potential(s)

Potential

$$V = m_{11}^2 |\Phi_1|^2 + m_{22}^2 |\Phi_2|^2 - m_{12}^2 (\Phi_1^\dagger \Phi_2 + h.c.) + \frac{m_S^2}{2} \Phi_S^2$$

$$+ \frac{\lambda_1}{2} (\Phi_1^\dagger \Phi_1)^2 + \frac{\lambda_2}{2} (\Phi_2^\dagger \Phi_2)^2 + \lambda_3 (\Phi_1^\dagger \Phi_1) (\Phi_2^\dagger \Phi_2) + \lambda_4 (\Phi_1^\dagger \Phi_2) (\Phi_2^\dagger \Phi_1)$$

$$+ \frac{\lambda_5}{2} [(\Phi_1^\dagger \Phi_2) + h.c.] + \frac{\lambda_6}{4} \Phi_S^4 + \frac{\lambda_7}{2} (\Phi_1^\dagger \Phi_1) \Phi_S^2 + \frac{\lambda_8}{2} (\Phi_2^\dagger \Phi_2) \Phi_S^2$$

with fields

$$\Phi_1 = \begin{pmatrix} \phi_1^+ \\ \frac{1}{\sqrt{2}}(v_1 + \rho_1 + i\eta_1) \end{pmatrix} \quad \Phi_2 = \begin{pmatrix} \phi_2^+ \\ \frac{1}{\sqrt{2}}(v_2 + \rho_2 + i\eta_2) \end{pmatrix} \quad \Phi_S = v_S + \rho_S$$

magenta \implies SM

magenta + blue \implies RxSM (also CxSM)

magenta + black \implies 2HDM (also C2HDM)

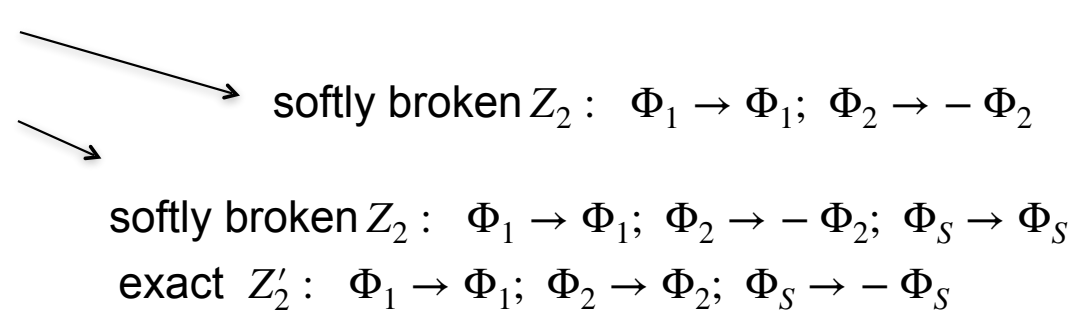
magenta + black + blue + red \implies N2HDM

• m_{12}^2 and λ_5 real 2HDM

• m_{12}^2 and λ_5 complex C2HDM

Particle (type) spectrum depends on the symmetries imposed on the model, and whether they are spontaneously broken or not. There are two charged particles and 4 neutral.

The model can be CP violating or not.



Constraints

- Should contain a SM-like Higgs boson
- Electroweak ρ parameter should be close to 1 (relation between W and Z mass)

$$\rho_{\text{exp}} = 1.0004^{+0.0003}_{-0.0004}$$

$$\rho = \frac{m_W^2}{m_Z^2 \cos^2 \theta_W} = \frac{\sum_i [4T_i(T_i + 1) - Y_i^2] |v_i|^2 c_i}{\sum_i 2Y_i^2 |v_i|^2}$$

$$Q = T_3 + Y/2$$

T_i $SU(2)_L$ Isospin

Y_i Hypercharge

v_i VEV

c_i 1(1/2) for complex (real) representations

- Perturbative unitarity
- Boundness from below

DM Direct detection

Distribution of Dark Matter in the galaxy

Hard problem - there are only averages over long volumes. There are attempts to measure locally and globally the shape of the Milky Way DM halo.

But what we really need is the kinematic distribution of DM in our solar system.

We assume the Standard Halo Model (SHM) with a density profile of $\rho(r) \sim r^{-2}$. The velocities obey a Boltzmann-Maxwell distribution. The local circular speed of DM is (218-246) Km/s. The velocity distribution is cut at the escape velocity, which is about 530 Km/s.

The prediction for the direct detection of DM on the Earth is separated into a kinematical part involving the velocity distribution and one part that deals with the collision. This allows us to compare different experiments independently of the local DM distribution.

MB distribution - system containing a large number of identical non-interacting, non-relativistic classical particles in thermodynamic equilibrium, the fraction of the particles within an infinitesimal element of the three-dimensional velocity space, centered on a velocity vector of magnitude v , is

$$f(v) d^3 v = \left(\frac{m}{2\pi kT} \right)^{3/2} e^{-\frac{mv^2}{2kT}} d^3 v,$$

Direct detection

We assume we have a WIMP that has an electroweak interaction that comes via some portal. Since the DM is coupled to a mediator (in the case of the scalar extension is the Higgs) and the mediator is coupled to the remaining SM particles, there will be an effective DM-SM interaction.

Also, we assume there is a local DM density ρ_0 in which the earth is traveling. The DM stream may interact with a nucleus and transfer a small amount of energy (recoil energy). So far no event was recorded and bounds were set on coupling vs. mass. The differential scattering can be written as

$$\frac{dR(E_R, t)}{dE_R} = N_T \frac{\rho}{m_\chi} \int_{v > v_{min}} v f(\vec{v} + \vec{v}_E(t)) \frac{d\sigma(E_R, v)}{dE_R} d^3v \quad [\sigma v n] = m^2 \frac{m}{s} \frac{1}{m^3} = \frac{1}{s}$$

where E_R is the recoil energy, N_T is the number of nuclei, v is the velocity in the rest frame of the experiment, f is the velocity distribution function and v_{min} is the minimum velocity of DM causing a recoil energy. The minimum velocity for elastic scattering is

$$v_{min} = \sqrt{\frac{m_N E_R}{2\mu^2}}, \quad \mu = \frac{m_N m_\chi}{m_N + m_\chi}$$

where m_N is the nucleon mass.

Direct detection

The differential rate can further be divided in a spin-dependent (SD) and a spin-independent (SI) part. The time integrated differential cross section is then written as

$$\frac{\sigma(E_R, \nu)}{dE_R} = \frac{m_N}{2\mu^2\nu^2} (\sigma^{SI} F_{SI}^2(E_R) + \sigma^{SD} F_{SD}^2(E_R))$$

where F are nuclear form factors. The DM velocity is non-relativistic, $\nu/c \approx 10^{-3}$, and therefore the recoil energies are low (order KeV) and the momentum transfer is of order GeV. This in turn means that nuclei cannot be treated as point-like in the scattering process with DM. The cross section with a target nucleus is

$$\sigma_i^{SI} = \frac{\mu_i}{\pi} |Z_i g_p^{SI} + (A_i - Z_i) g_n^{SI}|^2 |F_i(q)|^2$$

where i indicates the material and Z and A are the proton and mass numbers, respectively.

Now we need to find a way to link the quarks to the nucleons.

Let us see how exactly we can do this.

Intermission - EFTs

Let us go back to the Fermi theory of weak interactions, with Lagrangian

$$\mathcal{L}_{int} = \frac{G_F}{\sqrt{2}} \sum_{i,j} \bar{\psi}_i \gamma_\mu (1 - \gamma_5) \psi_i \bar{\psi}_j \gamma_\mu (1 - \gamma_5) \psi_j$$

In the electroweak theory this interaction would have been written as

$$\mathcal{L}_{int} = \frac{g^2}{8} \sum_{i,j} \bar{\psi}_i \gamma_\mu (1 - \gamma_5) \psi_i \frac{-1}{q^2 - m_W^2} \bar{\psi}_j \gamma_\mu (1 - \gamma_5) \psi_j$$

And in the limit $q^2 \ll m_W^2$ we can write

$$\mathcal{L}_{int} \approx \frac{g^2}{8m_W^2} \sum_{i,j} \bar{\psi}_i \gamma_\mu (1 - \gamma_5) \psi_i \bar{\psi}_j \gamma_\mu (1 - \gamma_5) \psi_j \quad (q^2 \ll m_W^2) \quad \frac{G_F}{\sqrt{2}} = \frac{g^2}{8m_W^2}$$

We say that we have matched the Wilson coefficient $G_F/\sqrt{2}$ to the coefficient of the actual model. This yields $G_F = 1.17 \times 10^{-5} \text{ GeV}^{-2}$. Theory works well for and energy well below the W boson mass. At higher energies one should use the proper electroweak theory.

Direct detection at LO

Write the effective Lagrangian

Wilson coefficients

$$\mathcal{L}^{\text{eff}} = \sum_{q=u,d,s} \mathcal{L}_q^{\text{eff}} + \mathcal{L}_G^{\text{eff}}$$

$$\mathcal{L}_q^{\text{eff}} = f_q \chi_\mu \chi^\mu m_q \bar{q} q + \frac{g_q}{m_\chi^2} \chi^\rho i \partial^\mu i \partial^\nu \chi_\rho \mathcal{O}_{\mu\nu}^q,$$

$$\mathcal{L}_G^{\text{eff}} = f_G \chi_\rho \chi^\rho G_{\mu\nu}^a G^{a\mu\nu}, \quad \mathcal{O}_{\mu\nu}^q = \frac{1}{2} \bar{q} i \left(\partial_\mu \gamma_\nu + \partial_\nu \gamma_\mu - \frac{1}{2} \not{\partial} \right) q.$$

Define the nucleon matrix elements

f_{Tq} denotes the fraction of the nucleon mass that is due to light quark q (lattice)

$$\langle N | m_q \bar{q} q | N \rangle = m_N f_{Tq}^N$$

$$-\frac{9\alpha_S}{8\pi} \langle N | G_{\mu\nu}^a G^{a,\mu\nu} | N \rangle = \left(1 - \sum_{q=u,d,s} f_{Tq}^N \right) m_N = m_N f_{TG}^N$$

SHIFMAN, VAINSHTEIN, ZAKHAROV, PLB78 443 (1978)

$$\langle N(p) | \mathcal{O}_{\mu\nu}^q | N(p) \rangle = \frac{1}{m_N} \left(p_\mu p_\nu - \frac{1}{4} m_N^2 g_{\mu\nu} \right) (q^N(2) + \bar{q}^N(2)),$$

fraction of the nucleon momentum carried by the quarks (PDFs)

And calculate the cross section

$$\sigma_N = \frac{1}{\pi} \left(\frac{m_N}{m_\chi + m_N} \right)^2 |f_N|^2.$$

$$f_N/m_N = \sum_{q=u,d,s} f_q f_{Tq}^N + \sum_{q=u,d,s,c,b} \frac{3}{4} (q^N(2) + \bar{q}^N(2)) g_q - \frac{8\pi}{9\alpha_S} f_{TG}^N f_G.$$

And now we need to get all the Wilson coefficients f_q, g_q, f_G at the order we are working at

Direct detection at LO for scalars

Write the effective Lagrangian

$$\mathcal{L}_{\text{eff}} = \sum_q C_S^q \mathcal{O}_S^q + C_S^g \mathcal{O}_S^g + \sum_q C_T^q \mathcal{O}_T^q$$

$$\begin{aligned} \mathcal{O}_S^q &= m_q \chi^2 \bar{q} q, \\ \mathcal{O}_S^g &= \frac{\alpha_s}{\pi} \chi^2 G_{\mu\nu}^a G^{a\mu\nu}, \\ \mathcal{O}_T^q &= \frac{1}{m_\chi^2} \chi i \partial^\mu i \partial^\nu \chi \mathcal{O}_{\mu\nu}^q. \end{aligned}$$

Quark contributions

$$\mathcal{A}_{\text{gen}} = \sum_i C_{\chi\chi h_i} C_{qq h_i} \frac{1}{q^2 - m_{h_i}^2} \bar{u}(\mathbf{p}) u(\mathbf{p} + \mathbf{q}) \xrightarrow{q^2 \rightarrow 0} - \sum_i C_{\chi\chi h_i} C_{qq h_i} \frac{1}{m_{h_i}^2} \bar{u}(\mathbf{p}) u(\mathbf{p})$$

Assuming scalar-like couplings we can write

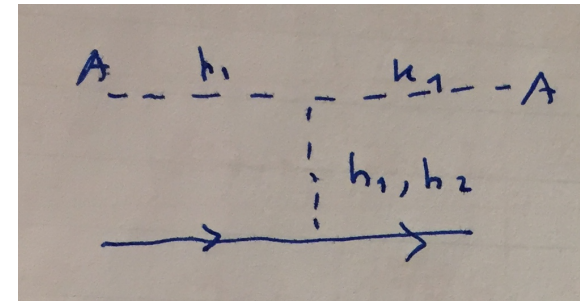
$$\mathcal{L}_{\text{eff}} \supset - \sum_i \frac{C_{\chi\chi h_i} C_{qq h_i}}{2m_{h_i}^2} \chi \chi \bar{q} q \quad \text{Term in the effective Lagrangian}$$

And so the Wilson coefficient is

$$C_S^q \supset - \sum_i \frac{C_{\chi\chi h_i} C_{qq h_i}}{2m_q m_{h_i}^2}$$

There can be additional contributions to the quark operators generated through other diagrams, even though at tree level the t-channel exchange is the only topology contributing to this operator in the models under investigation.

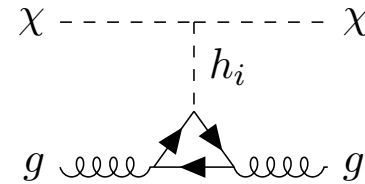
Exchanged momentum very small



Direct detection at LO for scalars

Gluon contributions

$$m_Q \bar{Q}Q \rightarrow -\frac{\alpha_s}{12\pi} G_{\mu\nu}^a G^{a\mu\nu}$$



This transformation can be used to write

$$\frac{f_N^{\text{LO}}}{m_N} = f_q^{\text{LO}} \left[\sum_{q=u,d,s} f_{T_q}^N + \sum_{q=c,b,t} \frac{2}{27} f_{T_G}^N \right]$$

And so the final cross section is

$$\sigma_N = \frac{1}{\pi} \left(\frac{m_N}{m_\chi + m_N} \right)^2 |f_N|^2.$$

And for normalisation the Wilson coefficient in a model with two scalars is

$$f_q = \frac{1}{2} \frac{g g_\chi}{m_W} \frac{\sin(2\alpha)}{2} \frac{m_{h_1}^2 - m_{h_2}^2}{m_{h_1}^2 m_{h_2}^2} m_\chi, \quad q = u, d, s, c, b, t$$

Nuclear form factors

We here present the numerical values for the nuclear form factors defined in Eq. (4.59). The values of the form factors for light quarks are taken from `micrOmegas` [75]

$$f_{T_u}^p = 0.01513, \quad f_{T_d}^p = 0.0191, \quad f_{T_s}^p = 0.0447, \quad (\text{A.99a})$$

$$f_{T_u}^n = 0.0110, \quad f_{T_d}^n = 0.0273, \quad f_{T_s}^n = 0.0447, \quad (\text{A.99b})$$

which can be related to the gluon form factors as

$$f_{T_G}^p = 1 - \sum_{q=u,d,s} f_{T_q}^p, \quad f_{T_G}^n = 1 - \sum_{q=u,d,s} f_{T_q}^n. \quad (\text{A.100})$$

The needed second momenta in Eq. (4.59) are defined at the scale $\mu = m_Z$ by using the CTEQ parton distribution functions [76],

$$u^p(2) = 0.22, \quad \bar{u}^p(2) = 0.034, \quad (\text{A.101a})$$

$$d^p(2) = 0.11, \quad \bar{d}^p(2) = 0.036, \quad (\text{A.101b})$$

$$s^p(2) = 0.026, \quad \bar{s}^p(2) = 0.026, \quad (\text{A.101c})$$

$$c^p(2) = 0.019, \quad \bar{c}^p(2) = 0.019, \quad (\text{A.101d})$$

$$b^p(2) = 0.012, \quad \bar{b}^p(2) = 0.012, \quad (\text{A.101e})$$

where the respective second momenta for the neutron can be obtained by interchanging up- and down-quark values.

Nuclear form factors

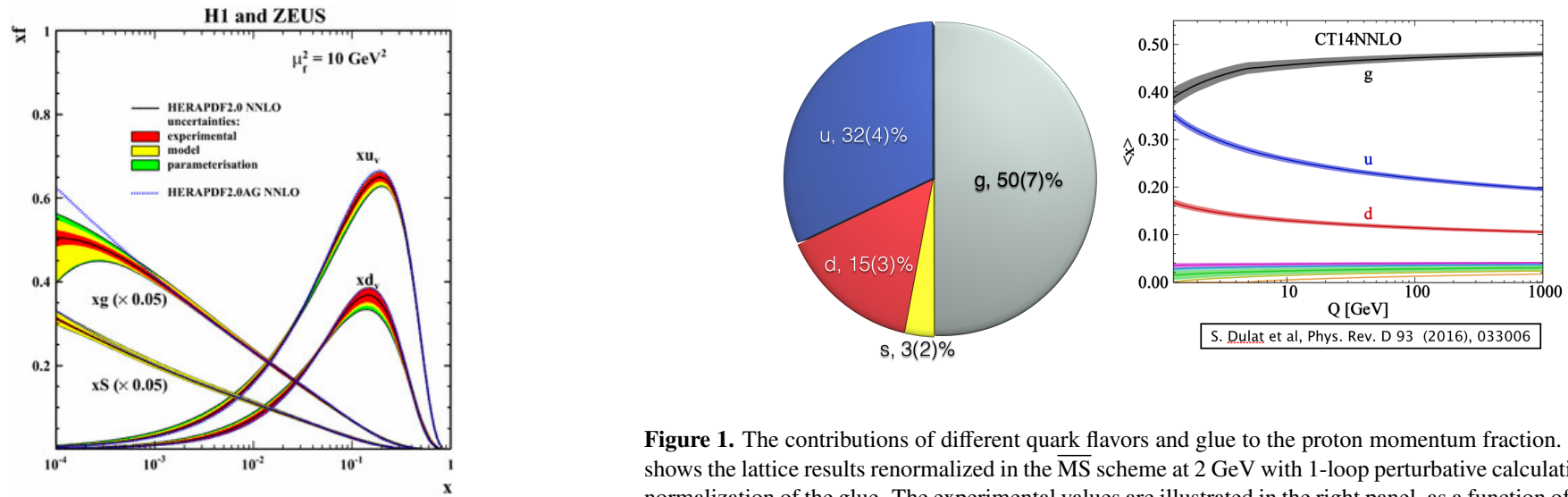


Figure 1. The contributions of different quark flavors and glue to the proton momentum fraction. The left panel shows the lattice results renormalized in the $\overline{\text{MS}}$ scheme at 2 GeV with 1-loop perturbative calculation and proper normalization of the glue. The experimental values are illustrated in the right panel, as a function of the $\overline{\text{MS}}$ scale. Our results agree with the experimental values at 2 GeV.

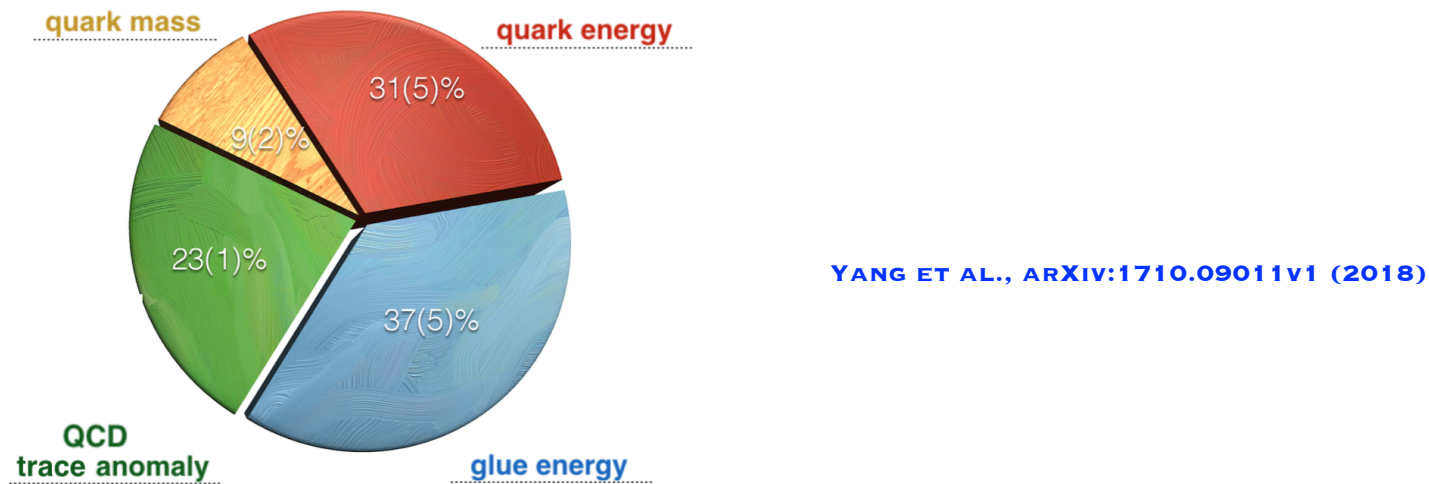


Figure 2. The pie chart of the proton mass decomposition, in terms of the quark mass, quark energy, glue field energy and trace anomaly.

The spin 0 extension - real

The SM is extended by an extra real scalar singlet S . The most general Lagrangian we can write is

$$\mathcal{L} = \mathcal{L}_{SM} + \frac{1}{2}(\partial_\mu S)(\partial^\mu S) - aS - bS^2 - cS^3 - dS^4 - \kappa_1 SH^\dagger H - \kappa_2 SH^\dagger H - \mu^2 H^\dagger H - \lambda(H^\dagger H)^2$$

And with a Z_2 symmetry $S \rightarrow -S$, the potential reduces to

$$V_N = bS^2 + dS^4 + \kappa_1 S^2 H^\dagger H + \mu^2 H^\dagger H + \lambda(H^\dagger H)^2$$

Let us consider the solution (for the minimum)

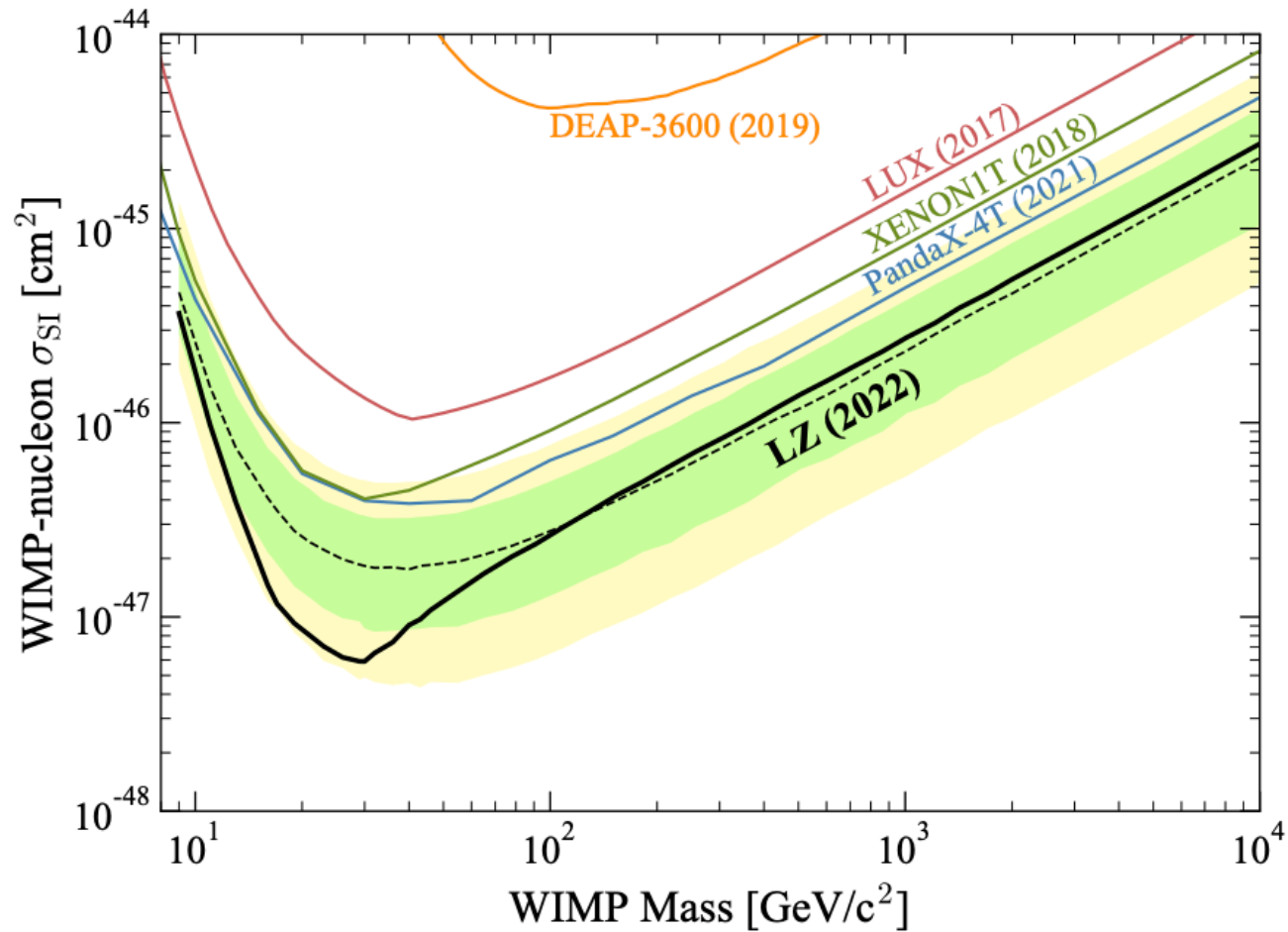
$$S = 0; h^2 = -\mu^2/(2\lambda);$$

P: Collect the relevant couplings for direct detection.

P: Calculate the amplitude.

DD measurements

This is what we have to compare to.



Back to the complex spin zero extension

Let us now consider the same process but in the complex extension. The relevant pieces of the Lagrangian are

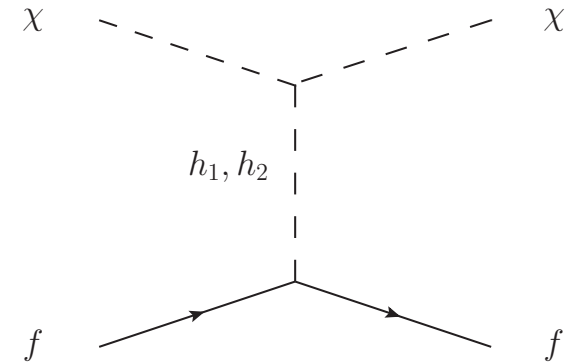
$$\mathcal{L} \supset \frac{v_s}{2} \chi^2 (\kappa_{\chi\chi h_1} h_1 + \kappa_{\chi\chi h_2} h_2)$$

$$\kappa_{\chi\chi h_1} = + m_{h_1}^2 / v_s^2 \sin \theta$$

$$\kappa_{\chi\chi h_2} = - m_{h_2}^2 / v_s^2 \cos \theta$$

And

$$\mathcal{L} \supset -(h_1 \cos \theta + h_2 \sin \theta) \sum_f \frac{m_f}{v} \bar{f} f$$



P: What is now the amplitude in the limit of zero exchanged momentum?

Direct detection at NLO

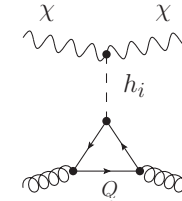
The NLO EW SI cross section can be obtained using the one-loop form factor

$$\frac{f_N^{\text{NLO}}}{m_N} = \sum_{q=u,d,s} f_q^{\text{NLO}} f_{T_q}^N + \sum_{q=u,d,s,c,b} \frac{3}{4} (q(2) + \bar{q}(2)) g_q^{\text{NLO}} - \frac{8\pi}{9\alpha_S} f_{T_G}^N f_G^{\text{NLO}}$$

with the Wilson coefficients at one-loop given by

$$\begin{aligned} f_q^{\text{NLO}} &= f_q^{\text{vertex}} + f_q^{\text{med}} + f_q^{\text{box}} \\ g_q^{\text{NLO}} &= g_q^{\text{box}} \\ f_G^{\text{NLO}} &= -\frac{\alpha_S}{12\pi} \sum_{q=c,b,t} (f_q^{\text{vertex}} + f_q^{\text{med}}) + f_G^{\text{top}} \end{aligned}$$

Box diagrams contribute to the two different quark operators.



The LO form factor is given by

$$\frac{f_N^{\text{LO}}}{m_N} = f_q^{\text{LO}} \left[\sum_{q=u,d,s} f_{T_q}^N + \sum_{q=c,b,t} \frac{2}{27} f_{T_G}^N \right]$$

And the cross section at one-loop is

$$\sigma_N = \frac{1}{\pi} \left(\frac{m_N}{m_\chi + m_N} \right)^2 [|f_N^{\text{LO}}|^2 + 2\text{Re}(f_N^{\text{LO}} f_N^{\text{NLO}*})]$$

ERTAS, KAHLHOEFER, JHEP06 052 (2019)
ABE, FUJIWARA, HISANO, JHEP 02, 028 (2019)

$$\mathcal{L}^{hhGG} = \frac{1}{2} d_G^{\text{eff}} h_i h_j \frac{\alpha_S}{12\pi} G_{\mu\nu}^a G^{a\mu\nu}$$

$$f_G^{\text{top}} = \left(d_G^{\text{eff}} \right)_{ij} C_{\Delta}^{ij} \frac{-\alpha_S}{12\pi}.$$

$$f_q = \frac{1}{2} \frac{g g_\chi}{m_W} \frac{\sin(2\alpha)}{2} \frac{m_{h_1}^2 - m_{h_2}^2}{m_{h_1}^2 m_{h_2}^2} m_\chi, \quad q = u, d, s, c, b, t$$

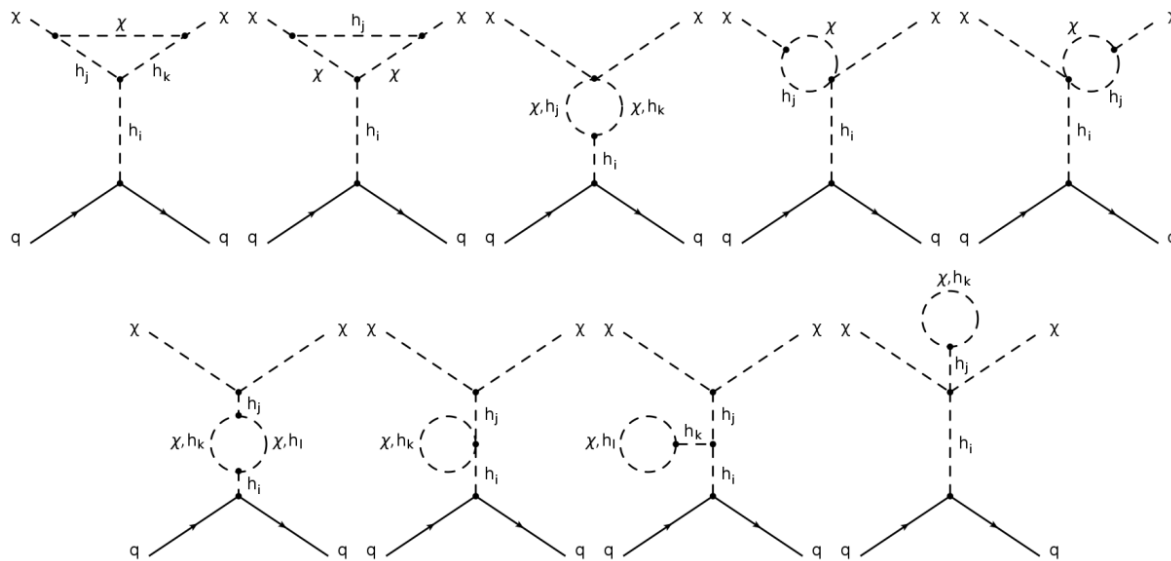
Direct detection at NLO

S2HDM - Now the SM is extended by one doublet and a complex singlet. There is an extra doublet compared to the previous model.

$$\mathcal{V} = \sum_{ij} m_{ij}^2 \phi_i^\dagger \phi_j + \sum_{ijkl} \lambda_{ijkl} \phi_i^\dagger \phi_j \phi_k^\dagger \phi_l + \sum_{ij} \kappa_{ij} |\mathbb{S}|^2 \phi_i^\dagger \phi_j - \mu_S^2 |\mathbb{S}|^2 + \lambda_S |\mathbb{S}|^4 + \mu^2 (\mathbb{S}^2 + \mathbb{S}^{*2})$$

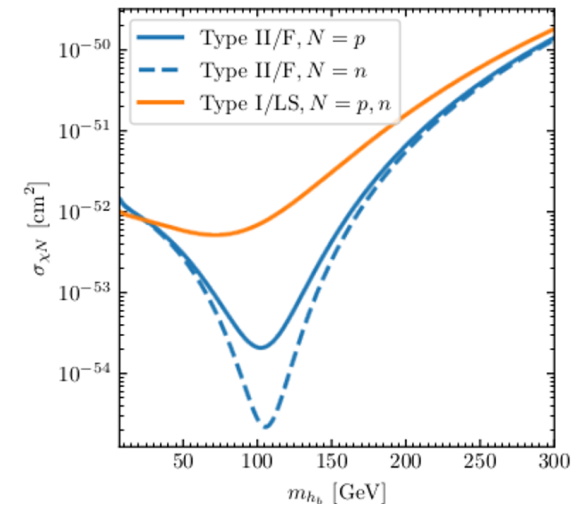
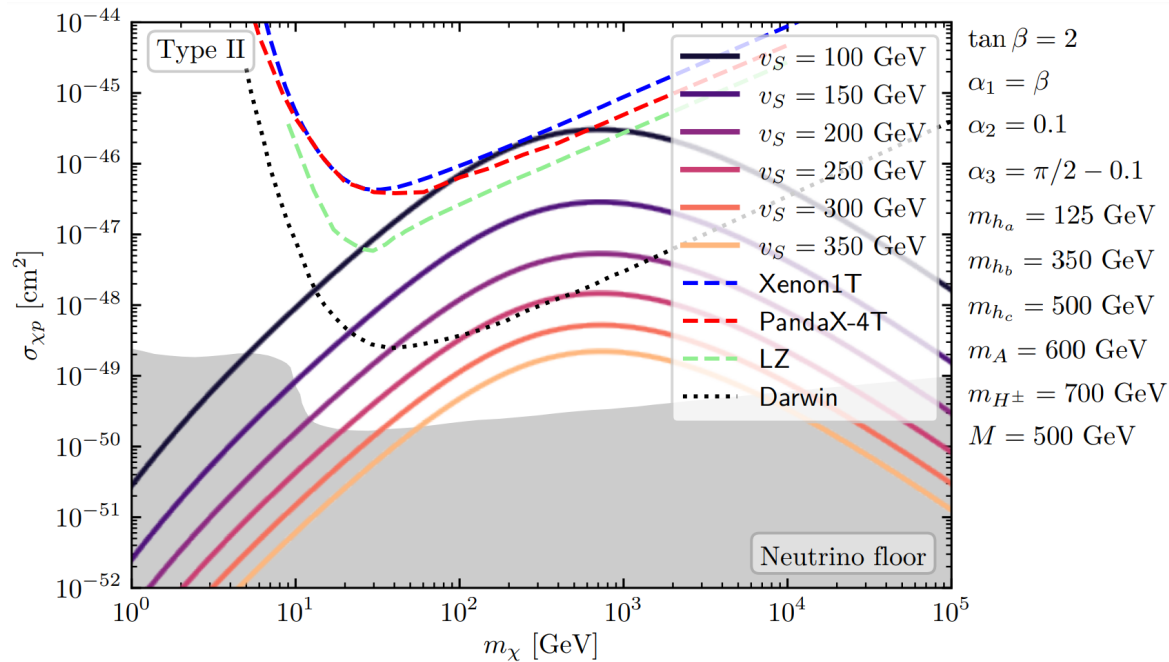
Extra particles: 2 CP-even scalars, 2 charged scalars and 1 CP-odd scalar and a DM particle. Free parameters $m_{h_{1,2,3}}, m_A, m_\chi, \alpha_{1,2,3}, \tan \beta, m_{12}^2, v_S$.

These models can lead to tree-level flavour changing neutral currents. These are very constrained by experiment. To solve this problem one usually forces the Yukawa Lagrangian to be invariant under a Z_2 symmetry. This leads to 4 possible Yukawa Lagrangians (the way scalars are combined with fermions).



Diagrams that survive. Same type of diagrams as for the CxSM but with more particles in the loop.

Direct detection at NLO



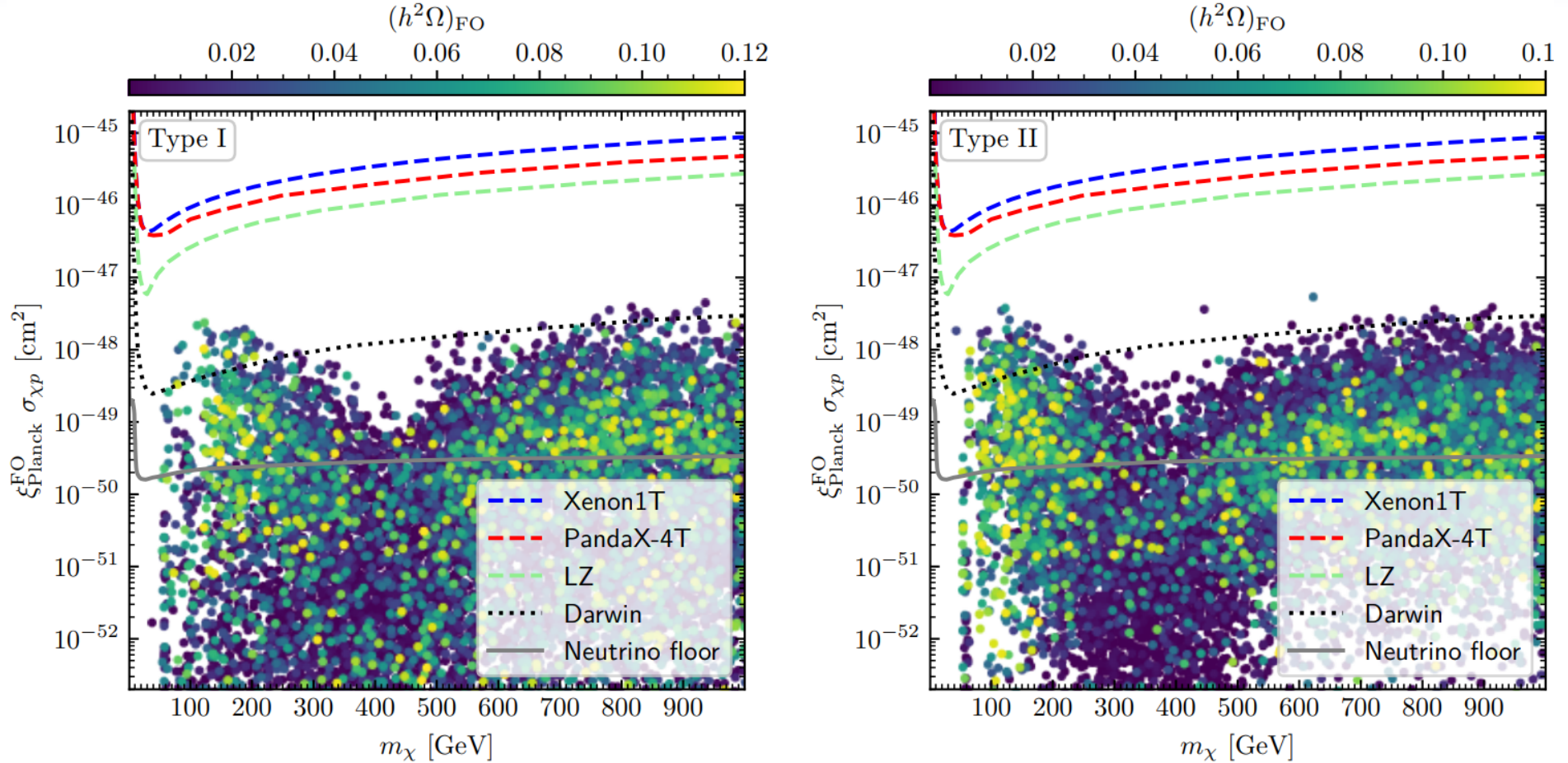
Type dependent blind-spots

Here we just fixed all input parameters except for the VEV of the singlet. The behaviour is similar for all values of the singlet VEV but as the VEV gets smaller a larger mass region in the WIMP region is excluded.

We also show Darwin as an example of some future projection. This is the total cross section.

Direct detection at NLO

Experimental prospect for direct detection in Types I and II



Type	m_{h_a}	$m_{h_b}, m_{h_c}, m_A, m_\chi$	m_{H^\pm}	$\alpha_{1,2,3}$	$\tan \beta$	M	v_S	
I	125.09	[30,1000]	[150,1000]	$[-\pi/2, \pi/2]$	[1.5,10]	[20, 1000]	[30,1000]	
Type	m_{h_a}	m_{h_b}, m_A	m_{H^\pm}	$m_{h_c, \chi}$	$\alpha_{1,2,3}$	$\tan \beta$	M	v_S
II	125.09	[200,1000]	[650,1000]	[30,1000]	$[-\pi/2, \pi/2]$	[1.5,10]	[450, 1000]	[30,1000]

Scalar DM but more interesting

Peculiar Scalar extensions of the SM

Some models have negligible dark matter direct detection (DD) cross section at zero momentum transfer (at leading order). **Barely affected by direct detection bounds.**

True for models with a pNG dark matter candidate with origin in a potential of the form

$$\mathcal{V} = \sum_{ij} m_{ij}^2 \phi_i^\dagger \phi_j + \sum_{ijkl} \lambda_{ijkl} \phi_i^\dagger \phi_j \phi_k^\dagger \phi_l + \sum_{ij} \kappa_{ij} |\mathbb{S}|^2 \phi_i^\dagger \phi_j - \mu_S^2 |\mathbb{S}|^2 + \lambda_S |\mathbb{S}|^4 + \mu^2 (\mathbb{S}^2 + \mathbb{S}^{*2})$$

with

$$\phi_i = \begin{pmatrix} c^\pm \\ \frac{1}{\sqrt{2}}(v_i + a_i + ib_i) \end{pmatrix} \quad \mathbb{S} = \frac{1}{\sqrt{2}}(v_S + S + iA)$$

which is a model with N Higgs Doublet Model plus a complex singlet.

The potential is invariant under

$$\mathbb{S} \rightarrow \mathbb{S}^* \quad \text{Stabilises } A$$

and without the red term it is also invariant under

$$\mathbb{S} \rightarrow e^{i\alpha} \mathbb{S}$$

The soft breaking term gives mass to the pNG dark matter.

One doublet and one complex singlet (CxSM)

The SM is extended by an extra complex scalar singlet \mathbb{S} which has a global U(1) symmetry

$$\mathbb{S} \rightarrow e^{i\alpha}\mathbb{S}$$

Softly break dark U(1) symmetry to the residual Z_2 symmetry in one of the singlet components

$$\mathcal{L} = \mathcal{L}_{SM} + (D_\mu \mathbb{S})^\dagger (D^\mu \mathbb{S}) + \mu_S^2 |\mathbb{S}|^2 - \lambda_S |\mathbb{S}|^4 - \kappa |\mathbb{S}|^2 H^\dagger H + \mu^2 (\mathbb{S}^2 + \mathbb{S}^{*2}) \quad \mathbb{S} \rightarrow \mathbb{S}^*$$

SM + dark matter candidate A + a new scalar that mixes with the CP-even field in the doublet such that

$$m_\pm = \lambda_H v_H^2 + \lambda_S v_S^2 \pm \sqrt{\lambda_H^2 v_H^4 + \lambda_S^2 v_S^4 + \kappa v_H^2 v_S^2 - 2\lambda_H \lambda_S v_H^2 v_S^2}$$

The mass eigenstates fields h_1 and h_2 are obtained from h and S via

$$\begin{pmatrix} h_1 \\ h_2 \end{pmatrix} = \begin{pmatrix} \cos \alpha & \sin \alpha \\ -\sin \alpha & \cos \alpha \end{pmatrix} \begin{pmatrix} h \\ S \end{pmatrix}$$

The conditions for the potential to be bounded from below are the same for the two models

$$\lambda_H > 0, \quad \lambda_S > 0, \quad \kappa > -2\sqrt{\lambda_H \lambda_S}.$$

The scalar mass matrix is

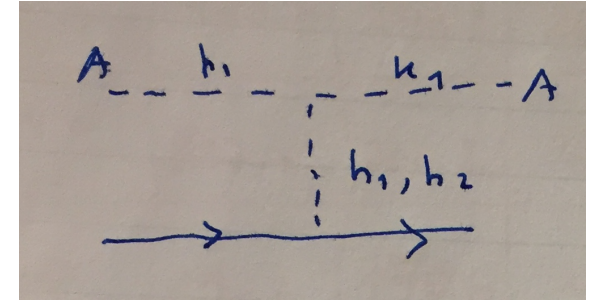
$$\mathcal{M}^2 = \begin{pmatrix} 2\lambda_H v^2 & \kappa v v_S & 0 \\ \kappa v v_S & 2\lambda_S v_S^2 & 0 \\ 0 & 0 & -4\mu^2 \end{pmatrix}$$

$$m_{DM} = -4\mu^2$$

One doublet and one complex singlet (CxSM)

The amplitude for the DM direct detection cross section

$$i\mathcal{M} \sim \sin\alpha \cos\alpha \left(\frac{im_{h_2}^2}{t - m_{h_2}^2} - \frac{im_{h_1}^2}{t - m_{h_1}^2} \right) \left(\frac{-im_f}{v} \right) \bar{u}_f(k_2)u_f(p_2) \sim 0 \quad (t \rightarrow 0)$$



And it **vanishes for zero momentum transfer**. Why? Going back to the Lagrangian,

$$\mathcal{L} = \mathcal{L}_{SM} + (D_\mu S)^\dagger (D^\mu S) + \mu_S^2 |S|^2 - \lambda_S |S|^4 - \kappa |S|^2 H^\dagger H + \mu^2 (S^2 + S^{*2}) \quad S \rightarrow S^*$$

Writing

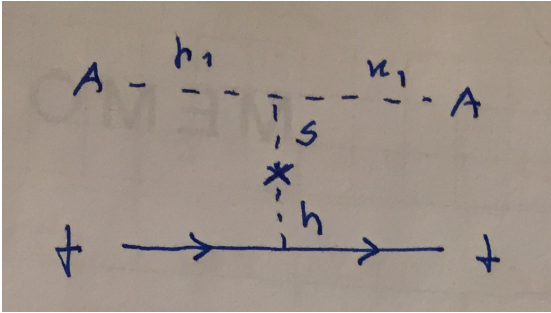
$$S = \frac{v_S + S}{\sqrt{2}} e^{i\frac{A}{v_S}} \Rightarrow V_{soft} = -\mu^2 (v_S + S)^2 \cos\left(\frac{2A}{v_S}\right) = -\mu^2 (v_S + S)^2 \left(1 - \frac{2A^2}{v_S^2}\right) + \dots$$

Including the kinetic term leads to the following Lagrangian interaction

$$\mathcal{L}_{SA^2} = \frac{1}{2v_S} (\partial^2 S) A^2 - \frac{1}{v_S} S A (\partial^2 + m_A^2) A$$

First term proportional to p^2 of S and the second term vanishes when the DM particle is on-shell. Amplitude is proportional to p^2 with A on-shell.

One doublet and one complex singlet (CxSM)



$$i\mathcal{M} \sim \left(\frac{-it}{v_S} \right) \frac{i}{t - m_S^2} (-i2\lambda_{SH} v v_S) \frac{i}{t - m_h^2} \left(\frac{-im_f}{v} \right) \bar{u}_f(k_2) u_f(p_2)$$

Which vanishes when $t = 0$

Note however if other soft breaking terms are added

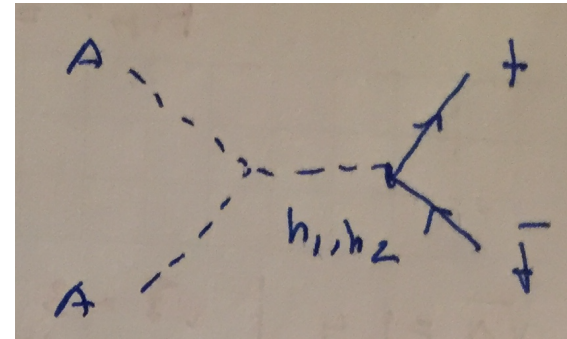
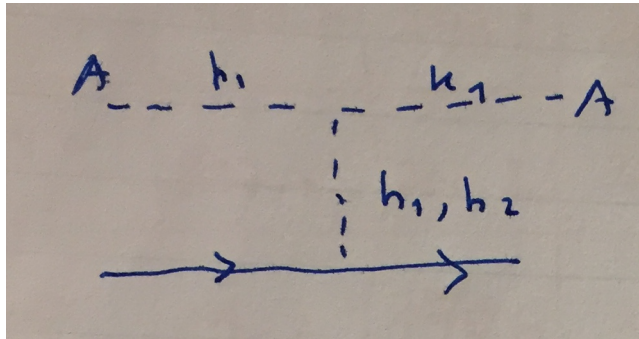
$$V'_{soft} = -\kappa_1^3 (S + S^*) - \kappa_2 |S|^2 (S + S^*) - \kappa_3 (S^3 + S^{*3})$$

the cancellation is lost except for fine-tuned values of the couplings

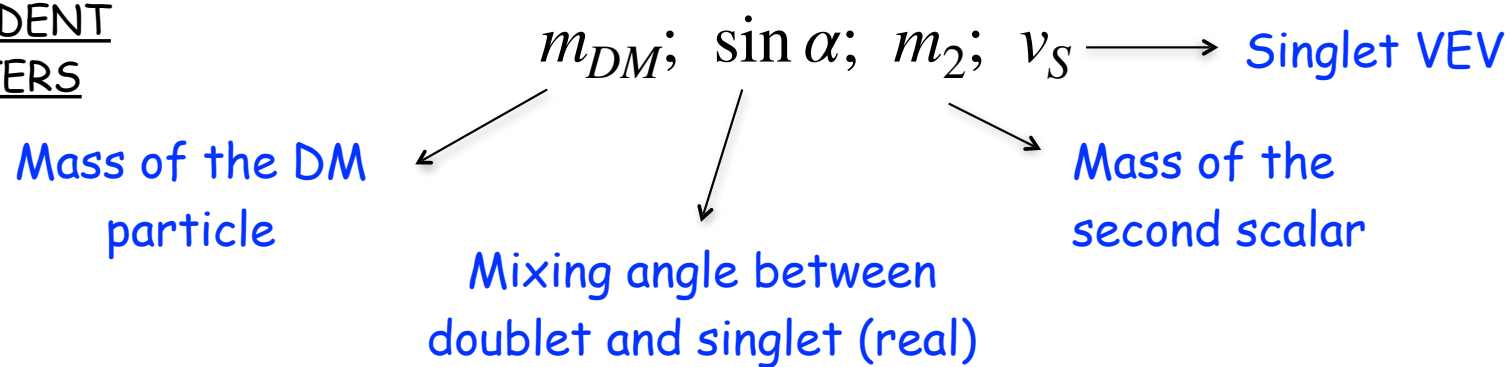
$$\kappa_1^3 = \frac{1}{2}(\kappa_2 + 9\kappa_3)v_S^2$$

One doublet and one complex singlet (CxSM)

Note that the cancellation does not happen in scattering



INDEPENDENT
PARAMETERS



There is obviously a 125 GeV Higgs (other scalar can be lighter or heavier).
Experimental and theoretical constraints included.

DM - scalar vs. vector

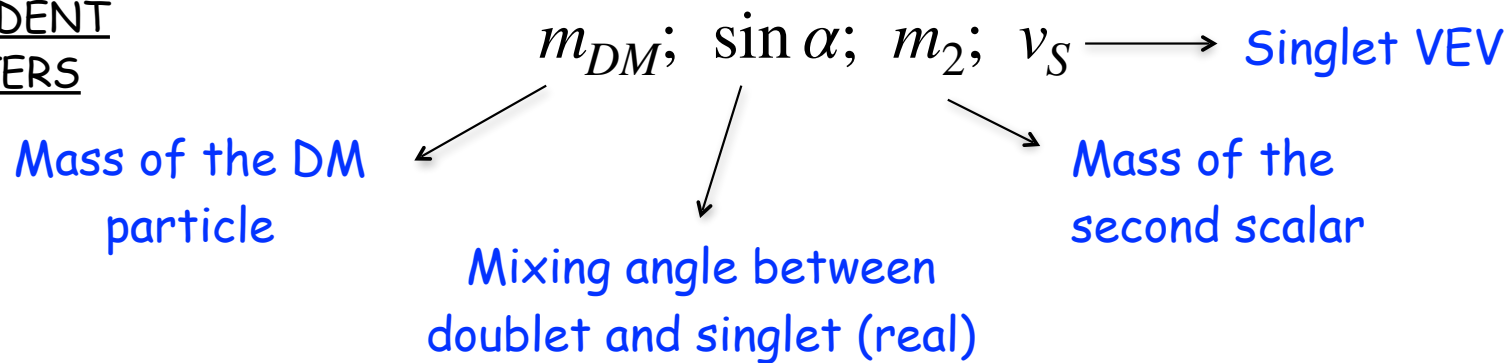
Scalar vs. vector

PARTICLE CONTENT

VDM: SM + vector dark matter + new scalar

SDM: SM + scalar dark matter + new scalar

INDEPENDENT PARAMETERS



Parameter	Range
SM-Higgs— m_1	125.09 GeV
Second Higgs— m_2	[1,1000] GeV
DM— m_{DM}	[1,1000] GeV
Singlet VEV— v_s	[1,10 ⁷] GeV
Mixing angle— α	$[-\frac{\pi}{4}, \frac{\pi}{4}]$

There is obviously a 125 GeV Higgs (other scalar can be lighter and heavier).

Experimental and theoretical constraints to be discussed next

Scalar vs. vector

Theoretical and collider constraints:

Points generated with ScannerS requiring

- absolute minimum
- boundedness from below
- that perturbative unitarity holds
- S, T and U

Signal strength: gives a constraint on $\cos\alpha$

Searches: BR of Higgs to invisible below 24%

Searches: for extra scalars imposed via HiggsBounds which gives a bound that is a function of the new scalar mass and $\cos\alpha$

Scalar vs. vector

Cosmological constraints:

DM abundance: we require

$$(\Omega h^2)_{DM} < 0.1186 \quad [\text{Calculated with MicroOmegas}]$$

or to be in the 5σ allowed interval from the Planck collaboration measurement

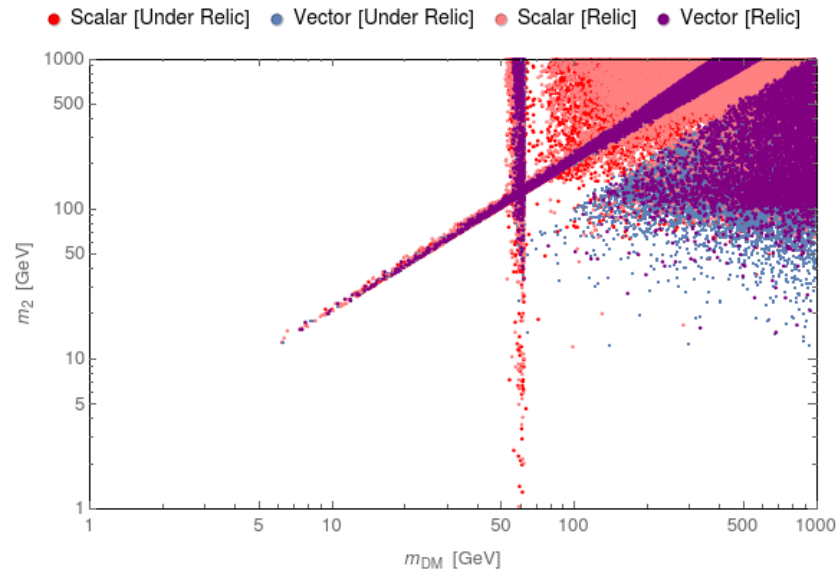
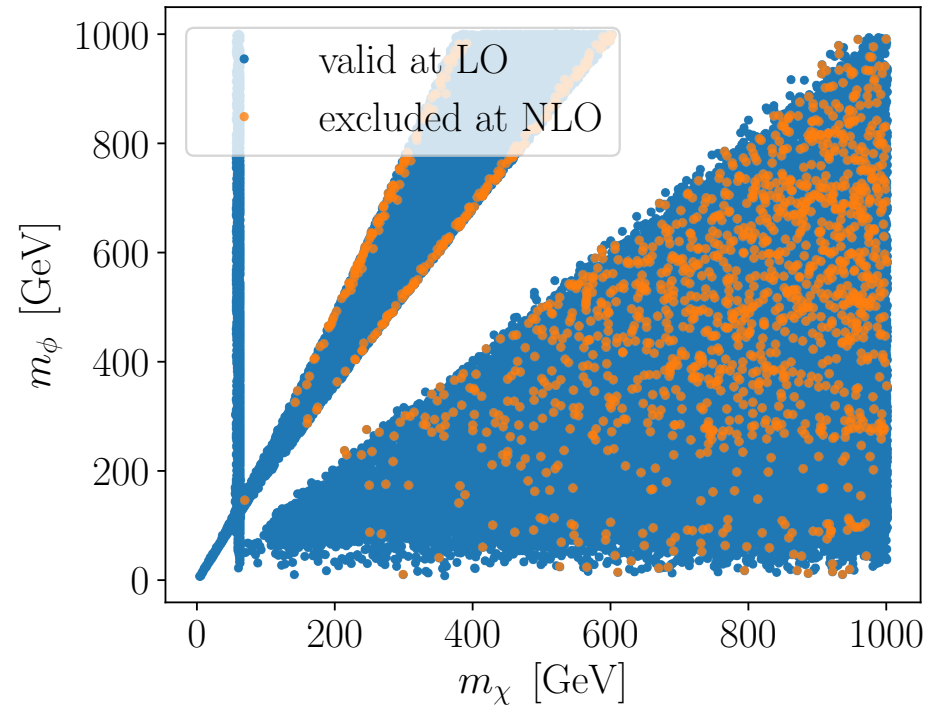
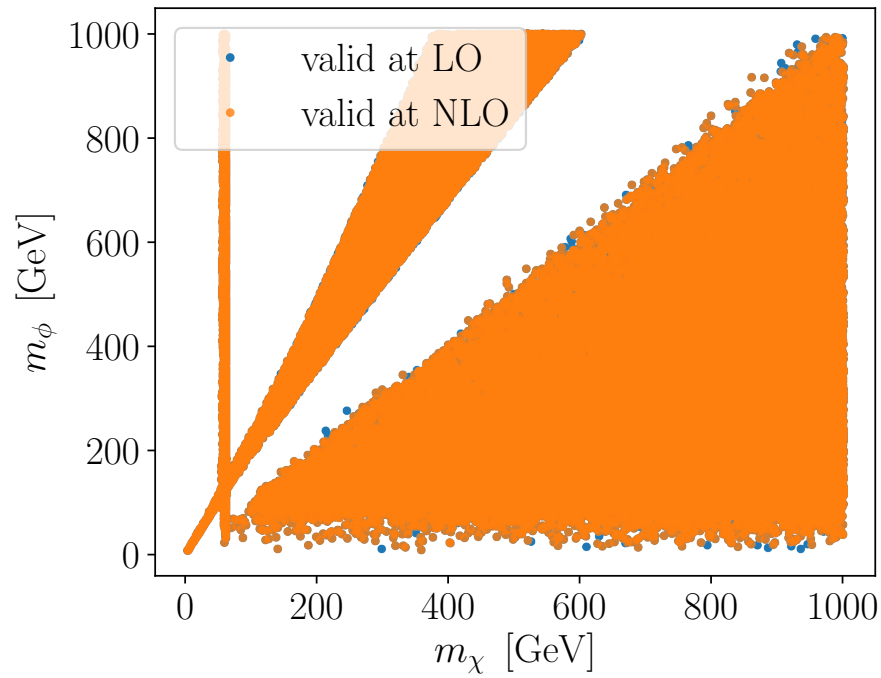
$$(\Omega h^2)_{DM}^{obs} = 0.1186 \pm 0.0020$$

Direct detection: we apply the latest XENON1T bounds

$$\sigma_{DM,N}^{eff} = f_{DM} \sigma_{DM,N} \quad \text{with} \quad f_{DM} = \frac{(\Omega h^2)_{DM}}{(\Omega h^2)_{DM}^{obs}} \quad [\text{Fraction contributing to the scattering}]$$

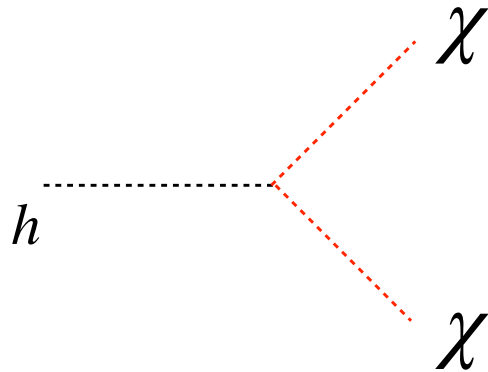
Indirect detection: for the DM range of interest, the Fermi-LAT upper bound on the dark matter annihilation from dwarfs is the most stringent. We use the Fermi-LAT bound on bb.

Scalar vs. vector



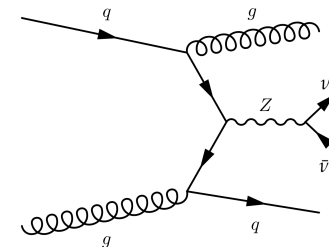
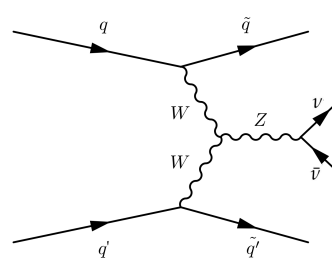
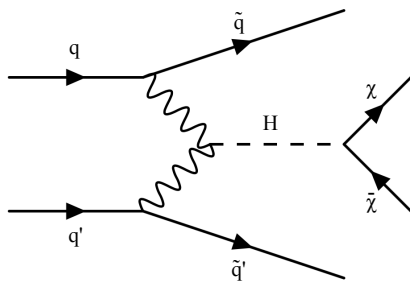
Back to colliders
- the Higgs invisible width

Back to colliders - Higgs invisible width



If the dark matter particle has a mass that is below half of Higgs mass, the Higgs can decay to a dark matter pair.

One of the many on-going searches is



The result gives us a bound on the BR of the Higgs to invisible

$$BR(h \rightarrow \chi\chi) = \frac{\Gamma(h \rightarrow \chi\chi)}{\Gamma_T(h)} \quad \Gamma_T(h) \approx 4.6 \text{ MeV}$$

Back to colliders - Higgs invisible width

The width is calculated using

49.4.2 Two-body decays

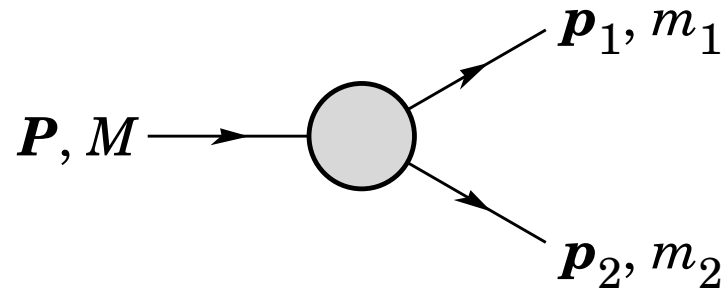


Figure 49.1: Definitions of variables for two-body decays.

In the rest frame of a particle of mass M , decaying into 2 particles labeled 1 and 2,

$$E_1 = \frac{M^2 - m_2^2 + m_1^2}{2M}, \quad (49.16)$$

$$|\mathbf{p}_1| = |\mathbf{p}_2| = \frac{1}{2M} \sqrt{\lambda(M^2, m_1^2, m_2^2)}, \quad (49.17)$$

and

$$d\Gamma = \frac{1}{32\pi^2} |\mathcal{M}|^2 \frac{|\mathbf{p}_1|}{M^2} d\Omega, \quad (49.18)$$

where $\lambda(\alpha, \beta, \gamma) = \alpha^2 + \beta^2 + \gamma^2 - 2\alpha\beta - 2\alpha\gamma - 2\beta\gamma$ is the Källén function and $d\Omega = d\phi_1 d(\cos \theta_1)$ is the solid angle of particle 1. The invariant mass M can be determined from the energies and momenta using Eq. (49.2) with $M = E_{\text{cm}}$.

Back to colliders - Higgs invisible width

Now calculate the invisible BR for the three models

Scalar - The SM is extended by an extra real scalar singlet S , with a Z_2 symmetry $S \rightarrow -S$

$$\mathcal{L} = \mathcal{L}_{SM} + \frac{1}{2}(\partial_\mu S)(\partial^\mu S) - V_N + V_{SM} \quad V_N = bS^2 + dS^4 + \kappa_1 S^2 H^\dagger H + \mu^2 H^\dagger H + \lambda(H^\dagger H)^2$$

Let us consider the solution (for the minimum)

$$S = 0; h^2 = -\mu^2/(2\lambda);$$

Vector - Dark $U(1)_X$ gauge symmetry: all SM particles are $U(1)_X$ neutral.

$$\mathcal{L} = \mathcal{L}_{SM} - \frac{1}{4}X_{\mu\nu}X^{\mu\nu} + (D_\mu S)^\dagger(D^\mu S) + \mu_S^2 |S|^2 - \lambda_S |S|^4 - \kappa |S|^2 H^\dagger H \quad D_\mu = \partial_\mu + ig_X X_\mu$$

with

$$H = \begin{pmatrix} G^\pm \\ \frac{1}{\sqrt{2}}(v_H + h + iG_0) \end{pmatrix} \quad S = \frac{1}{\sqrt{2}}(v_S + S + iA)$$

$$\begin{pmatrix} h_1 \\ h_2 \end{pmatrix} = \begin{pmatrix} \cos \alpha & \sin \alpha \\ -\sin \alpha & \cos \alpha \end{pmatrix} \begin{pmatrix} h \\ S \end{pmatrix}$$

Back to colliders - Higgs invisible width

Now choose a DM mass of 40 GeV and calculate the bound on the portal coupling

$$BR(h \rightarrow \chi\chi) = \frac{\Gamma(h \rightarrow \chi\chi)}{\Gamma_T(h)} \quad \Gamma_T(h) \approx 4.6 \text{ MeV}$$

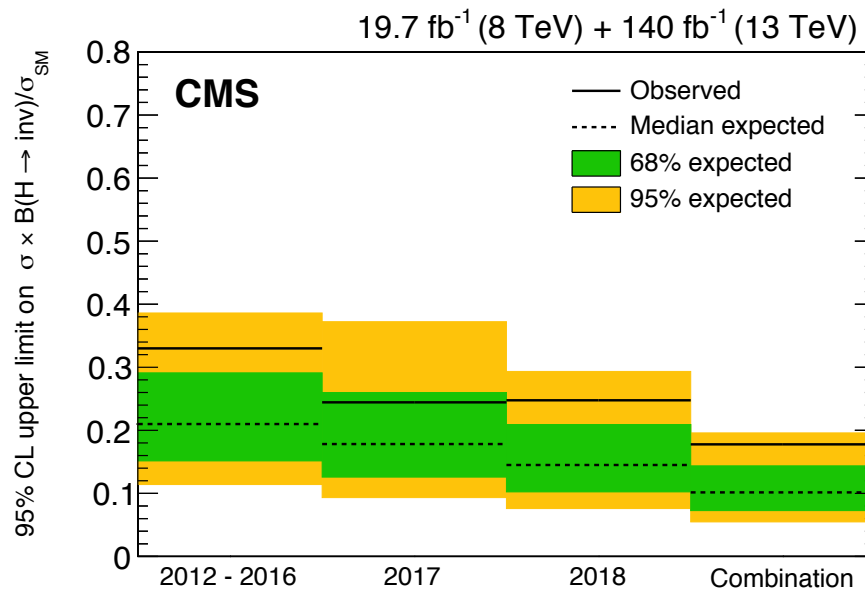


Figure 11: Observed and expected 95% CL upper limits on $(\sigma_H / \sigma_H^{\text{SM}}) \mathcal{B}(H \rightarrow \text{inv})$ for all data-taking years considered, as well as their combination, assuming an SM Higgs boson with a mass of 125.38 GeV.

Relic density, WIMP miracle
and thermal DM generation

Temperature fluctuations in the CMB

CMB are photons that decoupled from the thermal bath. The surface of last scattering is the one defined by the photons that could come freely to reach us today.

$$T_0 = (2.72548 \pm 0.00057)$$

The value of the variations is of the order $\delta T/T \leq 10^{-5}$ in the sphere of last scattering. If we study these variations in detail we can understand better the temperature fluctuations at that time. Temperature fluctuations on the sphere can be described via spherical harmonics, with the usual polar and azimuthal angles

$$\frac{\delta T(\theta, \phi)}{T_0} = \frac{T(\theta, \phi) - T_0}{T_0} = \sum_{l=0}^{\infty} \sum_{m=-l}^l a_{lm} Y_{ml}(\theta, \phi)$$

In order to analyse temperature fluctuations, the relevant measure is the variance of the temperature distribution

$$\frac{1}{4\pi} \int d\Omega \left(\frac{\delta T(\theta, \phi)}{T_0} \right)^2 = \frac{1}{4\pi} \sum_{m,l} |a_{lm}|^2$$

Temperature fluctuations in the CMB

The index m describes the angular momentum in a particular direction, but because there is no special direction in the sphere of last scattering the a_{lm} coefficients do not depend on m . Thus, the sum over m yields $2l+1$ identical terms. The average of $|a_{lm}|^2$ over m will be defined as the observed power spectrum

$$C_l = \frac{1}{2l+1} \sum_{m=-l}^l |a_{lm}|^2$$

The values of the coefficients C_l can be determined using

$$\frac{1}{4\pi} \int d\Omega \left(\frac{\delta T(\theta, \phi)}{T_0} \right)^2 = \frac{1}{4\pi} \sum_{l=0}^{\infty} \frac{2l+1}{4\pi} C_l$$

Temperature fluctuations measured by PLANCK allows to calculate C_l .

The peaks are generated by acoustic oscillations which occur in the baryon-photon fluid at the time of photon decoupling.

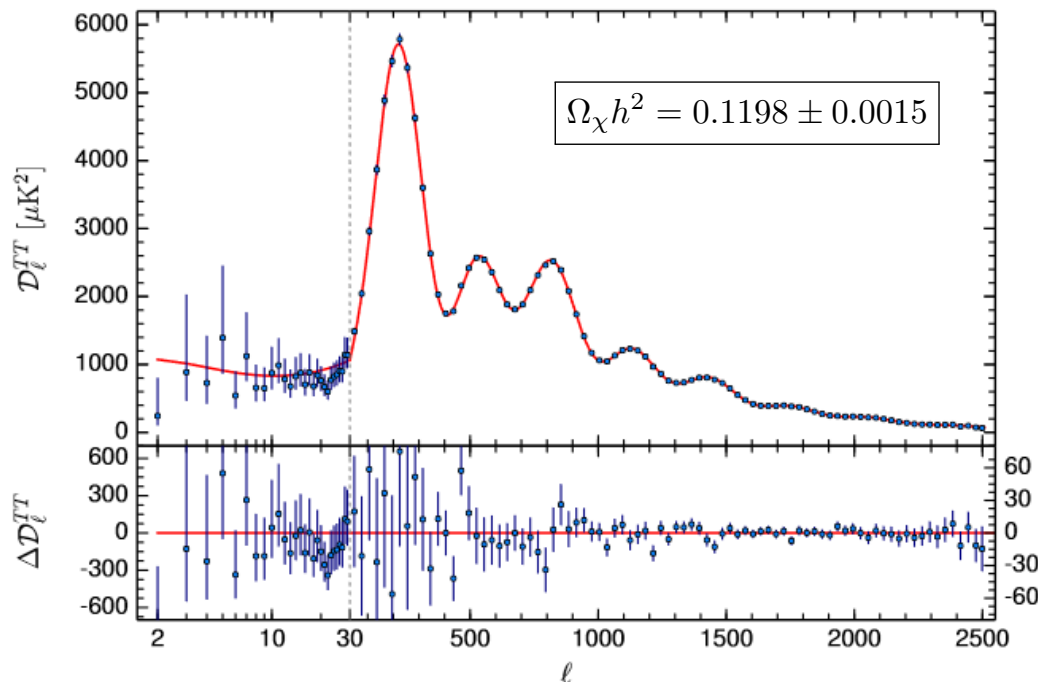
Regions with a large accumulation of DM form gravitational wells, which pull the baryon-photon fluid inside it resulting in a compression of the fluid.

At the same time the relativistic photons exert a pressure that counteracts the gravitational pull, which results in a rarefaction of the fluid.

These counteracting forces create oscillations in the baryon-photon fluid and lead to temperature fluctuations in the photon spectrum during decoupling.

Temperature fluctuations in the CMB

The odd numbered peaks correspond to the decoupling of photons during a compression phase, while even numbered peaks correspond to a decoupling during a rarefaction phase.



To fit the data points given in a model with 6 independent cosmological parameters is used under the assumption of a flat universe. This model is referred to as the "base Λ CDM", which includes the Hubble constant H , and the baryon and DM fraction

The first peak corresponds to the time of last scattering where the fluid compressed once. Determining its position gives information about the curvature of the universe.

The second peak corresponds to one compression and one rarefaction of the fluid. A large relative baryon content in the baryon-photon fluid would lead to an increase in amplitude of the compression peaks and at the same time to a decrease of the rarefaction peaks. Therefore, by measuring the ratio between the first and the second peak, the baryon content of the universe can be obtained.

The height of the third peak determines the amount of DM in the universe. Since, DM does not interact with photons, it only contributes to the strength of the compression peaks. Therefore, a large third peak is a sign of a sizeable DM component in the universe.

Mechanisms of thermal DM generation - freeze-out

The relic density is calculated using the Boltzmann equation which describes the change of a number density $n(t)$ with time. If $a(t)$ is the linear dimension of the universe,

$$0 = \frac{d}{dt}[n(t) a(t)^3] = \dot{n}(t)a(t)^3 + 3n(t)a(t)^2\dot{a}(t) \quad \Rightarrow \quad \dot{n}(t) + 3H(t)n(t) = 0$$

Where H is the Hubble constant. This would be the equation that would hold if the density of all particles would be constant with time. The evolution of the density of DM is also related to the production or annihilation of DM

$$\dot{n}(t) = -3H(t)n(t) - \langle \sigma v \rangle_{\chi\chi} (n^2(t) - n_{eq}^2)$$

where $\langle \sigma v \rangle_{\chi\chi}$ is the thermal averaged cross section (luminosity), and n_{eq} is the equilibrium density. Note that

$$[\sigma v n] = m^2 \frac{m}{s} \frac{1}{m^3} = \frac{1}{s}$$

The thermal averaged cross section is given by

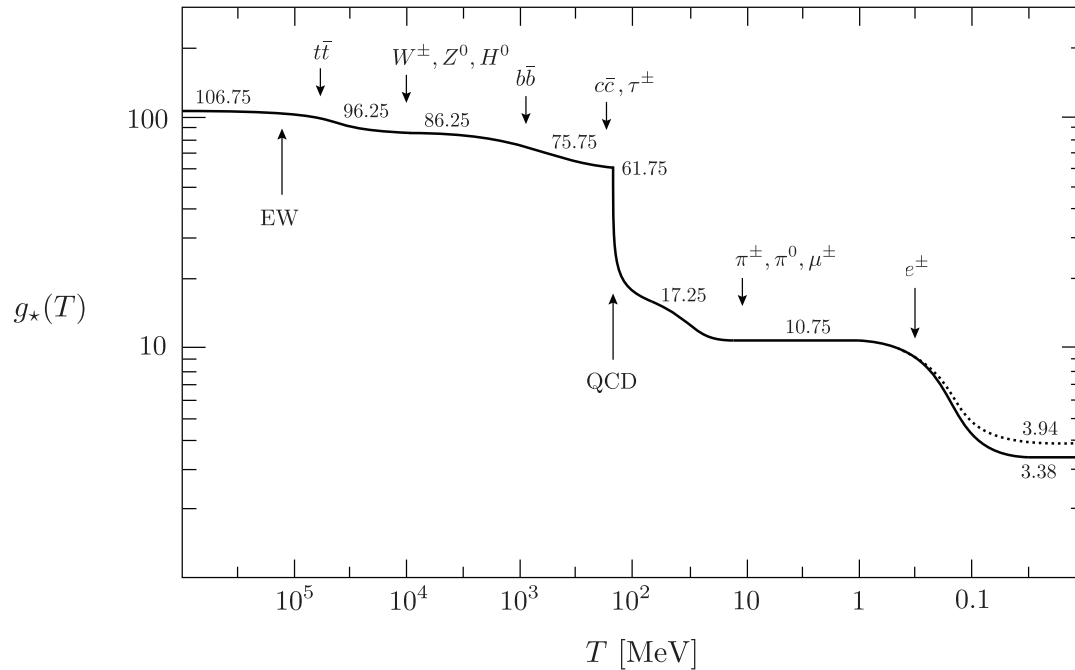
$$\langle \sigma v \rangle_{\chi\chi} = \frac{\int d^3p_{\chi,1} \int d^3p_{\chi,2} e^{-(E_{\chi,1}+E_{\chi,2})/T} \sigma_{\chi\chi} v}{\int d^3p_{\chi,1} \int d^3p_{\chi,2} e^{-(E_{\chi,1}+E_{\chi,2})/T}} \quad v = \frac{\sqrt{(p_{\chi,1} p_{\chi,2}) - m_{\chi}^4}}{E_{\chi,1} E_{\chi,2}}$$

Mechanisms of thermal DM generation - freeze-out

The equation is usually simplified with a change of variables $Y = ns$, leading to

$$\frac{dY}{dx} = -\sqrt{\frac{\pi}{45G}} \frac{g_*^{1/2} m_\chi}{x^2} \langle \sigma v \rangle_{\chi\chi} (Y^2 - Y_{\text{eq}}^2)$$

Where $x = m_\chi/T$, G is the gravitational constant and g_* are the relativistic degrees of freedom (that evolve over time). We have assumed that the total entropy on the universe remains constant with time.



$g_b = 28$ photons (2), W^\pm and Z^0 ($3 \cdot 3$), gluons ($8 \cdot 2$), and Higgs (1)
 $g_f = 90$ quarks ($6 \cdot 12$), charged leptons ($3 \cdot 4$), and neutrinos ($3 \cdot 2$)

$$g_* = g_b + \frac{7}{8} g_f = 106.75$$

Figure 3.4: Evolution of relativistic degrees of freedom $g_*(T)$ assuming the Standard Model particle content. The dotted line stands for the number of effective degrees of freedom in entropy $g_{*S}(T)$.

Mechanisms of thermal DM generation - freeze-out

Going back to the Boltzmann equation in the form

$$\frac{dY}{dx} = -\sqrt{\frac{\pi}{45G}} \frac{g_*^{1/2} m_\chi}{x^2} \langle \sigma v \rangle_{\chi\chi} (Y^2 - Y_{\text{eq}}^2) \quad s' = h_{\text{eff}}(T) \frac{2\pi^2}{45} T^3, \quad \rho = g_{\text{eff}}(T) \frac{\pi^2}{30} T^4$$

We can now integrate the equation to get the value of the Yield today.

The relic density can be calculated via

$$\Omega_\chi = \frac{\rho_{\chi,0}}{\rho_c} = \frac{m_\chi n_0}{\rho_c} = \frac{m_\chi s_0 Y_0}{\rho_c}$$

where s_0 is the entropy density today and $\rho_c = 3H^2/(8\pi G)$ is the critical density that separates a expanding from a collapsing universe. To match the definition of the observed relic density we need to multiply the above equation by

$$h^2 = \left(\frac{H}{100 \frac{\text{km}}{\text{sMpc}}} \right)^2$$

Mechanisms of thermal DM generation - freeze-out

Introducing numerical values we get the following expression

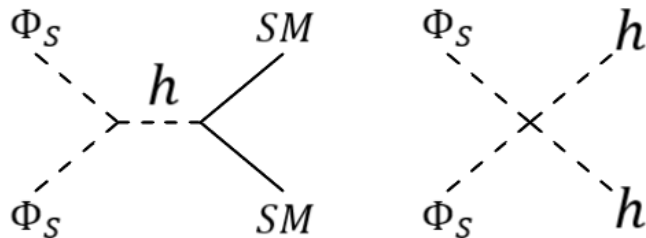
$$\Omega_\chi h^2 = m_\chi s_0 Y_0 \frac{8\pi G}{3H^2} \approx 2.742 \times 10^8 \frac{m_\chi}{\text{GeV}} Y_0$$

Experimental value

$$\Omega_\chi h^2 = 0.1198 \pm 0.0015$$

Now we just need to calculate Y_0 . And we start with our favourite model

$$V = \mu^2 \Phi^\dagger \Phi + \lambda (\Phi^\dagger \Phi)^2 + \mu_S^2 \Phi_S^2 + \lambda_S \Phi_S^4 + \lambda_3 \Phi^\dagger \Phi \Phi_S^2$$



Note that the notation keeps changing!

We need to calculate the cross section for all possible processes, multiply by the relative velocity and find the thermal average.

But before that, the WIMP miracle.

The WIMP miracle

We assume that DM is in thermal equilibrium with the SM particles, and is able to annihilate. At the point of thermal decoupling DM freezes-out with a density that is approximate the one that we measure today. The process of annihilation is



The interaction rate corresponding to the scattering process just compensates the increasing scale factor at the point of decoupling

$$\Gamma(T_{dec}) = H(T_{dec})$$

If we assume that the interaction rate is set by the electroweak interactions and use the Z-boson coupling and mass, the cross section of the above process is of the order

$$\sigma_{\chi\chi} = \frac{\pi\alpha^2 m_\chi^2}{c_w^2 m_Z^4}$$

And after assuming a lot of other stuff (that could change the order of magnitude but not by much) we reach the conclusion

$$\Omega_\chi h^2 \approx 0.12 \left(\frac{13 \text{ GeV}}{m_\chi} \right)^2 .$$

known as the WIMP miracle.

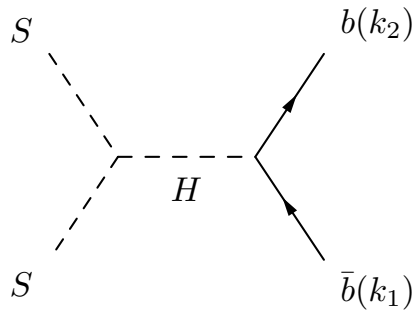
Mechanisms of thermal DM generation - freeze-out

Scalar - The SM is extended by an extra real scalar singlet S , with a Z_2 symmetry $S \rightarrow -S$

$$\mathcal{L} = \mathcal{L}_{SM} + \frac{1}{2}(\partial_\mu S)(\partial^\mu S) - V_N + V_{SM}$$

Let us consider the solution (for the minimum) $S = 0$; $h^2 = -\mu^2/(2\lambda)$;

And now let us calculate a specific process of DM annihilation to a b-quark pair



First we calculate the cross section. After that we make an approximation of averaging over a constant. Then we calculate Y today by approximating whatever we can to constants.

What do we need?

$$v = 2\sqrt{\frac{s}{4m_\chi^2} - 1} \quad \Omega_\chi h^2 = m_\chi s_0 Y_0 \frac{8\pi G}{3H^2} \approx 2.742 \times 10^8 \frac{m_\chi}{\text{GeV}} Y_0 \quad m_P = \sqrt{\frac{hc}{2\pi G}} = 1.22 \times 10^{19} \text{ GeV}$$

Mechanisms of thermal DM generation - freeze-out

Now we integrate from x_f (at freeze-out) to infinity

$$\frac{dY}{dx} = -\lambda \frac{Y^2}{x^2} \quad x = \frac{m_\chi}{T} \quad \lambda = \sqrt{\frac{\pi}{45G}} g_*^{1/2} m_\chi \langle \sigma v \rangle_{\chi\chi}$$

The result is

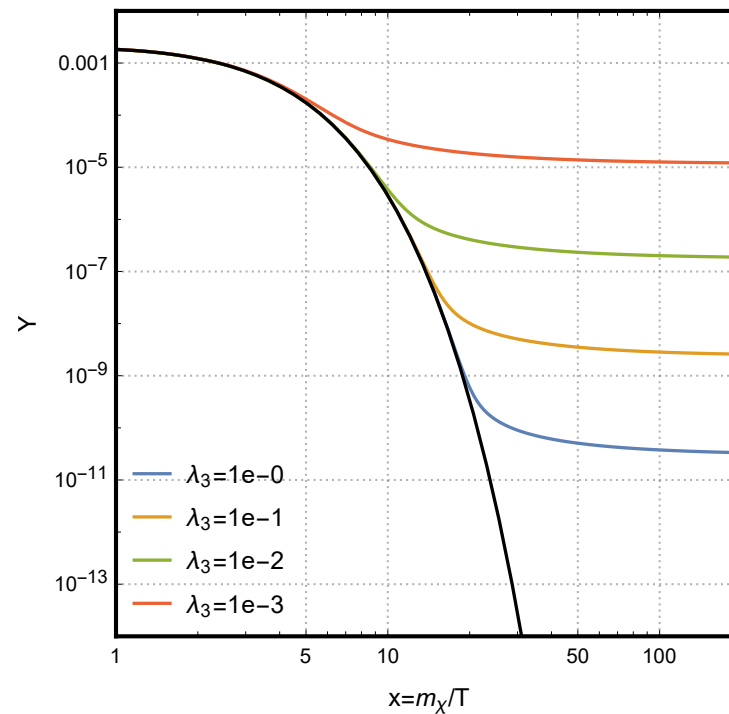
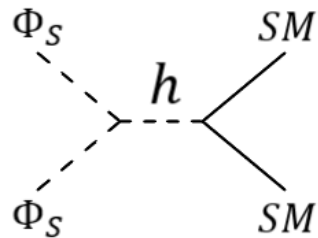
$$Y_0 = Y_\infty \approx \frac{x_f}{\lambda}$$

Considering $x_f = 10$ calculate the coupling for a DM of 100 GeV.

$$\Omega_\chi h^2 = m_\chi s_0 Y_0 \frac{8\pi G}{3H^2} \approx 2.742 \times 10^8 \frac{m_\chi}{\text{GeV}} Y_0$$

Mechanisms of thermal DM generation - freeze-out

Back to the complex singlet and considering only the final state with b quarks



$$\Omega_\chi h^2 = m_\chi s_0 Y_0 \frac{8\pi G}{3H^2} h^2 \approx 2.742 \cdot 10^8 \frac{m_\chi}{\text{GeV}} Y_0$$

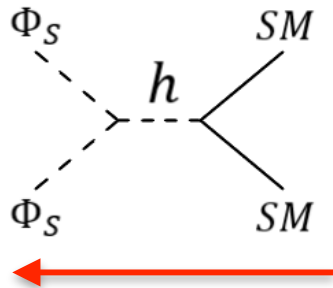
The figure shows the evolution of $Y(x)$ as a function of x for different cross sections, that is, for different portal couplings. The larger the coupling the smaller the yield. The reason is that the thermal averaged cross section is a measure of how strongly the SM and the DM bath are coupled. A larger coupling means a more efficient interaction rate. This in turn means a smaller temperature and a larger x .

Mechanisms of DM generation - freeze-in

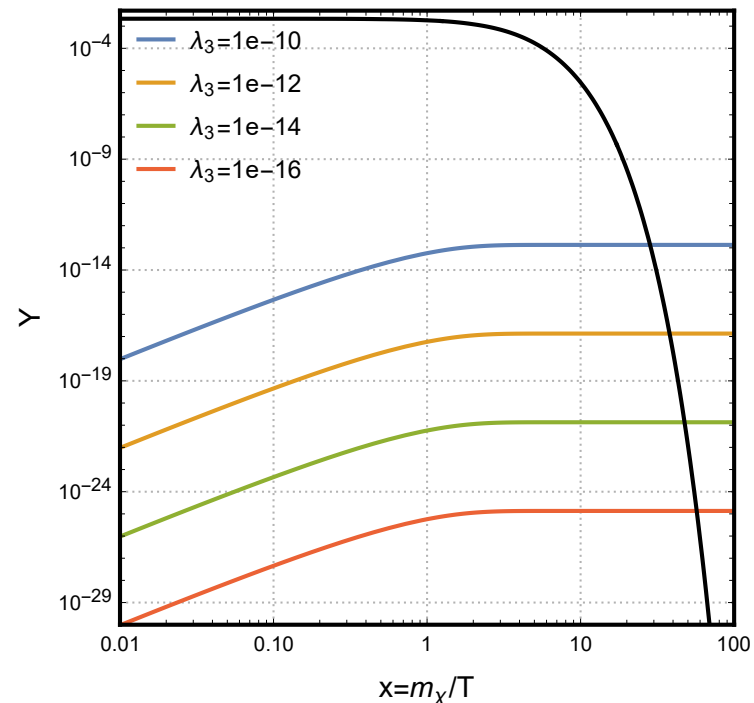
Freeze-out may not happen if the portal coupling is too small. In that case the DM annihilation channels are not efficient enough to produce the current relic density.

In this regime of very weakly interacting massive particles, also called Feebly Interacting Massive Particles (FIMPs) the mechanism of freeze-in may come to the rescue.

In contrast to freeze-out, the DM particles do not start in thermal equilibrium with the SM and have a low initial abundance. Processes favour the direction of DM production from SM particles instead of annihilation of DM particles into SM particles.



This production happens until the SM coupling to DM is too small to accommodate for the expansion of the universe.



Mechanisms of thermal DM generation - freeze-in

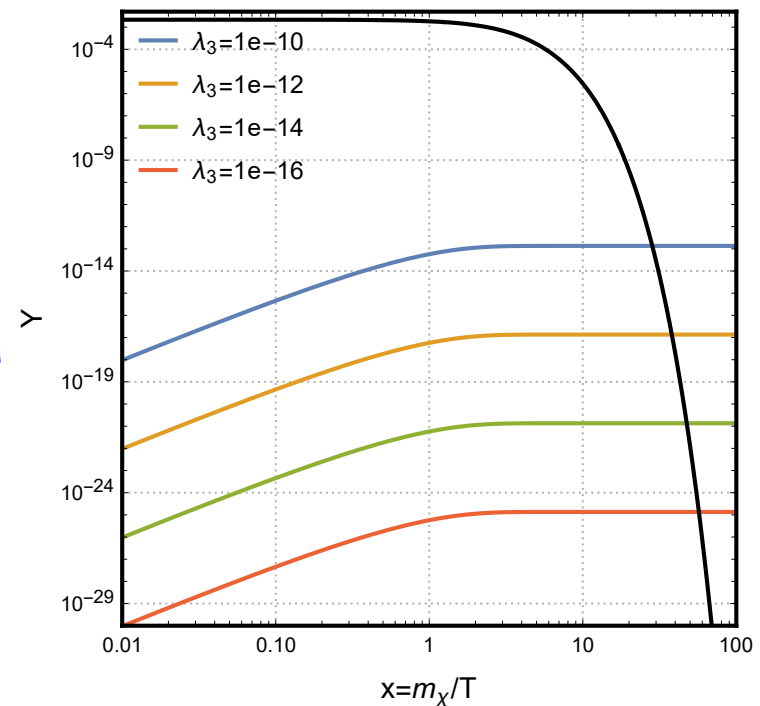
The calculation of the relic density via freeze-in is in general more involved than for freeze-out. Due to the fact that during freeze-in the DM particles are not in thermal equilibrium with the SM particles, the newly produced heavy DM particles have in general less kinetic energy than at equilibrium.

In terms of Y and x the Boltzmann equation now is

$$\frac{dY}{dx} = \sqrt{\frac{\pi}{45G}} \frac{g_*^{1/2} m_\chi}{x^2} \sum_{i,j=1}^N \langle \sigma v \rangle_{ij} (Y_{i,eq} Y_{j,eq} - Y_i Y_j)$$

The figure shows the relation between the coupling λ_3 from the potential and the evolution of Y . As for freeze-out a higher value of λ_3 results in a larger TAC. In contrast to freeze-out though, a larger TAC results in a larger yield (and therefore relic density), because the annihilation of SM particles into DM is more efficient.

At temperatures lower than the dark matter mass, the bath no longer has enough energy to produce dark matter. At this point, the amount of dark matter has "frozen-in," there are no other ways to produce more dark matter.



Mechanisms of DM generation - pandemic

This is a mechanism that complements freeze-in and freeze-out production in a generic way, opening new parameter space to explain the observed DM abundance.

To make this work we need at least two DM particles (χ, ψ). ψ is already in thermal equilibrium with the SM bath in the early universe. χ has a small initial value abundance created by freeze-in. Interaction between ψ and χ leads to an exponential growth of χ that shuts down at some point.

In this scenario we extend the SM with two real singlet scalar fields χ, ψ that are odd under Z_2 and all SM particles are even. The most general renormalisable Lagrangian is

$$\begin{aligned} \mathcal{L}_{\text{scalar,int}} = & -m_{11}^2 \Phi_1^\dagger \Phi_1 + m_{22}^2 \Phi_2^2 + m_{33}^2 \Phi_3^2 + m_{23} \Phi_2 \Phi_3 \\ & + \lambda_1 (\Phi_1^\dagger \Phi_1)^2 + \lambda_2 \Phi_2^4 + \lambda_3 \Phi_3^4 + \lambda_{12} (\Phi_1^\dagger \Phi_1) \Phi_2^2 + \lambda_{13} (\Phi_1^\dagger \Phi_1) \Phi_3^2 \\ & + \lambda_{23} \Phi_2^2 \Phi_3^2 + \lambda_{123} (\Phi_1^\dagger \Phi_1) \Phi_2 \Phi_3 + \lambda_{223} \Phi_2^3 \Phi_3 + \lambda_{332} \Phi_3^3 \Phi_2. \end{aligned}$$

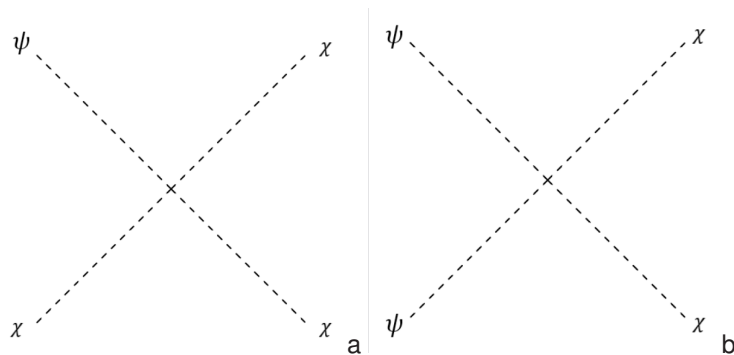


Figure: Feynman diagram of (a) the exponential growth process and (b) of the freeze-in process

Here the terms which leads to freeze-in and exponential growth are highlighted.

$$\frac{dY_\chi}{dt} = -\sqrt{\frac{\pi}{45G}} \frac{g_*^{1/2} m_\psi}{x^2} (\langle \sigma v \rangle_{\text{tr}} Y_\psi^{\text{eq}} Y_\chi - \langle \sigma v \rangle_{\text{fi}} (Y_\psi^{\text{eq}})^2).$$

This is an x!

Mechanisms of DM generation - pandemic



Karlsruher Institut für Technologie
Institut für Theoretische Physik
Wolfgang-Gaede-Straße 1
76131 Karlsruhe
https://www.itp.kit.edu/

Faculdade de Ciências da Universidade de Lisboa
Centro de Física Teórica e Computacional
Campo Grande, Edifício C8
1749-016 Lisboa, Portugal
https://ciencias.uilisboa.pt/



Dark Matter Production in a Pandemic Model

Ultralight Dark Matter Summer School

Rodrigo Capucha, Karim Elyauti, Johann Plotnikov

Motivation

With **Dark Matter (DM)** being among the most convincing hints towards **new physics** there is a need to study and understand the processes that lead to the currently observed DM relic density in the universe. In this work we investigate the **pandemic model** [1], a novel DM production mechanism, with respect to **freeze-in** and **freeze-out** for the generation of DM. This mechanism complements freeze-in and freeze-out production, opening new parameter space to explain the observed DM abundance.

Pandemic process requirements

- At least **two dark sector particles** ψ and χ .
- ψ is already in thermal equilibrium with the Standard Model (SM) heat bath in the early universe.
- χ starts with a small initial abundance generated by the **freeze-in** process.
- Interaction between ψ and χ leads to an **exponential growth** of χ , which shuts off at some point.
- The DM number density can then be evaluated by the **Boltzmann equation** [1, 2]

$$\frac{dY_\chi}{dx} = \sqrt{\frac{g}{45G}} \frac{g_\psi}{x^2} m_\psi (\langle\sigma v\rangle_\psi Y_\psi^2 Y_\chi + \langle\sigma v\rangle_\psi (Y_\psi Y_\chi^2)). \quad (1)$$

Here Y (Y_{eq}) being the (equilibrium) yield, G the gravitational constant, $g^{1/2}$ given in [2], m_ψ the mass of ψ and $\langle\sigma v\rangle$ the thermal average cross section times the relative velocity v .



Figure 1: Generic diagram for exponential growth (left) and freeze-in (right).

Toy model

- Standard Model extended by **two real singlet scalars** ϕ_2 and ϕ_3 (TRSM) connected to the SM via Higgs portal.
- Z_2 symmetry forbidding DM decay into SM pairs.
- Most general renormalizable Lagrangian invariant under Z_2 symmetry,

$$\mathcal{L}_{\text{interact}} = -m_\phi^2 \phi_i^2 + m_{\phi_2}^2 \phi_2^2 + m_{\phi_3}^2 \phi_3^2 + \lambda_1 \phi_1 \phi_2^2 + \lambda_2 \phi_1 \phi_3^2 + \lambda_3 \phi_2 \phi_3^2 + \lambda_4 (\phi_1 \phi_2)^2 + \lambda_5 (\phi_1 \phi_3)^2 + \lambda_6 (\phi_2 \phi_3)^2 + \lambda_7 \phi_1 \phi_2 \phi_3 + \lambda_8 \phi_1^2 \phi_2 \phi_3 + \lambda_9 \phi_1^2 \phi_3^2 + \lambda_{10} \phi_2^2 \phi_3^2. \quad (2)$$

Terms responsible for **freeze-in** and **exponential growth**.

Results

- With **freeze-in** (Figure 2), the exponential growth phase allows to satisfy the relic density constraint for **significantly smaller freeze-in couplings**, λ_{fi} , opening up new parameter space of interest.

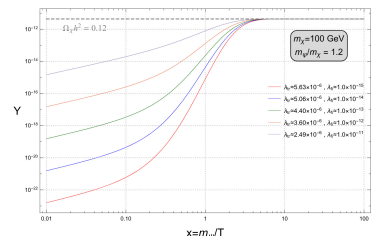


Figure 2: Evolution of the yield, Y , as a function of $x = m_\psi/T$ for the freeze-in and exponential growth processes. The parameters λ_{tr} and λ_{fi} are adjusted to provide the measured DM relic density of $\Omega_\chi h^2 = 0.12$, for $m_\psi/m_\chi = 1.2$ and $m_\chi = 100$ GeV.

Results

- This is further illustrated in Figure 3, where we show the λ_{tr} and λ_{fi} combinations, for fixed mass ratios m_ψ/m_χ , that result in $\Omega_\chi h^2 \approx 0.12$, via **different DM production mechanisms**.

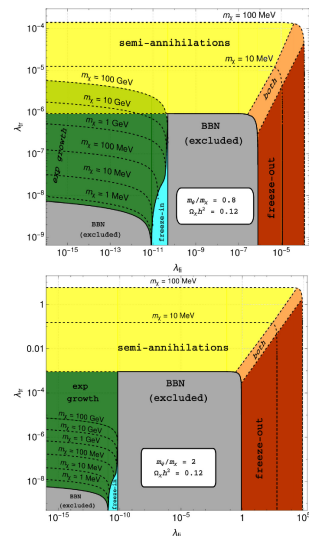


Figure 3: Phase diagram for λ_{tr} and λ_{fi} . These couplings are chosen such that the measured DM amount is generated. Top (bottom): $m_\psi/m_\chi = 0.8$ (2). The colored regions represent the main mechanism responsible for DM production; the dashed lines indicate the required value of m_ψ , and the gray zones are excluded by the Big Bang Nucleosynthesis (BBN) constraints.

Conclusion

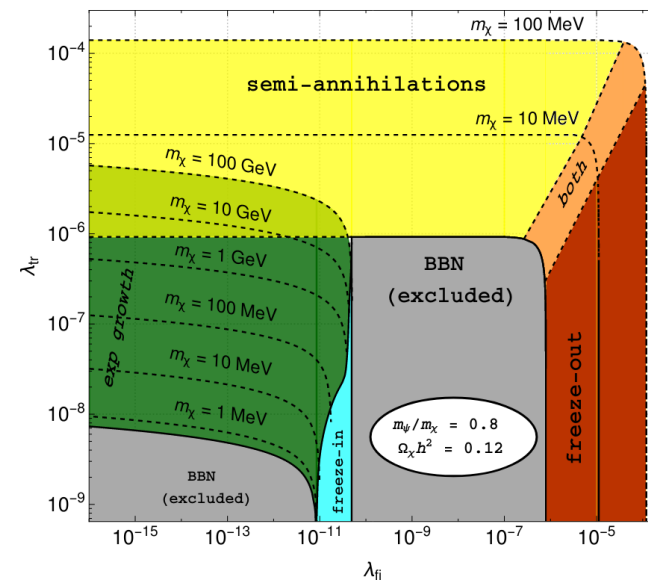
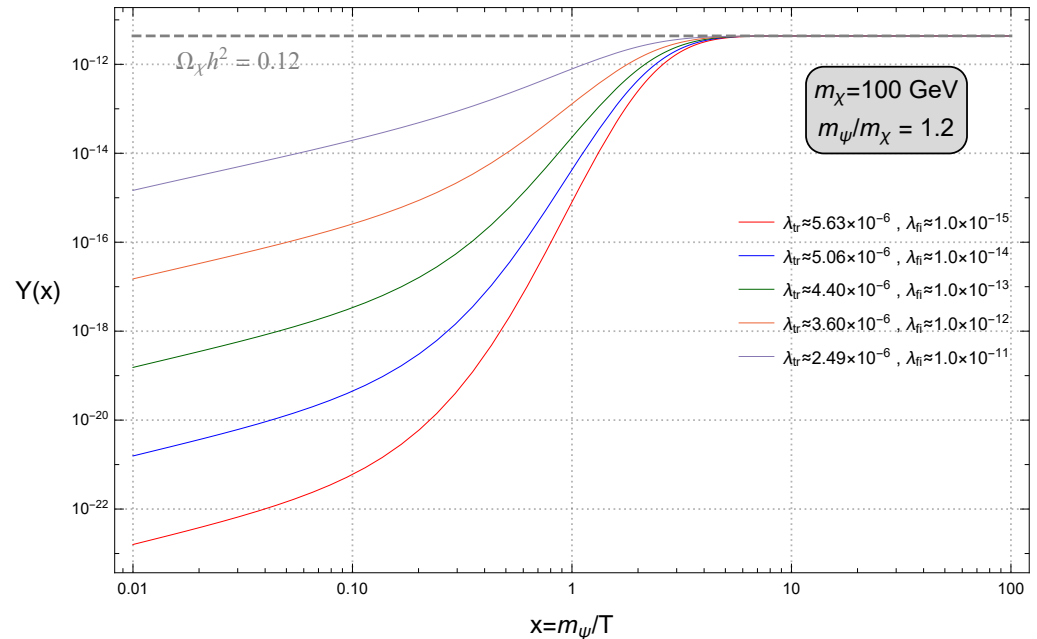
The pandemic process allows a wider range of parameters for specific models not attainable through purely freeze-in/out. A possible specific model under investigation is **CP in the dark** [3].

References

- [1] T. Bringmann et al. "Dark Matter from Exponential Growth". In: *Physical Review Letters* 127:19 (2021).
- [2] P. Gondolo and G. Gelmini. "Cosmic abundances of stable particles: Improved analysis". In: *Nuclear Physics B* 350:1 (1991), pp. 145–179. ISSN: 0550-3213.
- [3] Duarte Azevedo et al. "CP in the dark". In: *Journal of High Energy Physics* 2018 (11 2018), p. 91. ISSN: 1029-8479.

Acknowledgments:

RC is supported by the Portuguese Foundation for Science and Technology (FCT), under contracts UIDB/00618/2020, UIDP/00618/2020, PTDC/FISPAR/31000/2017, CERN/FISPAR/014/2019, and by the FCT grant 2020.08221.BD.



Mechanisms of DM generation - freeze-out

$$\mathcal{M} = \bar{u}(k_2) \frac{-im_f}{v_H} v(k_1) \frac{-i}{(k_1 + k_2)^2 - m_H^2 + im_H \Gamma_H} (-2i\lambda_3 v_H)$$

$$\begin{aligned} \sum_{\text{spin}} |\mathcal{M}|^2 &= 4\lambda_3^2 m_f^2 \left(\sum_{\text{spin}} v(k_1) \bar{v}(k_1) \right) \left(\sum_{\text{spin}} u(k_2) \bar{u}(k_2) \right) \frac{1}{|(k_1 + k_2)^2 - m_H^2 + im_H \Gamma_H|^2} \\ &= 4\lambda_3^2 m_f^2 \text{Tr}[(\not{k}_1 - m_f \mathbf{1})(\not{k}_2 + m_f \mathbf{1})] \frac{1}{[(k_1 + k_2)^2 - m_H^2]^2 + m_H^2 \Gamma_H^2} \\ &= 4\lambda_3^2 m_f^2 4 [k_1 k_2 - m_f^2] \frac{1}{[(k_1 + k_2)^2 - m_H^2]^2 + m_H^2 \Gamma_H^2} \\ &= 8\lambda_3^2 m_f^2 \frac{(k_1 + k_2)^2 - 4m_f^2}{[(k_1 + k_2)^2 - m_H^2]^2 + m_H^2 \Gamma_H^2} . \end{aligned}$$

$$\overline{\sum_{\text{spin,color}} |\mathcal{M}|^2} = N_c 8\lambda_3^2 m_b^2 \frac{s - 4m_b^2}{(s - m_H^2)^2 + m_H^2 \Gamma_H^2}$$

$$\begin{aligned} \sigma(SS \rightarrow b\bar{b}) &= \frac{1}{16\pi s} \sqrt{\frac{1 - 4m_b^2/s}{1 - 4m_S^2/s}} \overline{\sum |\mathcal{M}|^2} \\ &= \frac{N_c}{2\pi\sqrt{s}} \lambda_3^2 m_b^2 \sqrt{\frac{1 - 4m_b^2/s}{s - 4m_S^2}} \frac{s - 4m_b^2}{(s - m_H^2)^2 + m_H^2 \Gamma_H^2} \end{aligned}$$

$$\begin{aligned} \langle \sigma v \rangle \Big|_{SS \rightarrow b\bar{b}} &\equiv \sigma v \Big|_{SS \rightarrow b\bar{b}} \\ &\stackrel{\text{Eq.(3.19)}}{=} v \frac{N_c \lambda_3^2 m_b^2}{2\pi\sqrt{s}} \frac{\sqrt{1 - 4m_b^2/s}}{m_S v} \frac{s - 4m_b^2}{(s - m_H^2)^2 + m_H^2 \Gamma_H^2} \\ &\stackrel{\text{threshold}}{=} \frac{N_c \lambda_3^2 m_b^2}{4\pi m_S^2} \sqrt{1 - \frac{m_b^2}{m_S^2}} \frac{4m_S^2 - 4m_b^2}{(4m_S^2 - m_H^2)^2 + m_H^2 \Gamma_H^2} \\ &\stackrel{m_S \gg m_b}{=} \frac{N_c \lambda_3^2 m_b^2}{\pi} \frac{1}{(4m_S^2 - m_H^2)^2 + m_H^2 \Gamma_H^2} . \end{aligned}$$

Indirect detection

Indirect detection

There are many on-going experiments with the goal of detecting the products of DM annihilation in our Galaxy, or beyond.

We assume that DM annihilation is strongly suppressed after thermal freeze-out. However, it can still occur today and the chances of discovery can be maximised by searching in regions of very high DM density.

For most extensions of the SM, DM can annihilate to most of the SM particles.

We will just focus on photon final states. Depending on the model, DM can annihilate directly into a pair of photons, or into other SM states that then produce photons. The gamma-rays propagate essentially unperturbed, and can be detected by a satellite or ground-based telescope on Earth.

Let us consider that there are multiple DM annihilation channels, each with velocity-averaged cross section $\langle\sigma_i v\rangle$. The annihilation rate per particle is

$$\sum_i \frac{\rho[r(\ell, \psi)]}{m_\chi} \times \langle\sigma_i v\rangle$$

where r is the radial distance between the annihilation event and the Galactic Center—it is a function of the line-of-sight (l.o.s.) distance, l , which is oriented an angle ψ away from the Galactic plane.

Indirect detection

The total annihilation rate in the volume $dV = l^2 dl d\Omega$ is obtained by multiplying the previous equation by the total number of particles in the volume

$$\left(\sum_i \frac{\rho[r(\ell, \psi)]}{m_\chi} \langle \sigma_i v \rangle \right) \times \left(\frac{\rho[r(\ell, \psi)]}{2 m_\chi} dV \right) \quad \text{Factor of 2 because we need to DM particles to annihilate}$$

The photon flux is the annihilation rate multiplied by dN_i/dE_γ , that is, the number of photons at a given energy E_γ produced in the i^{th} annihilation channel. The differential photon flux $d\Phi/dE_\gamma$ in the observational volume oriented in the direction ψ is

$$\frac{d\Phi}{dE_\gamma}(E_\gamma, \psi) = \frac{1}{4\pi} \int_{\Delta\Omega} d\Omega \int_{\text{l.o.s.}} d\ell \rho[r(\ell, \psi)]^2 \sum_i \frac{\langle \sigma_i v \rangle}{2m_\chi^2} \frac{dN_i}{dE_\gamma}$$

All the astrophysical uncertainties in the determination of the flux are absorbed by the J-factor

$$J = \frac{1}{\Delta\Omega} \int d\Omega \int_{\text{l.o.s.}} d\ell \rho[r(\ell, \psi)]^2$$

The larger the J-factor, the more interesting the astrophysical target is for DM annihilation. The J-factors for dwarf galaxies are roughly $J \sim 10^{19-20} \text{ GeV}^2/\text{cm}^5$. For our nearest neighbour, the Andromeda galaxy, $J \sim 10^{20} \text{ GeV}^2/\text{cm}^5$. For our own Galactic Center, $J \sim 10^{22-25} \text{ GeV}^2/\text{cm}^5$ (10^{22-24}) within 0.1° (1°).

Indirect detection

The final state particles are stable leptons or protons propagating large distances in the Universe. While the leptons or protons can come from many sources, the anti-particles appear much less frequently. One key experimental task in many indirect dark matter searches is therefore the ability to measure the charge of a lepton, typically with the help of a magnetic field. For example, we can study the energy dependence of the antiproton–proton ratio or the

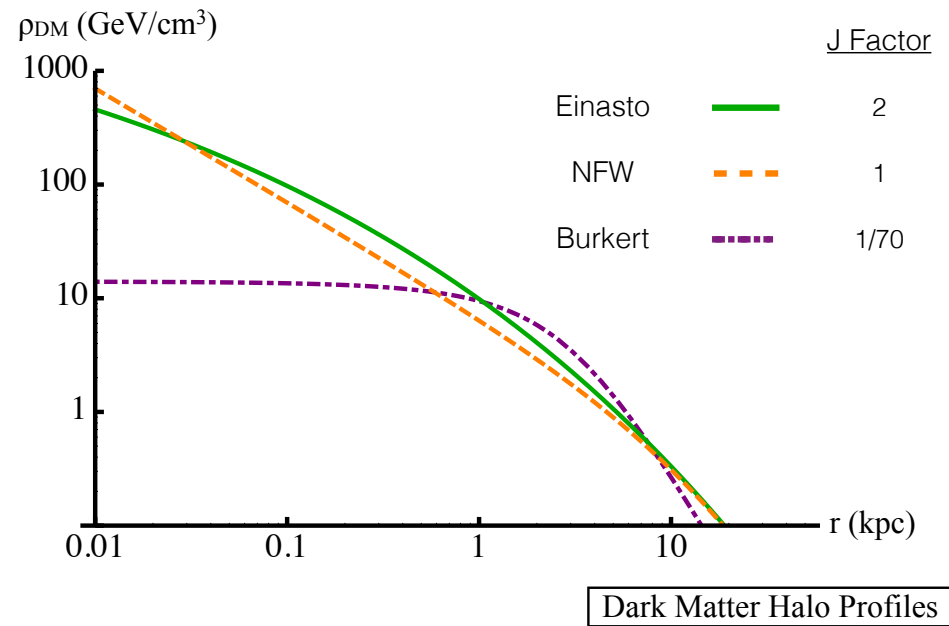


Figure 14: Dark matter galactic halo profiles, including standard Einasto and NFW profiles along with a Burkert profile with a 3 kpc core. J factors are obtained assuming a spherical dark matter distribution and integrating over the radius from the galactic center from $r \simeq 0.05$ to 0.15 kpc. J factors are normalized so that $J(\rho_{\text{NFW}}) = 1$. Figure from Ref.[12]

Indirect detection

However, when we choose a good target, there is a balance between the size of the J-factor and the potential backgrounds that has to be taken into account.

As an example, dwarf galaxies are DM-dominated and therefore some of the cleanest systems to search for DM because they contain very few stars and little gas. In contrast, a signal from the center of the Galaxy, while enhanced due to the DM density and proximity, has to contend with large systematic uncertainties on the astrophysical backgrounds.

The particle physics input to the flux is the factor (in most cases the velocity-averaged cross section can be pulled out of the integral)

$$\frac{\langle \sigma v \rangle_{\chi\chi}}{m_\chi^2} \frac{dN}{dE_\gamma}$$

The kinematics of the annihilation event determine the basic properties of the photon energy spectrum. Consider, first, the case where the DM annihilates directly into one or two photons: $\chi\chi \rightarrow \gamma X$, where $X = \gamma, Z, H$ or some other neutral state. In the non-relativistic limit, energy conservation gives

$$2m_\chi = E_\gamma + \sqrt{E_\gamma^2 + m_X^2} \longrightarrow E_\gamma \approx m_\chi \left(1 - \frac{m_X^2}{4m_\chi^2} \right)$$

E_γ is the energy of the outgoing photon in the CM frame and m_X is the mass of the X state.

The $\gamma\gamma$ final state results in a monochromatic energy line at the DM mass. For a γZ final state, the gamma line is still monochromatic, but is shifted to lower energies.

Indirect detection

Blue lines - energy spectrum for a $\gamma\gamma$ final state where the measured energy resolution is $\Delta E/E = 0.15$ (solid) or 0.02 (dotted). The observation of such a gamma-ray 'line' would be spectacular evidence for DM annihilation. However, the production of a pair of gamma-rays is typically loop-suppressed (and therefore sub-dominant) in many theories.

Red lines - how the spectrum changes if photons are radiated off of virtual charged particles in the loop.

Green lines - illustrate the box spectrum, which arises when the DM annihilates to a new state φ (e.g., $XX \rightarrow \varphi\varphi$) that then decays to a photon pair ($\varphi \rightarrow \gamma\gamma$).

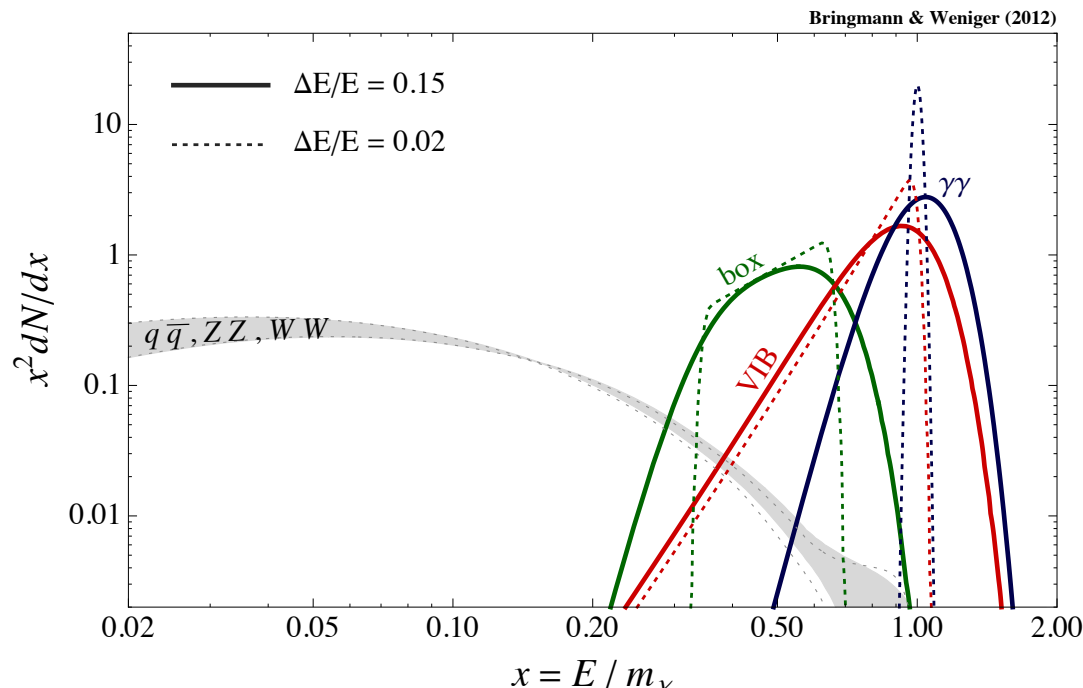


Figure 10: Illustration of the photon energy spectrum for the $\gamma\gamma$ final state without (blue) and with (red) virtual internal bremsstrahlung. The box spectrum (green) can be produced if the DM annihilates to a new state, that then decays to photons, as described in the text. The dotted versus solid lines compare two separate energy resolutions: $\Delta E/E = 0.02$ and 0.15, respectively. The spectrum for photons resulting from the annihilation into gauge bosons and quarks is shown by the gray band. Figure from [96].

Indirect detection

Another possibility is that the DM annihilates to leptons, gauge bosons, or quarks, which may produce secondary photons either through final-state radiation or in the shower of their decay products. The photon energy spectrum dN/dE_ν depends on the exact details of the final-state radiation, and must be determined with Monte Carlo tools like Pythia.

In the case of secondary photon production, the energy spectrum does not have a very distinctive shape, and one must search for a continuum excess over the background. The grey band in shows an example of the spectrum for annihilation to quarks or gauge bosons.

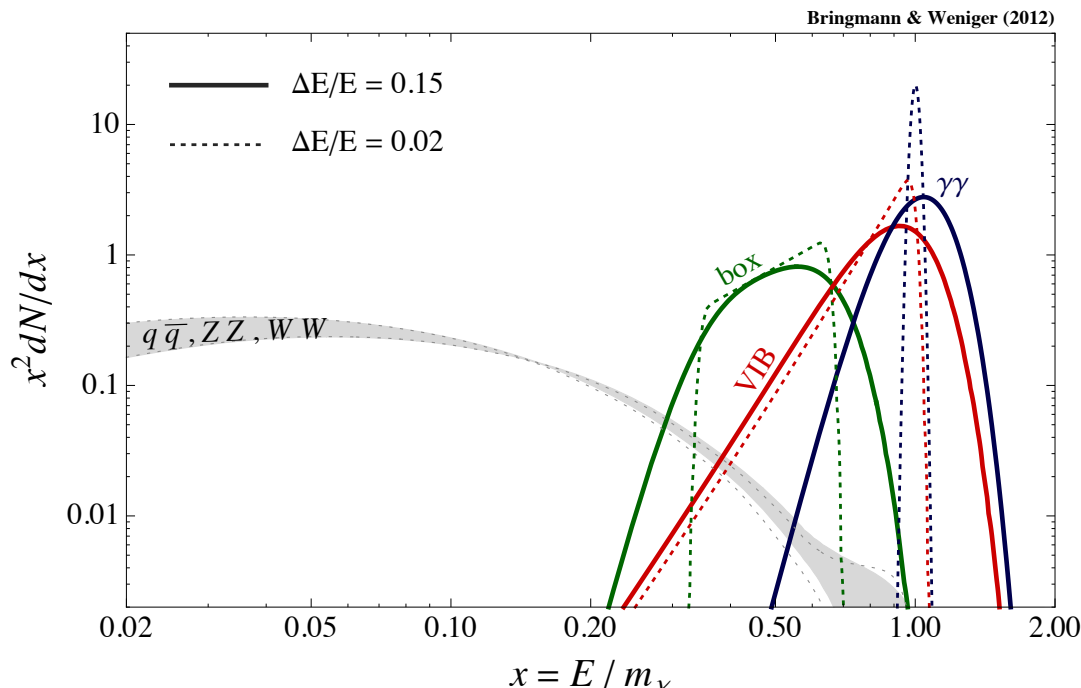


Figure 10: Illustration of the photon energy spectrum for the $\gamma\gamma$ final state without (blue) and with (red) virtual internal bremsstrahlung. The box spectrum (green) can be produced if the DM annihilates to a new state, that then decays to photons, as described in the text. The dotted versus solid lines compare two separate energy resolutions: $\Delta E/E = 0.02$ and 0.15 , respectively. The spectrum for photons resulting from the annihilation into gauge bosons and quarks is shown by the gray band. Figure from [96].

Indirect detection

The details of the annihilation mechanism are in the velocity-averaged cross section $\langle\sigma v\rangle$. This cross section is the same in many simple models as what appears in the relic density calculation.

In addition, we automatically have an interesting target scale for the cross section: $3 \times 10^{-26} \text{ cm}^3 \text{ s}^{-1}$. This regime was probed by the best gamma-ray observatories. For example, the Fermi Large Area Telescope has searched for signals of DM annihilation in the Milky Way's dwarf galaxies.

Figure show the results for DM annihilation (from FermiLAT) to $b\bar{b}$ (left) and tau tau (right)

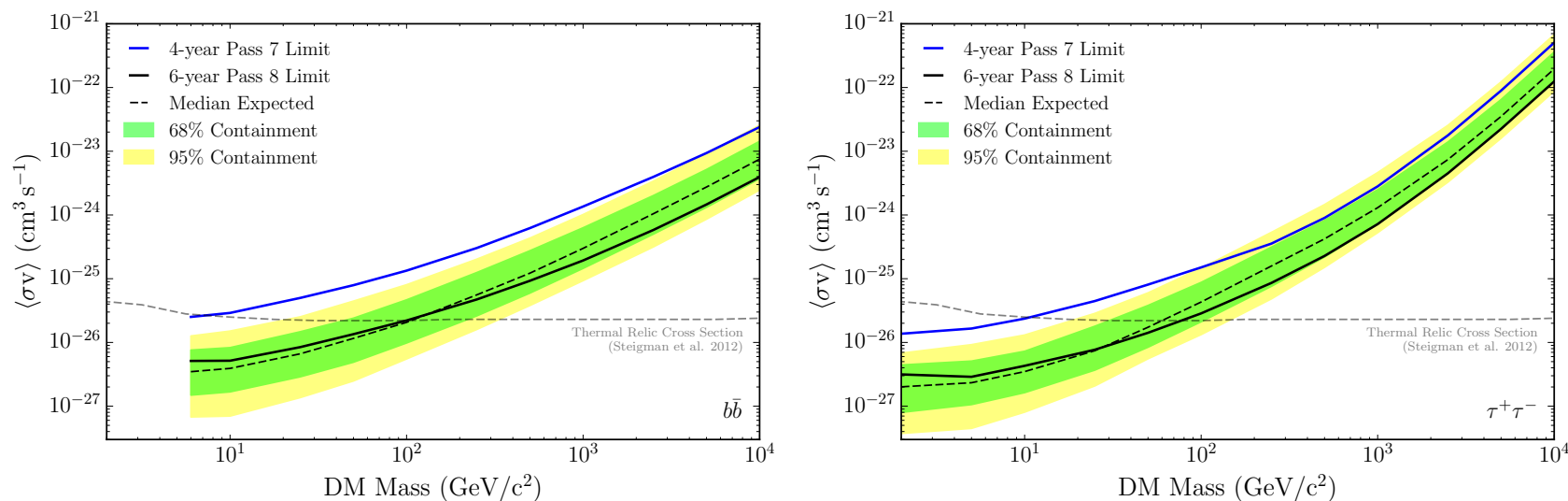
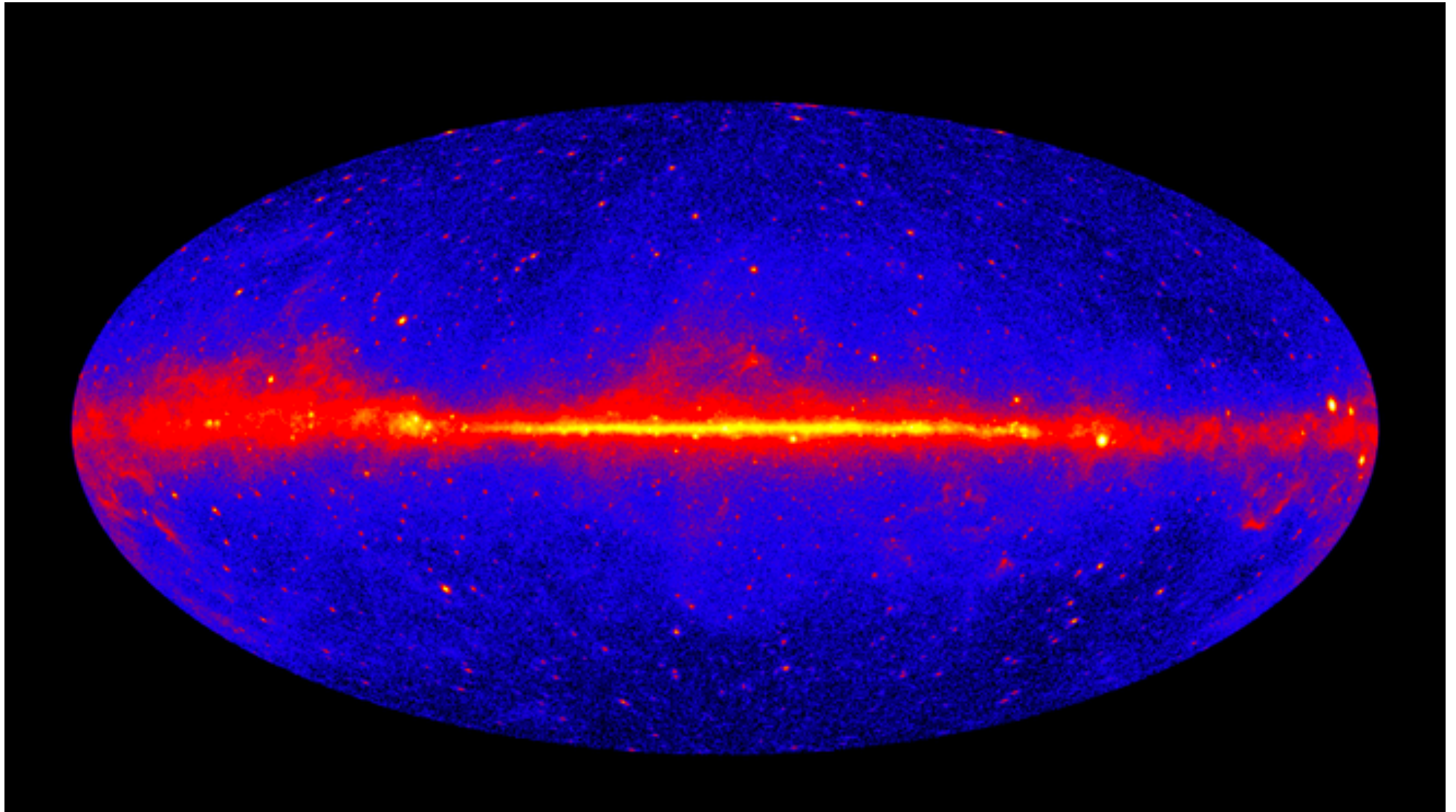


Figure 11: *Fermi* LAT limits on DM annihilation into $b\bar{b}$ (left) and $\tau^+\tau^-$ (right) final states. The dashed black line is the expected bound with 68% and 95% contours shown in green and yellow, respectively. The solid black line is the observation with six-year Pass 8 data. Figure from [99].

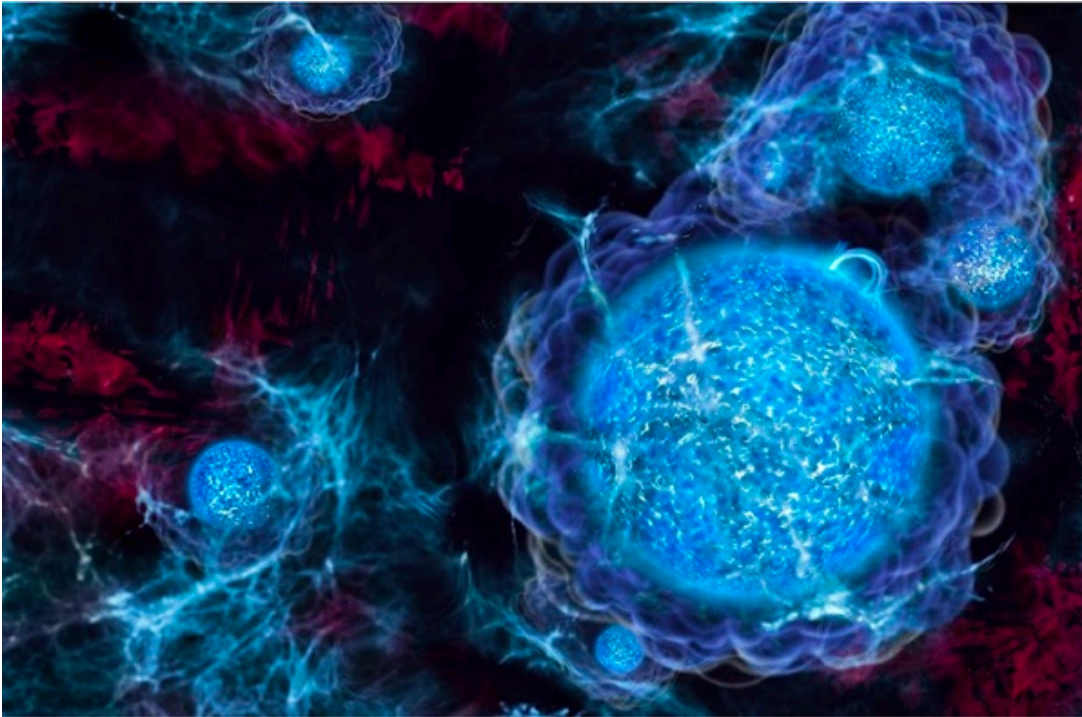
Indirect detection



Ultralight DM

Ultralight DM

Dark matter can be ultra-light. If DM is in the mass range of $10^{-20} - 10^{-10}$ eV, it can produce compact objects that in turn may produce *Gravitational Waves (GW)* that can be probed by current and future experiments. These objects are known as boson stars.



The production mechanisms in this case are: the misalignment mechanism, decay of thermal relics, freeze-out and decay of topological defects (Domain Walls and Cosmic Strings).

An ultralight DM thermally produced is hard, because it behaves as hot dark matter and it can jeopardise the period of structure formation.

However, if the pNGB has an extremely small coupling with the SM particles, it ensures it will not be thermally produced.

We can use the same extension of the SM that we have used for the scalar DM. This DM candidate has can be ultralight dark matter.

Ultralight DM

Dark matter can be ultra-light. If DM is in the mass range of $10^{-20} - 10^{-10}$ eV, it can produce compact objects that in turn may produce Gravitational Waves (GW) that can be probed by current and future experiments. These objects are known as boson stars.

Using the exact same potential for a complex scalar field invariant under U(1) with a soft breaking term we can describe such a light particle.

$$V(H, \phi) = V_0(H) + \mu_\phi^2 \phi \phi^* + \frac{1}{2} \lambda_\phi |\phi \phi^*|^2 + \lambda_{H\phi} H^\dagger H \phi \phi^* + V_{\text{soft}},$$

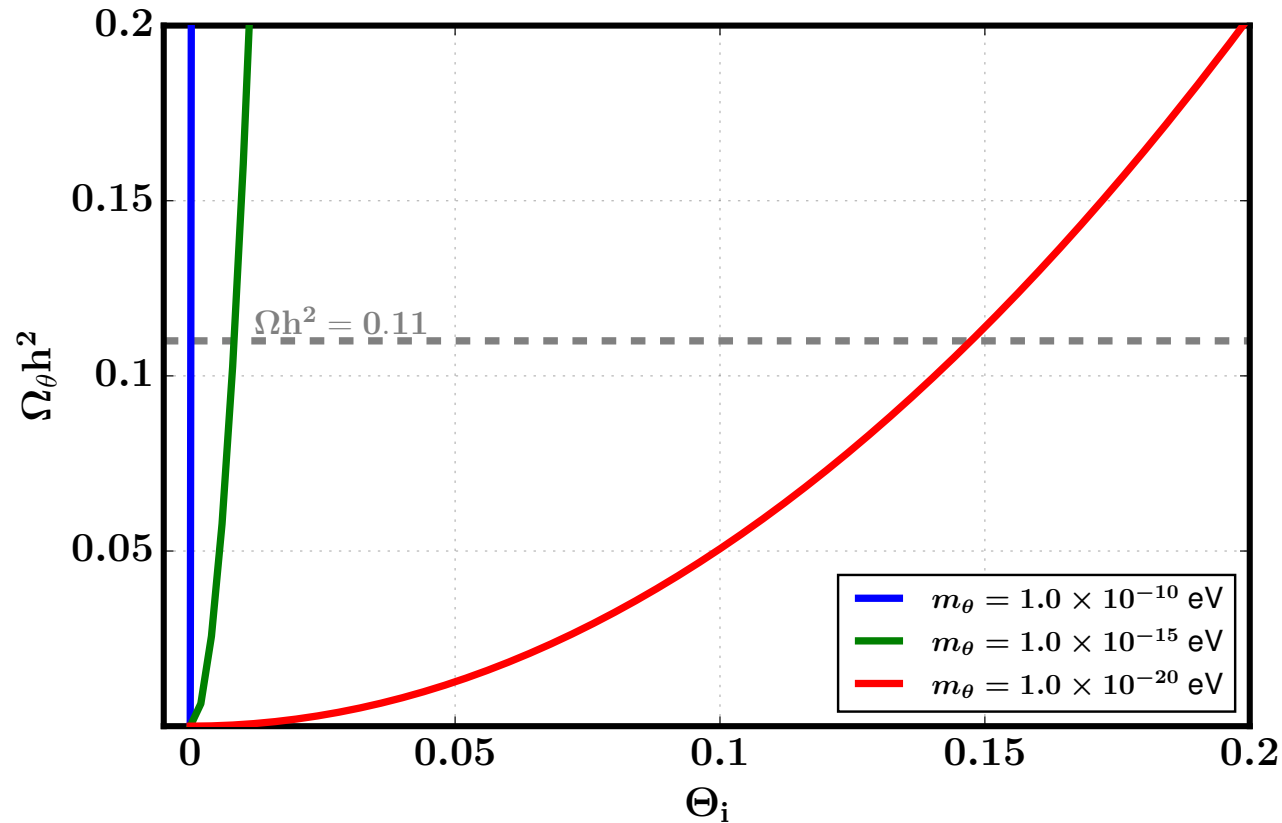
$$V_0(H) = \mu_H^2 H^\dagger H + \frac{1}{2} \lambda_H (H^\dagger H)^2 \quad V_{\text{soft}} = \frac{1}{2} \mu_s^2 (\phi^2 + \phi^{*2})$$

Resulting in a very small self-interaction

$$\phi = \frac{1}{\sqrt{2}} (\sigma + \nu_\sigma) e^{i\theta/\nu_\sigma} \quad \lambda_{\theta\theta\theta\theta} = -\frac{m_\theta^2}{6\nu_\sigma^2}$$

Ultralight DM

Ultralight non-thermal DM produced via the misalignment mechanism.



$$V_{\text{soft}} = \frac{\mu_s^2}{2} (\sigma + \nu_\sigma)^2 \cos\left(2\frac{\theta}{\nu_\sigma}\right)$$

Figure 1: Abundance of ultralight DM for the case where the SSB occurs before the end of inflation, for $m_\theta = 10^{-10}$ eV, 10^{-15} eV and 10^{-20} eV for blue, green and red curves, respectively. Here, we fixed $\nu_\sigma = 10^{17}$ GeV.